Systematic approaches to overcoming limitations of MAPK pathway inhibition in melanoma

(Article begins on next page)

Systematic approaches to overcoming limitations

of MAPK pathway inhibition in melanoma

A dissertation presented

by

David Joseph Konieczkowski

to

The Division of Medical Sciences

In partial fulfillment of the requirements

for the degree of

Doctor of Philosophy

in the subject of

Biological Chemistry and Molecular Pharmacology

Harvard University

Cambridge, Massachusetts

June 2013

Dissertation Advisor: Dr. Levi A. Garraway David Joseph Konieczkowski

Systematic approaches to overcoming limitations

of MAPK pathway inhibition in melanoma

Abstract

Metastatic melanoma is an aggressive, incurable cancer with historically few therapeutic options. The discovery that 60% of melanomas harbor the oncogenic BRAF^{V600E} mutation, which constitutively activates the MAPK pathway, has provided a promising new therapeutic axis. Although MAPK pathway inhibitor therapy has shown striking clinical results in BRAF^{V600}-mutant melanoma, this approach faces three limitations. First, 10-20% of BRAF^{V600}-mutant melanomas never achieve meaningful response to MAPK pathway inhibitor therapy (intrinsic resistance). Second, among BRAF^{V600}-mutant melanomas initially responding to MAPK pathway inhibitor therapy, relapse is universal (acquired resistance). Third, approximately 40% of melanomas lack BRAF^{V600} mutations and so are not currently candidates for MAPK pathway inhibitor therapy. We sought to address each of these problems: by characterizing the phenomenon of intrinsic MAPK pathway inhibitor resistance, by finding ways to perturb mechanisms of acquired MAPK pathway inhibitor resistance, and by identifying novel dependencies in melanoma outside of the MAPK pathway. Intriguingly, the NF-κB pathway emerged as a common theme across these investigations. In particular, we establish that MAPK

pathway inhibitor sensitive and resistant melanomas display distinct transcriptional signatures. Unlike most BRAF^{V600}-mutant melanomas, which highly express the melanocytic lineage transcription factor MITF, MAPK pathway inhibitor resistant lines display low MITF expression but high levels of NF-κB signaling. These divergent transcriptional states, which arise in melanocytes from aberrant MAPK pathway activation by BRAF^{V600E}, remain plastic and mutually antagonistic in established melanomas. Together, these results characterize a dichotomy between MITF and NF-κB cellular states as a determinant of intrinsic sensitivity versus resistance to MAPK pathway inhibitors in BRAF^{V600}-mutant melanoma. In separate investigations, we have shown that, NFKB1 p105, a member of the NF-κB family, intimately regulates levels of COT, a known effector of resistance to MAPK pathway inhibitors. Moreover, we have used shRNA screening to nominate particular nodes within the NF-κB pathway, including MYD88 and IRF3, as candidate melanoma lineage-specific dependencies. Cumulatively, although these studies use diverse approaches to investigate the limitations of MAPK pathway inhibitor therapy in melanoma, they converge in nominating the NF-κB pathway as a previously underappreciated feature of melanoma biology and suggest the relevance of this pathway for future investigation.

CONTENTS

CHAPTER 1. INTRODUCTION

Clinical aspects of melanoma

Unlike other skin cancers, melanoma is an aggressive and clinically intractable disease.

Melanoma is the sixth most common cancer in the North America, and the incidence of

melanoma has increased dramatically over the past several decades [1], suggesting the need for

better prevention, screening, and therapeutic approaches.

Melanoma risk factors

Melanoma risk is partly environmental and partly genetic. The primary environmental risk

factor for melanoma, at least in non-Hispanic whites, is UV exposure.[2] Genetically,

approximately 10% of melanoma cases are familial [3]. High-risk loci for inherited melanoma

include CDKN2A [4, 5] in which loss of function mutations impair inhibition of the cyclin-

dependent kinase CDK4 and cell cycle progression; CDK4 itself, in which mutations render it

unable to be inhibited by CDN2A [6]; and Rb [7, 8]. Other genetic factors have also been

recently associated with melanoma risk, including MC1R mutations conferring redheadedness

(even in the absence of UV exposure) [9, 10], MITF mutation (rendering it defective in

SUMOylation) [11], and promoter mutations in TERT (putatively leading to enhanced TERT

transcription) [12].

Melanoma growth phases

Phenotypically, melanoma behavior is divided into two growth phases: radial and vertical.

Radial growth phase melanomas are thin, epidermal, and relatively slow growing. After a

variable (or no) period in radial growth phase, melanomas enter vertical growth phase, invading

into the dermis and gaining metastatic potential. Once in vertical growth phase, the probability

of metastasis is directly correlated with depth of invasion (Breslow depth). [13] It is a measure

of the aggressiveness of melanoma that it is perhaps the only cancer where a primary tumor measured in millimeters at the time of excision is nonetheless likely to be fatal.

Melanoma histologies

Histologically, melanomas are divided into superficial spreading melanoma (the most common type, accounting for around 75% of melanomas), nodular melanoma (which progresses immediately into vertical growth phase), lentigo maligna melanoma (arising as macular lesions on aged, sun-damaged skin), and acral lentiginous melanoma (arising on palmar, plantar, and subungual surfaces).[14] Other rare classes of melanoma exist, including desmoplastic melanoma, which features spindle-shaped cells and a lack of MITF staining.[15-17]. However, these histologic subtypes do not directly correlate with clinical behavior.

Conventional treatment options for melanoma

Conventional treatment options for melanoma include surgery and chemotherapy. For primary melanoma in which complete resection can be achieved, surgical excision is curative.[18] Once metastasis has occurred, however, the mainstay of therapy has traditionally been cytotoxic chemotherapy. However, the standard agent, dacarbazine, has never been shown to have clinical benefit in metastatic melanoma relative to no treatment.[19] As a result, the median overall survival for metastatic melanoma has historically been approximately 6 months.[20]

Genomic landscape of melanoma

The historically dire therapeutic situation for metastatic melanoma has suggested the importance of a comprehensive understanding of oncogenic alterations in melanoma in order identify more effective therapeutic options.

Mutations

The most biologically significant mutations in melanoma appear to be those activating the MAPK pathway (Ras → RAF → MEK → ERK). Of these, the most common are activating, oncogenic mutations in codon 600 (V) of BRAF. (These alleles, commonly encoding mutations to residues E, D, or K, will hereafter be referred to collectively as BRAF^{V600} mutant.) [21] BRAF^{V600} mutations permit BRAF to signal even in the absence of normally required upstream stimulus from Ras. Therefore, BRAF^{V600} mutations constitutively activate the MAPK pathway. This effect is oncogenic in melanoma; moreover, in melanoma cell lines harboring the mutation, BRAF^{V600E} is required for sustained ERK phosphorylation and cell division. [22-24]

However, BRAF is not the only MAPK pathway derangement in melanoma: around one-third of melanomas harbor activating NRAS mutations. [25, 26] Notably, NRAS mutations are mutually exclusive with BRAF^{V600} mutations, implying either redundancy or even possibly synthetic lethality between these two oncogenes. The remainder of melanomas have generally been considered MAPK pathway wildtype; however, a recent report has demonstrated activating MEK mutations in some BRAF-mutant, NRAS-mutant, and BRAF-wildtype/NRAS-wildtype, suggesting that at least some melanomas previously characterized as MAPK pathway wildtype may in fact have MAPK activation at the level of MEK. [27]

Regardless of how the MAPK pathway is activated, it is clear—particularly in BRAF^{V600}-mutant melanoma—that sustained ERK activation drives continued melanoma proliferation and survival. The canonical role of ERK is to drive transcriptional output by phosphorylating transcription factors. While the transcriptional factors dependent on activation by ERK in melanoma have yet to be systematically characterized, among the most important so far appears

3

to be MITF, a master melanocyte regulator and melanoma oncogene discussed in greater detail below.

Recent sequencing studies have revealed other noteworthy mutations in melanoma: oncogenic mutations in the histone acetyltransferase co-activator TTRAP, apparent loss-of-function mutations in the glutamate receptor GRIN2A [28], loss-of-function oncogenic mutations in the PTEN-interacting protein PREX2 [29], and a highly recurrent mutation in the small GTPase RAC1 [30]. Perhaps most strikingly, highly recurrent (~70% prevalence) mutations have been identified in the TERT promoter, generating gain-of-function consensus ETS binding sites and potentially upregulating TERT transcription. [12, 31] Nonetheless, in contrast to mutations affecting the MAPK pathway, functional understanding of these mutations is generally either preliminary or nonexistent, and these mutations have not yet been therapeutically targeted in melanoma.

Certain other recurring themes have been noted in recent melanoma sequencing studies. First, the mutation rate among melanomas is highly variable (over nearly two orders of magnitude) and is approximately proportional to estimate sun exposure. Second, particularly in melanomas from sun-exposed lesions, the mutation rates observed (up to 100 mutations/Mb) are among the highest of cancers so far sequenced. Finally, for melanomas arising on sun-exposed surfaces, there is a highly significant excess of C→T or G→A transitions. [27, 30, 32-34] This mutational signature is consistent with that generated by UV irradiation and emphasizes the causal role of UV exposure in melanoma development.

Copy number

Copy number alterations in melanoma have been extensively characterized. Among the most

frequent targets of deletion are the tumor suppressors PTEN and CDKN2A, whereas TERT and

CCND1 are frequent targets of amplification. [27, 30, 35]

MITF in melanoma

Perhaps the canonical melanoma copy number alteration is amplification of the transcription

factor MITF. This amplification is found in approximately 10-20% of melanomas, although it

may be essential even in melanomas not harboring amplification [34, 36] Extensive work over

the past several decades has characterized the MITF transcription factor as the master regulator

of the melanocyte lineage (reviewed in [37]). In melanocytes, MITF orchestrates the

transcriptional program associated with pigment production and tanning in response to UV

irradiation (reviewed in [38]). In melanoma, MITF also has oncogenic functions distinct from is

pigmentation role. It drives cell cycle progression by directly inducing CDK2 transcription [39]

and bypasses senescence in nevi by suppressing expression of CDKN1A and CDKN2A [40].

Moreover, MITF potentiates cellular survival and evasion of apoptosis by inducing the

expression of BCL2 [41] and BIRC7 [42]. Thus, MITF is not only a key regulator of normal

melanocyte biology, but also an important melanoma oncogene.

The NF-κB pathway

Although the NF-κB pathway has not generally been considered critical in melanoma, it emerged

as a recurring theme in our studies. Therefore, a brief background is presented on it here.

Overview of the NF-κB pathway

An overview diagram of the NF-κB pathway is presented in **Fig 1.1**.
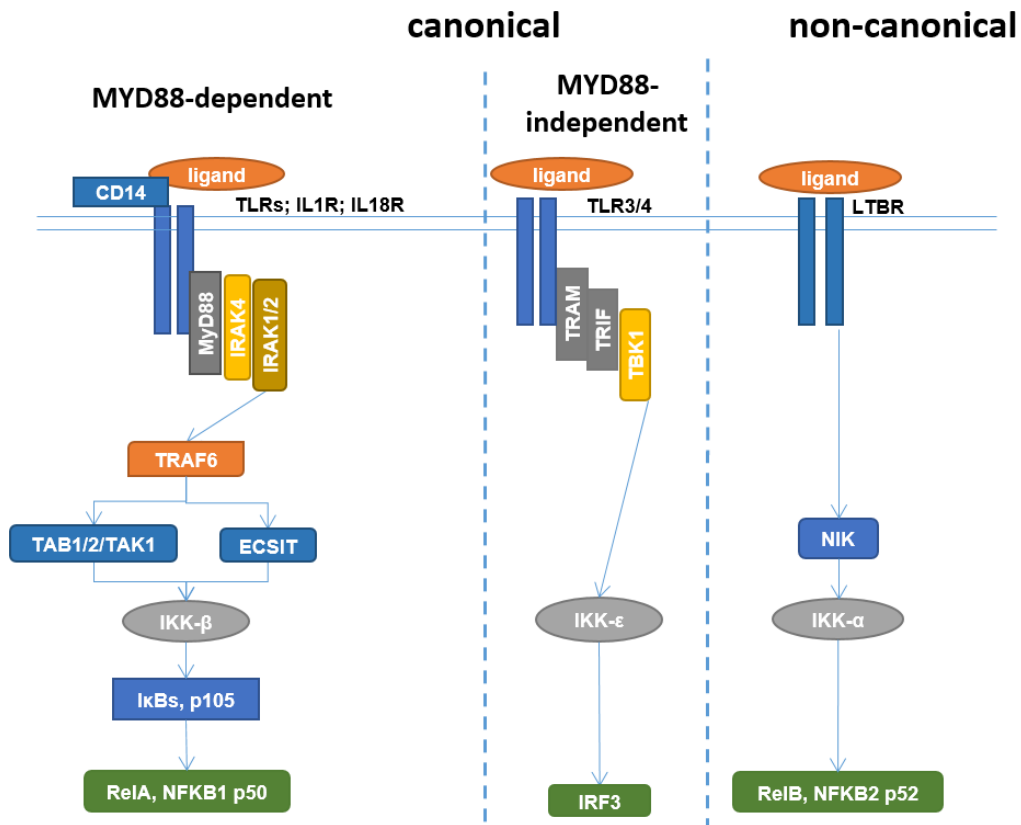
Figure 1.1. Schematic of the NF-κB pathway.
The NF-κB pathway can be divided into 3 arms, each incorporating different upstream ligands, adapter proteins, signal transduction networks, and downstream transcription factors. See text for more complete description.

The NF-κB family includes five transcription factors—RelA (p65), RelB, c-rel, NFKB1 (p105/p50), and NFKB2 (p100/p52)—that function as dimers. Because NFKB1/2 lack transcriptional activation domains, they drive transcription only when heterodimerized with a Rel protein. NFKB1 and NFKB2 have a C terminal inhibitory ankyrin repeat domain, which masks a nuclear localization signal and must be removed to allow nuclear localization and transcription. In contrast, inhibition of the Rel proteins is accomplished by the IκB proteins, which contain ankyrin repeats homologous to the C terminal of NFKB1/NKFB2. After upstream pathway activation, IκBs are phosphorylated and degraded at the proteasome, releasing Rel-containing NF-κB dimers for transcriptional activity. [43-45]

NF-κB dimers and their upstream activation can be divided into two pathways, canonical and non-canonical. [46] The canonical pathway favors RelA/NFKB1 dimers, whereas the non-canonical pathway includes RelB/NFKB2 dimers. In the canonical pathway, IκB is marked for degradation by phosphorylation by the IκB kinase IKK-β. IKK-β is activated by many upstream stimuli: for example, IL-1β and LPS signal through their receptors to MYD88 to IRAK1/2/4, TRAF6, and the TAB/TAK complex or ECSIT to IKK-β. IKK-β subsequently phosphoactivates NFKB1 and RelA. A MYD88-independent arm of the non-canonical pathway transduces signals from TLR3 ligands (e.g., viral dsRNA) through IKK-ε to the transcription factor IRF3. The non-canonical pathway, by contrast, depends on IKK-α, which is phosphoactivated by NIK [46] downstream of receptors such as the lymphotoxin β receptor (LTBR). [47]

NF-κB activation can have diverse consequences. Two relevant for cancer are control of cell cycle progression and induction of anti-apoptotic factors. NF-κB activity directly drives cell cycle progression because the promoter of cyclin D1 contains an NF-κB binding site. As regards apoptosis, NF-κB can drive transcription of anti-apoptotic genes such as BCL2 and BCL-XL.

The NF-κB pathway in cancer

The cancer relevance of NF-κB was first suggested by the fact that the v-rel Avian reticuloendotheliosis virus encodes a modified, oncogenic version of c-rel. [48-51] Many cancers also carry alterations in endogenous NF-κB genes. For example, diffuse large B cell lymphoma (DLBCL) harbors diverse NF-κB derangements including Rel amplification [52-54], constitutively active B cell receptor/CARD11 signaling [55-57], and loss of the NF-κB inhibitory protein A20/TFNAIP3 [58-60]. In solid tumors, one example is the status of IKBKE as a breast cancer oncogene. [61] Even in the absence of genomic derangements in the NF-κB pathway, there may exist latent NF-κB dependency. While activated Ras drives NF-κB activation [62-65], Ras-transformed cells also require NF-κB activity to survive the oncogenic stress of Ras activation and transformation [66-68]. Thus, NF-κB appears to play an important role in many types of cancer.

The NF-κB pathway in melanoma

Despite its roles in other cancers, the NF-κB pathway has been relatively little studied in melanoma. Some melanoma cell lines and tumors show increased activity of IKK-α, IKK-β, RelA, and NFKB1 p50 [69-71], with activation correlating with disease-specific mortality.[72] NIK—the kinase that activates IKK-α in the non-canonical pathway—is highly expressed in melanoma and apparently driven by ligand-independent signaling downstream of LTBR [73, 74] In an HRAS^{V12} / p16I^{NK4A} mouse model of melanoma, NF-κB activity was required for tumor formation; similar results have also been obtained with xenografts and IKK-β inhibitors. [75-77] However, to date, there has been no comprehensive assessment of the role of the NF-κB pathway in melanoma.

Targeted therapeutic approaches to melanoma

At present, two broad class of targeted therapeutic agents exist in melanoma: immune

modulatory agents, and MAPK pathway inhibitors.

Immune modulatory agents

Immune modulatory agents operate on the principle that melanoma is a highly antigenic cancer.

[78] Although there often exists a host immune response against melanoma, it is typically not

sufficient to contain the tumor. Therefore, enhancing the anti-tumor immune response has the

potential to generate therapeutic benefit. The most successful such approach to date has been

blockade of immune checkpoints inhibiting T-cell activation, leading to enhanced tumor killing

by cytotoxic T cells. This strategy, exemplified by ipilimumab (targeting the T cell inhibitor co-

receptor CTLA4) [79, 80] and anti-PDL1 antibodies (targeting PD1/PDL1 interaction) [81], has

recently shown significant clinical promise in melanoma ([82, 83], reviewed in [84]). However,

immune modulatory therapies are not the focus of this work.

MAPK pathway inhibition

In contrast, this dissertation focuses on the potential as well as the limits of MAPK pathway

inhibition. The rationale for MAPK pathway therapeutics in melanoma comes from two

fundamental discoveries. First was the elucidation that that approximately 60% of melanomas

harbor the activating, oncogenic $BRAF^{V600E}$ mutation, which constitutively activate the MAPK

pathway.[21] This biological discovery was translated to therapeutic implication by the

discovery that $BRAF^{V600E}$ mutation predict sensitivity to MAPK pathway inhibitors.[85]

Ultimately, these discoveries were brought to fruition by the development of vemurafenib

(PLX4032; its preclinical analogue PLX4720 was used in these studies), a specific inhibitor of

V600-mutant BRAF. [86] In Phase II and III trails in BRAF^{V600}-mutant melanoma patients, vemurafenib has achieved clinical benefit in 80-90% of patients and RECIST responses in approximately 50% of patients, yielding approximately 7 months progression-free survival and lengthening overall survival to approximately 16 months. [87, 88] An improvement on this approach has been to combine RAF inhibition with MEK inhibition to achieve more complete blockade of the MAPK pathway; in this regime, trials of dabrafenib (a RAF inhibitor) plus trametinib (a MEK inhibitor) have yielded response rates approaching 75% and progression-free survival of 9.4 months.[89] Thus, MAPK pathway inhibition has shown significant clinical efficacy in BRAF^{V600}-mutant melanoma.

Limitations to MAPK pathway inhibition

<u>Resistance to MAPK pathway inhibition</u>

This advance, however, has been tempered by two realizations. First, a subset of melanoma patients, despite harboring BRAF^{V600} mutations, do not respond to MAPK pathway therapeutics. [87-89] This phenomenon is termed intrinsic resistance. Second, of those patients who do initially respond, all will eventually relapse. [87] This phenomenon is termed acquired resistance.

Because of its profound clinical relevance, resistance to MAPK pathway inhibition has garnered significant research interest. Cumulatively, a picture of acquired resistance mechanisms has begun to emerge. A common theme in resistance to targeted therapeutics is drug target alterations; indeed, aberrant BRAF splicing can generate a truncated version of BRAF, resistant to inhibition by PLX4720, that is capable of aberrant self-dimerization and activation. [90] Alternatively, instead of re-activating BRAF, other kinases—including CRAF [91] and COT [92], a MAP3K—can substitute for BRAF and reactivate pERK. Resistance can also be

achieved by driving flux through the MAPK pathway in a $BRAF^{V600}$-independent fashion. Specifically, signaling from upstream Ras appears to proceed primarily through CRAF rather than BRAF. Therefore, even in the context of $BRAF^{V600E}$ inhibition, Ras activation can restore MAPK pathway activity and viability. Thus, gain of NRAS mutation [93], loss of NF1 [94] (a negative regulator of Ras), or loss of MAPK-driven negative feedback onto Ras [95] leads to BRAF-independent signaling flux into the MAPK pathway and inhibitor resistance. Similarly, driving endogenous signaling through Ras by HGF stimulus (whether exogenous or supplied by tumor stroma) of the upstream receptor kinase MET can cause resistance. [96] Conversely, inhibition of BRAF becomes ineffective if the normal output of BRAF is restored. Thus, activating alleles in MEK that re-activate pERK in a BRAF-independent fashion are sufficient to cause resistance [97]; moreover, even below the level of ERK, re-engagement of the MAPK transcriptional output BCL2A1 confers resistance. [98]

Together, these studies have begun to paint a unified picture of acquired resistance to inhibition of $BRAF^{V600E}$ in melanoma. Two points are important to note. First, these studies have largely identified mechanisms that reactive either the MAPK pathway or its output; in other words, resistance to MAPK inhibition in these cases occurs because the MAPK pathway or its output is no longer effectively inhibited. Second, these studies have largely begun from the premise of making a resistant cell sensitive; thus, they are conceptually targeted towards characterization of acquired, rather than intrinsic, resistance. For these reasons, the extent to which non-MAPK pathway mechanisms of resistance might be relevant, particularly in the setting of intrinsic resistance, remains to be elucidated.

Thus, despite its promise, MAPK pathway inhibition in melanoma faces three fundamental limitations. First, 10-20% of $BRAF^{V600}$-mutant melanomas are intrinsically resistant to MAPK pathway inhibition. Second, of the 80-90% of $BRAF^{V600}$-mutant melanomas who initially respond to MAPK pathway inhibition, all will eventually acquire resistance and relapse. Third, for both those melanomas harboring $BRAF^{V600}$ mutations as well as those lacking them, durable control is likely to require the identification of therapeutically tractable vulnerabilities beyond the MAPK pathway. In this work, we sought to address each of these issues in a systematic fashion.

CHAPTER 2. UNDERSTANDING INTRINSIC MAPK PATHWAY INHIBITOR RESISTANCE: AN MITF/NF-κB MELANOMA CELL STATE DICHOTOMY INFLUENCES SENSITIVITY TO MAPK PATHWAY INHIBITORS.

Abstract

Most melanomas harbor the oncogenic $BRAF^{V600E}$ mutation, which constitutively activates the MAPK pathway. Although MAPK pathway inhibition has shown clinical benefit in $BRAF^{V600}$-mutant melanoma, 10-20% of patients fail to respond to this approach. Using a panel of $BRAF^{V600}$-mutant melanoma cell lines, we found that MAPK pathway inhibitor sensitive and resistant melanomas display distinct transcriptional profiles. Whereas most $BRAF^{V600}$-mutant melanoma cell lines showed high expression of the melanocytic lineage transcription factor MITF and its target genes, MAPK pathway inhibitor resistant lines displayed low MITF expression but high levels of NF-κB signaling. Clinically, melanomas with low pre-treatment MITF expression showed less durable responses to MAPK pathway inhibitor therapy. In melanocytes, establishment of a cell state characterized by robust NF-κB-related gene expression was achieved by introduction of $BRAF^{V600E}$ but blocked by activation of MITF. Moreover, in established melanoma cell lines, this cellular state is plastic; MITF expression antagonized maintenance of the NF-κB transcriptional state, whereas NF-κB activation antagonized MITF expression and induced both resistance marker gene expression and MAPK pathway inhibitor resistance. These results suggest that a dichotomy between MITF and NF-κB transcriptional states in $BRAF^{V600}$-mutant melanoma may influence intrinsic resistance to MAPK pathway inhibitors.

13

Attributions

This chapter is reprinted from a manuscript in preparation.

All experiments and analyses were performed by David Konieczkowski except as follows:

Analysis for **Fig. 2.1B, 2.1D, 2.1A, 2.8A, 2.8E** was performed by Pablo Tamayo and Omar Abudayyeh.

Sectioning and staining for **Fig. 2.3D** and **2.7** were performed by Zac Cooper and Dennie Frederick. Scoring was performed by Adriano Piris.

Experiments in **Fig. 2.8A** were performed by William Kim.

Experiments in **Fig. 2.12** were performed by Kris Wood and previously published as: Wood KC, Konieczkowski DJ, … Garraway LA, Sabatini DM. MicroSCALE screening reveals genetic modifiers of therapeutic response in melanoma. *Sci Signaling* 2012.

Experiments in **Fig. 2.8B, 2.8C, 2.8D, 2.9, 2.14** and **2.10D** were performed by Cory Johannessen; lines in **Fig 2.10D** were derived by Krishna Vasudevan and Ravid Straussman.

Introduction

The discovery that activating $BRAF^{V600}$ mutations (present in 50-60% of melanomas) [21] predict sensitivity to mitogen-activated protein kinase (MAPK) pathway inhibition [85] has revolutionized therapeutic approaches to melanoma. MAPK pathway inhibitors—including the RAF inhibitors vemurafenib and dabrafenib and the MEK inhibitor trametinib—achieve clinical benefit in 80-90% of $BRAF^{V600}$-mutant melanoma patients, with RECIST response rates between 50% (for vemurafenib alone) and 70% (for dabrafenib+trametinib) ([87, 89, 99]. However, among patients whose tumors respond to MAPK pathway inhibitors, relapse is universal

(acquired resistance); moreover, 10-20% of patients never achieve meaningful response to therapy (intrinsic resistance). Recent studies have characterized diverse mechanisms of acquired resistance to MAPK pathway inhibitors in BRAF^{V600}-mutant melanoma.[90-92, 94-98] In contrast, we sought to elucidate molecular features that might contribute to intrinsic resistance to MAPK pathway inhibition in BRAF^{V600}-mutant melanoma.

Results

1. <u>Association of expression classes with differential MAPK pathway inhibitor sensitivity in BRAF^{V600}-mutant melanoma.</u>

We hypothesized that cell-intrinsic features such as gene expression programs might partly account for intrinsic resistance to MAPK pathway inhibitors. To test this hypothesis, we examined 29 BRAF^{V600}-mutant melanoma cell lines from the Cancer Cell Line Encyclopedia [100] for which gene expression and pharmacological sensitivity data was available (**Fig. 2.1A**). Although most lines were sensitive to the RAF inhibitor PLX4720 (GI$_{50}$ $\leq$ 2 uM), a subset exhibited intrinsic resistance to this agent as well as to MEK inhibitors (PD0325901 and AZD6244, **Fig. 2.1B**). Using this panel, we identified genes whose expression across the cell lines was strongly correlated or anti-correlated with their PLX4720 GI$_{50}$ values. *MITF*, which encodes a melanocyte lineage regulatory transcription factor and melanoma oncogene [36], emerged as the single gene best correlated with sensitivity to PLX4720 (**Fig. 2.1B, 2.1C, 2.2**). Conversely, *MITF*, its target genes, and a transcriptional signature of MITF activity [11] were poorly expressed in the resistant lines. Instead, intrinsically resistant BRAF^{V600E} melanoma cell lines expressed gene sets associated with NF-κB activation, as well as individual marker genes including *AXL*, *TPM1*, *NRP1*, and *CDH13*. (**Fig. 2.1B, 2.1C**)

15

This reciprocity between MITF and NF-κB transcriptional profiles, which correlated with MAPK inhibitor sensitivity in BRAF^{V600}-mutant melanoma cell lines, was reminiscent of prior transcriptional [101] and histopathologic [102] analyses of melanoma tumors. However, links to intrinsic vemurafenib or dabrafenib/trametinib resistance in BRAF^{V600}-mutant melanomas have not previously been defined. The reciprocity between MITF and NF-κB expression signatures was confirmed using a collection of primary and metastatic BRAF^{V600}-mutant melanomas (**Fig. 2.1D**) (data from The Cancer Genome Atlas, https://tcga-data.nci.nih.gov/tcga/). Thus, the transcriptional class distinction that distinguished MAPK pathway inhibitor sensitive and resistant cell lines *in vitro* was also readily discernible *in vivo*. Cumulatively, these results nominate an expression dichotomy between NF-κB and MITF, present in both melanoma cell lines and tumors, as correlated with intrinsic resistance versus sensitivity to MAPK pathway inhibition.

Figure 2.1. Association of expression classes with differential MAPK pathway inhibitor sensitivity in BRAF^{V600}-mutant melanoma.
(**a**) PLX4720 sensitivity across a collection of BRAF^{V600}-mutant melanoma cell lines.
(**b**) Relationship between PLX4720 sensitivity and MITF-high versus NF-κB-high classes.
(**c**) Expression of selected markers by Western blot.
(**d**) Expression dichotomy in BRAF^{V600}-mutant melanoma tumor samples.
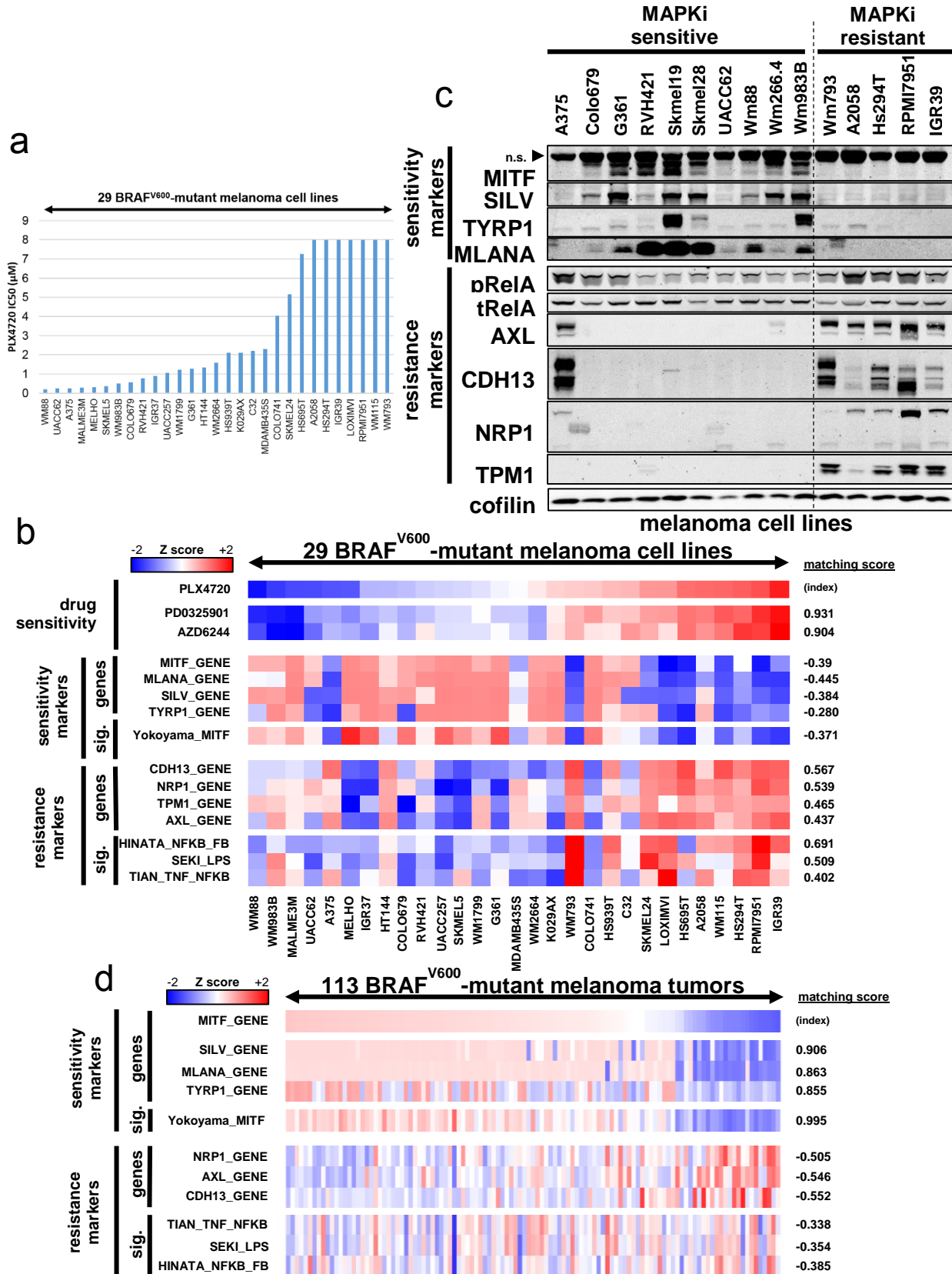
Figure 2.1 (continued)

18
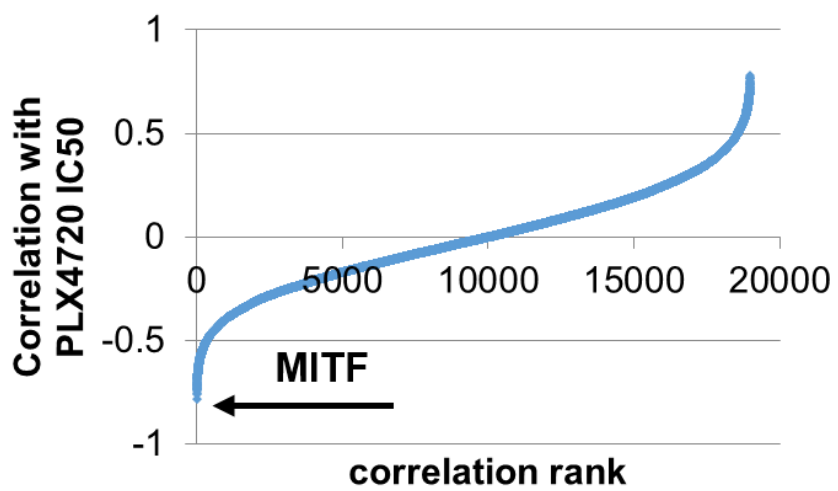
Figure 2.2.
Correlation of MITF expression with MAPK pathway inhibitor sensitivity in a panel of 29 BRAF^{V600}-mutant melanoma cell lines.

2.   NF-κB-high/MITF-low melanomas represent a reproducible subclass distinguished by resistance to MAPK pathway inhibition

To verify the association between the MITF/NF-κB class distinction and sensitivity to MAPK pathway inhibition, we examined a collection of patient-derived BRAF^{V600}-mutant melanoma short-term cultures for which gene expression data, but not pharmacological sensitivity data, was available. As in other datasets, we identified the MITF and NF-κB signatures at both the transcriptional (**Fig. 2.3A**) and protein expression (**Fig. 2.4**) levels. We then performed pharmacologic growth inhibition studies on 7 "MITF-high" and 3 "NF-κB-high" short-term cultures. Notably, all 7 MITF-high/NF-κB-low short-term cultures were sensitive to RAF and MEK inhibition, whereas each of the three NF-κB-high/MITF-low short-term cultures were resistant to these agents (**Fig. 2.3B**). These finding supported the premise that the MITF-low, NF-κB-high transcriptional signature correlated with intrinsic resistance to MAPK pathway inhibition in BRAF^{V600}-mutant melanoma.

In addition to single-agent RAF and MEK inhibitor resistance, we found that MITF-low, NF-κB-high short-term cultures (**Fig. 2.3B**) and cell lines (**Fig. 2.5**) also showed resistance to both combined RAF+MEK inhibition and ERK inhibition. The intrinsic resistance phenotype was not attributable to an inability of these agents to suppress MAPK pathway signaling, because the reduction of ERK phosphorylation in these lines was comparable to that observed in drug-sensitive lines (**Fig. 2.3C, 2.4, 2.6**). These findings suggest that a molecularly definable subset of MITF-high, NF-κB-low BRAF^{V600}-mutant melanomas are "indifferent" to MAPK pathway inhibition.

To assess whether the resistance phenotype linked to this class distinction *in vitro* might be similarly evident in melanoma tumors, we examined a series of pre-treatment biopsy specimens

obtained from metastatic BRAF^{V600}-mutant melanoma patients, subsequently treated with

combined RAF/MEK inhibition, for whom clinical response data was available. Using AXL

expression as a proxy for the NF-κB-high cellular state (**Fig. 2.1B-D, 2.3A, 2.4**), we stratified the

cohort into MITF-high/NF-κB-low (n=4) and MITF-low/NF-κB-high (n=8) groups on the basis

of immunohistochemistry (**Fig. 2.3D, 2.7, Table 2.1**). Following dabrafenib + trametinib

therapy, progression-free survival was significantly shorter (median 5.0 months versus 14.5

months, p=0.0313) in the MITF-low/NF-κB-high group (**Fig. 2.3E**), thus providing preliminary

support for the therapeutic relevance of this molecular dichotomy.

Figure 2.3. NF-κB-high, MITF-low melanomas represent a reproducible subclass distinguished by resistance to MAPK pathway inhibition

(**a**) Expression dichotomy in BRAFV600-mutant melanoma short-term cultures.

(**b**) Relationship between expression class and MAPK pathway inhibitor sensitivity in short-term cultures.

(**c**) Effects of MAPK pathway inhibitors on pERK and pFRA1 across sensitive and resistant cell lines. Uniquely, RPMI-7951 harbors amplification of MAP3K8 (COT), which is known to re-activate the MAPK pathway. D, DMSO; P, 2 µM PLX4720; A, 200 nM AZD6244; P+A, PLX4720+AZD6244; E, VTX11, 2 µM.

(**d**) Examples of AXL and MITF expression in pre-treatment melanoma biopsies.

(**e**) Comparison of progression-free survival between MITF-positive/AXL-negative and MITF-negative/AXL-positive classes.

Figure 2.3 (continued)

c

melanoma cell lines	1 hr	4d	1 hr	4d	1 hr	4d	1 hr	4d

pERK   pFRA1   tERK   cofilin

sensitive: Skmel19, G361, RVH421

resistant: IGR39, A2058, Hs294T, Wm793, RPMI7951

d

MITF   AXL

MITF + AXL -

MITF - AXL +

e

BRAFi + MEKi

p=0.0313

months PFS

MITF-pos   AXL-pos

IHC class
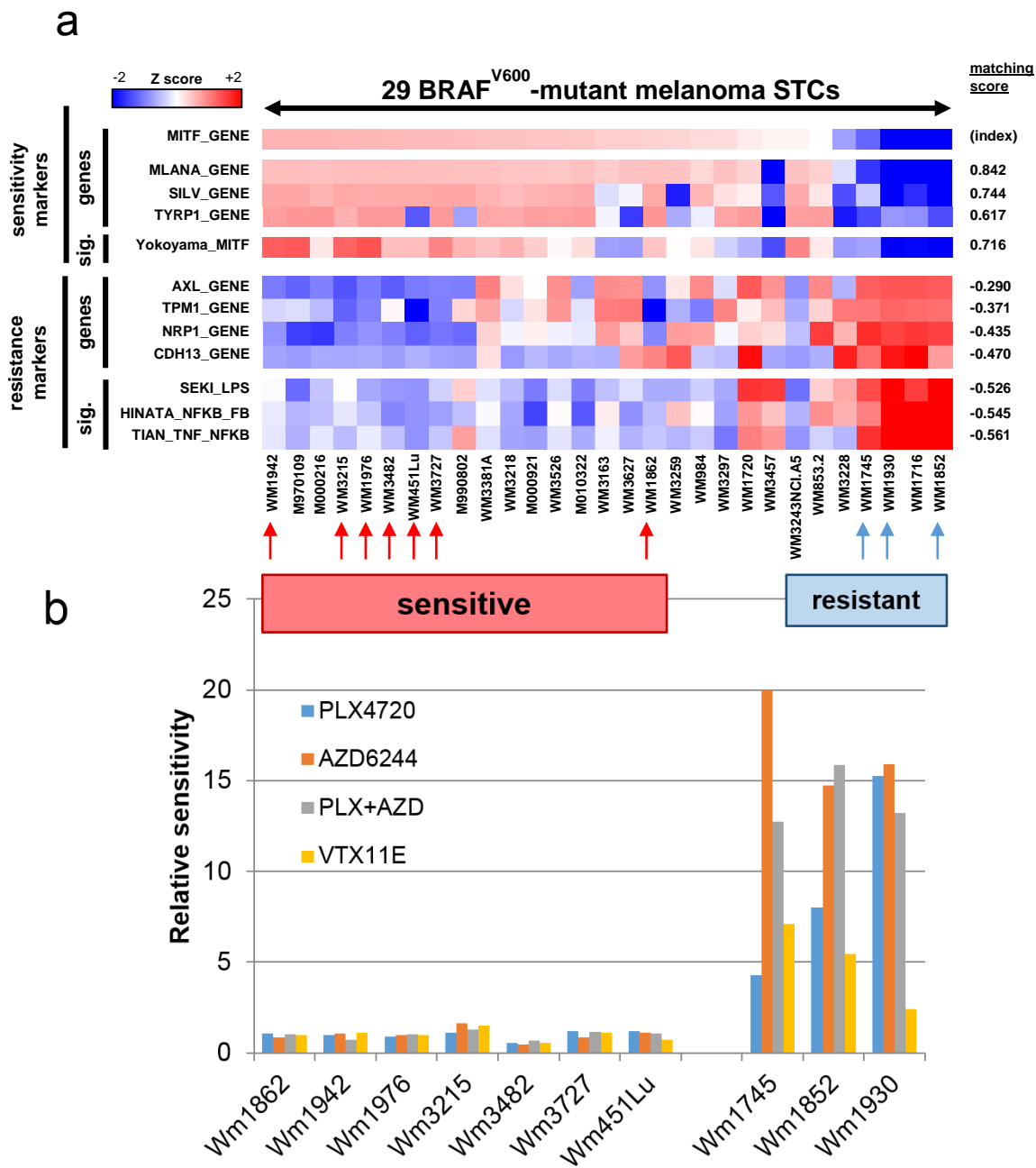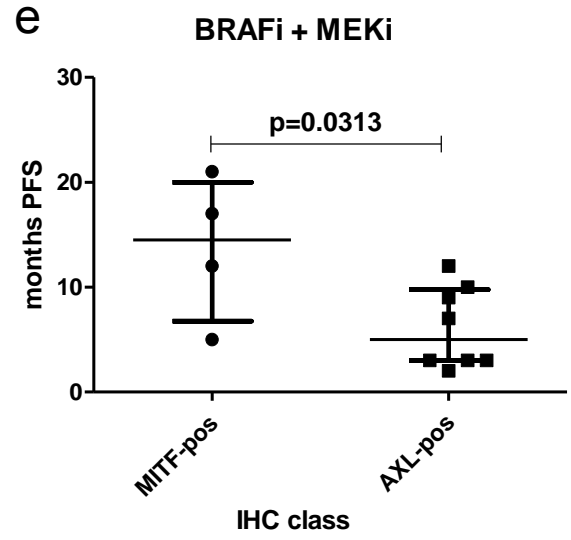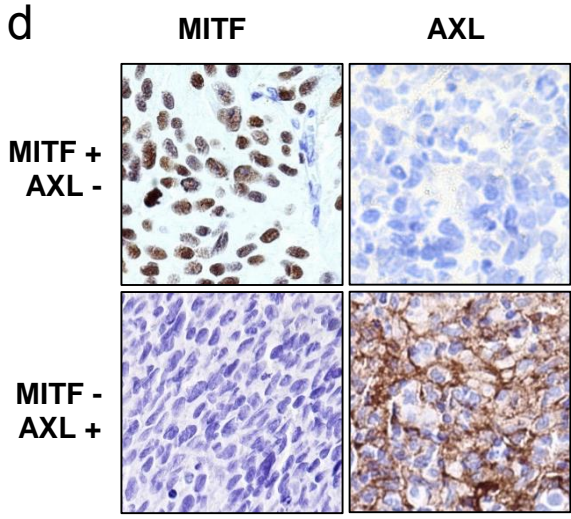
Figure 2.3 (continued)
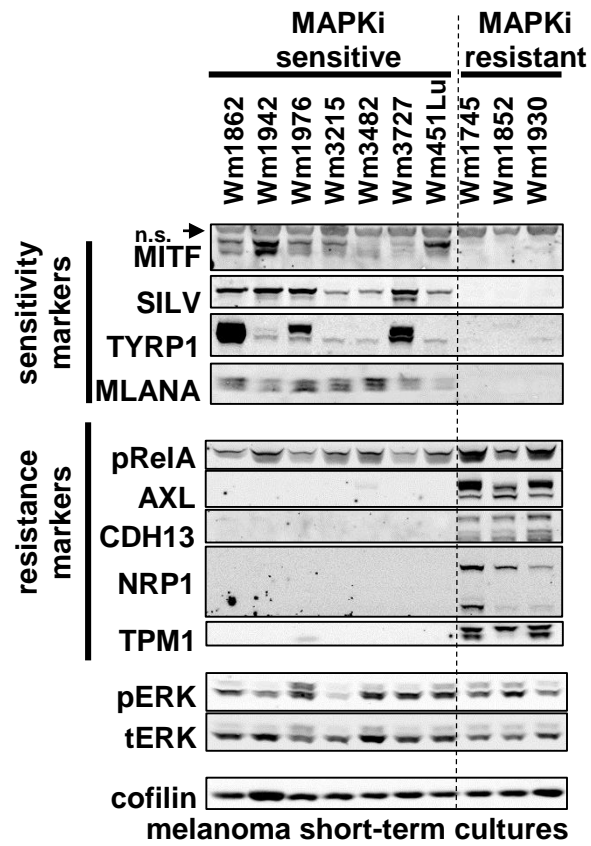
Figure 2.4.
Basal ERK phosphorylation and MITF/NF-κB marker expression in MAPK pathway inhibitor sensitive and MAPK pathway inhibitor resistant melanoma short-term cultures.
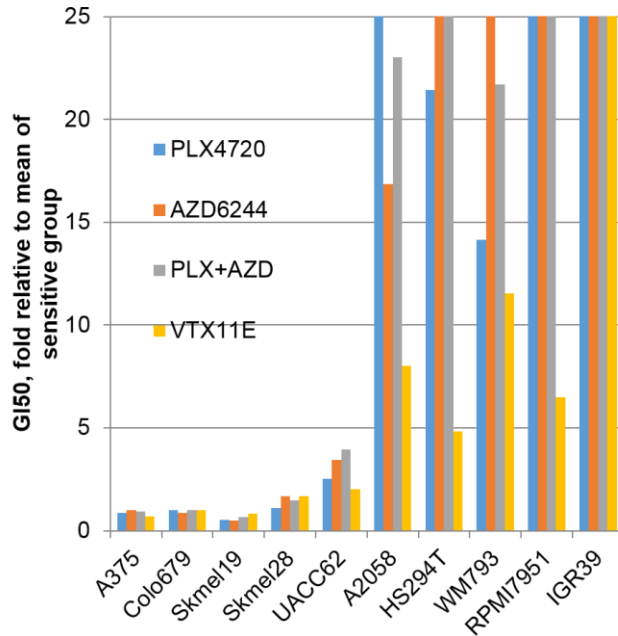
Figure 2.5.
Sensitivity profile of selected melanomas to inhibition of BRAF (PLX7420), MEK
(AZD6244), RAF+MEK, and ERK (VTX11E).
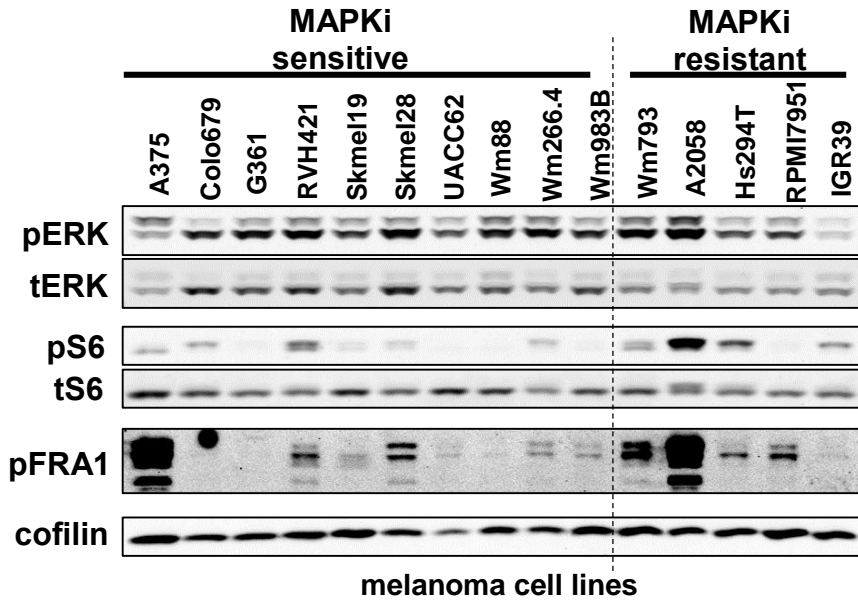
Figure 2.6.
Basal MAPK pathway activity, as measured by pERK, pS6, and pFRA1, in MAPK pathway
inhibitor sensitive and MAPK pathway inhibitor resistant melanoma cell lines.
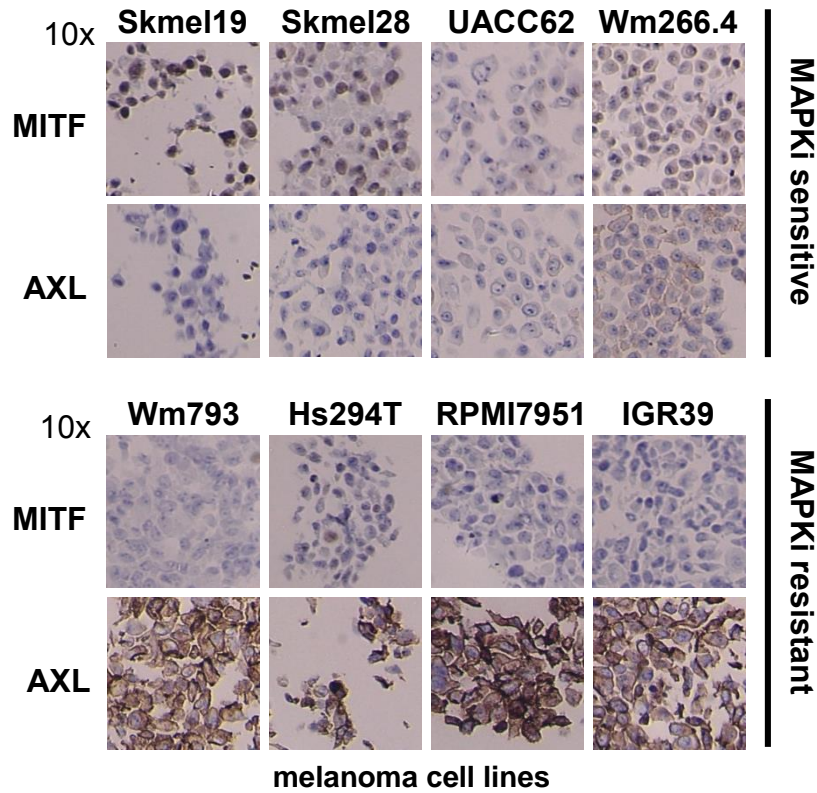
Figure 2.7.
Immunocytochemistry for MITF and AXL in MAPK pathway inhibitor sensitive and resistant melanoma cell lines.

Table 2.1.
Pre-treatment immunohistochemistry results and progression-free survival (PFS) following dabrafenib + trametinib therapy.

		MITF		AXL	
sample	PFS (mo)	distribution	intensity	distribution	intensity
R4	5	diffuse	2	negative	0
R9	12	diffuse	1	negative	0
6A	21	diffuse	3	negative	0
19A	17	diffuse	2	negative	0
9A	7	negative	0	diffuse	2
R8	2	negative	0	focal	2
R10	3	negative	0	focal	2
11A	10	negative	0	focal	2
13A	9	negative	0	diffuse	2
22A	3	negative	0	focal	2
25A	3	negative	0	focal	2
12A	12	negative	0	diffuse	2

3. Establishment of two-class dichotomy in melanocytes.

Having observed that sensitivity and resistance to MAPK pathway inhibitors can be associated with distinct transcriptional states, we sought to understand whether both of these states could be established from the same precursor cell. At baseline, we found that immortalized primary human melanocytes expressed high levels of both MITF and its target genes, reminiscent of MITF-high/NF-κB-low melanoma cell lines. Consistent with the aforementioned transcriptional class distinction in melanoma, expression of NF-κB-associated signatures and marker genes was low in these cells. (**Fig. 2.8A and 2.8B**)

In order to model the BRAF^{V600}-mutant status of our cell line panels, we first introduced BRAF^{V600E} into these melanocytes. As expected, ectopic BRAF^{V600E} expression augmented ERK phosphorylation (**Fig. 2.8B**). Consistent with prior observations[36], introduction of BRAF^{V600E} abrogated expression of MITF and its target genes at both the transcriptional (**Fig. 2.8A**) and protein levels (**Fig. 2.8B**). Interestingly, expression of BRAF^{V600E} also induced NF-κB pathway activation, as measured by NF-κB associated gene set expression (**Fig. 2.8A**), RelA phosphorylation (**Fig. 2.8B**), and expression of markers such as AXL and TPM1 (**Fig. 2.8A, 2.8B**). Thus, ectopic expression of BRAF^{V600E} in melanocytes phenocopied the expression pattern of intrinsically resistant melanomas. Comparable results were obtained even after prolonged (8-12 week) expression of BRAF^{V600E} in melanocytes (**Fig. 2.8C**), suggesting that these phenotypic patterns are durable. MEK^{DD} similarly suppressed MITF and up-regulated AXL, whereas MAPK pathway inhibitors largely reversed these effects. (**Fig. 2.8A, 2.8B**) These results suggest that aberrant MAPK pathway signaling is both necessary and sufficient for BRAF^{V600E} to effect these transcriptional changes. In addition, BRAF^{V600E}-mediated induction

of AXL (though not loss of MITF) was partially antagonized by an IκBα super-repressor (**Fig. 2.9**), suggesting that NF-κB activation induced by BRAF^{V600E} contributes at least partially to expression of marker genes associated with the NF-κB-high class. Altogether, these results suggest that, while melanocytes begin in an NF-κB-low/MITF-high state, the NF-κB-high/MITF-low phenotype can be induced by gain of BRAF^{V600E}.

Although BRAF^{V600E} can induce a NF-κB-high/MITF-low cell state in melanocytes *in vitro* ([36], **Fig. 2.8A-2.8C**), most BRAF^{V600}-mutant melanomas exhibit the opposite (i.e., MITF-high/NF-κB-low) cell state both *in vitro* and *in vivo*. Because MITF expression is a prominent feature of the low-NF-κB state, we hypothesized that concomitant MITF dysregulation might block or even reverse BRAF^{V600E}-induced transition to the high-NF-κB state. To test this, we ectopically expressed MITF in melanocytes simultaneously with either BRAF^{V600E} or MEK^{DD}. Indeed, expression of MITF blocked the ability of BRAF^{V600E} or MEK^{DD} to induce AXL expression (**Fig. 2.8D**), implying a blunted transition into the NF-κB-high transcriptional state. This effect was dependent on the ability of MITF to bind DNA, as a DNA binding-deficient mutant (MITF(R217Δ)) was unable to suppress AXL expression (**Fig. 2.8D**). Consistent with this data, we found an enrichment of MITF amplification in MITF-high/NF-κB low melanoma cell lines relative to MITF-low/NF-κB-high lines (**Fig. 2.8E**). In some cases, we also observed up-regulation of a gene set associated with cAMP signaling (**Fig. 2.8E**), which is known to induce MITF expression [103, 104]. These observations suggest that, even in the presence of BRAF^{V600E}, MITF dysregulation can result in maintenance of a high-MITF/low-NF-κB state.

Collectively, these data imply that both MITF-low/NF-κB-high and MITF-high/NF-κB-low cellular states can be established from the same precursor melanocyte through discrete genetic perturbations. They also raise the possibility that a key determinant of transcriptional states

29

associated with resistance versus sensitivity is the balance between, on the one hand, BRAF^{V600E}-mediated MAPK activation and subsequent NF-κB induction, and, on the other, sustained MITF expression.

Figure 2.8. Establishment of two-class dichotomy in melanocytes.
(**a**) Effects of aberrant MAPK pathway activation on whole-genome expression profiles.
(**b**) Effects of aberrant MAPK pathway activation on markers of the MITF-high and NF-κB-high classes; E, VTX11E (ERKi); P, PLX4720 (BRAFi); A, AZD6244 (MEKi), all overnight at 2 μM.
(**c**) Effects of chronic BRAFV600E expression of markers of the MITF-high and NF-κB-high classes. Experiments were performed in TICVA medium (+) or Ham's F10 (-) as indicated.
(**d**) Effect of MITF overexpression on MAPK pathway-induced expression changes.
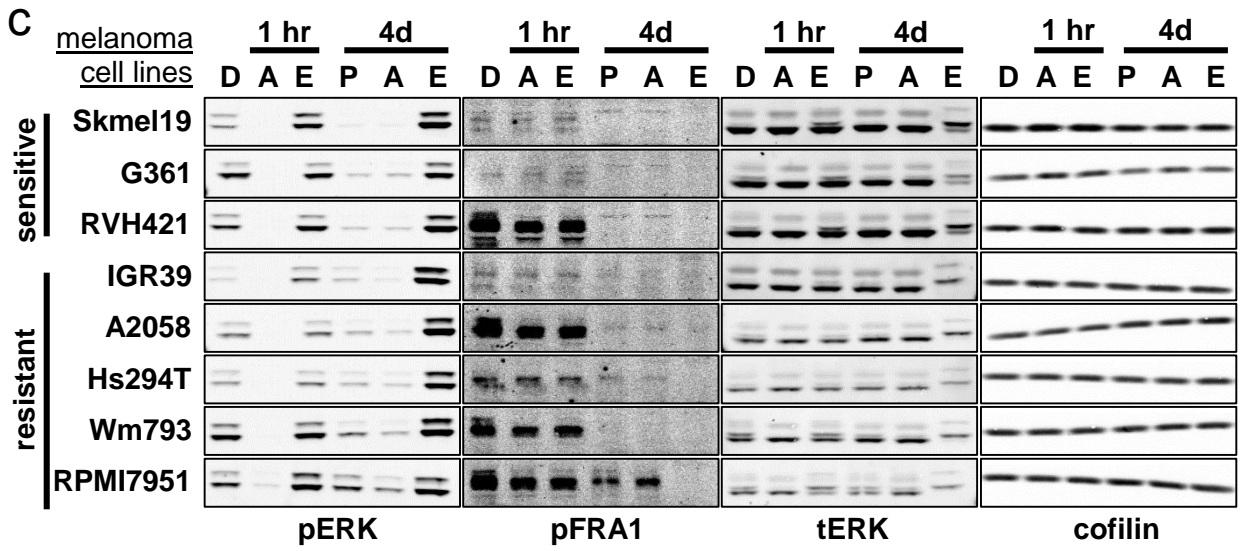(**e**) Relationship between MITF expression levels and MITF amplification.
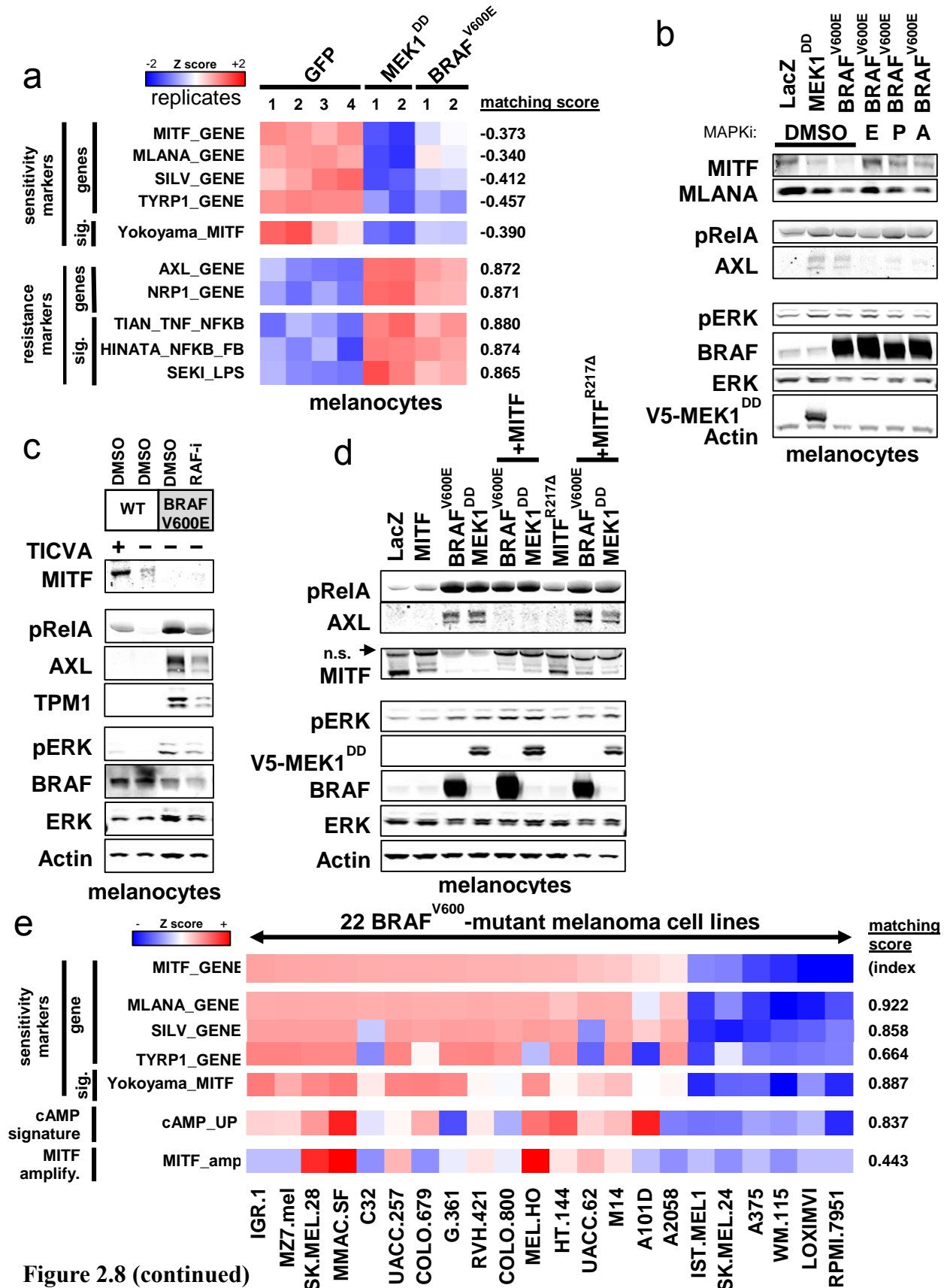
Figure 2.8 (continued)
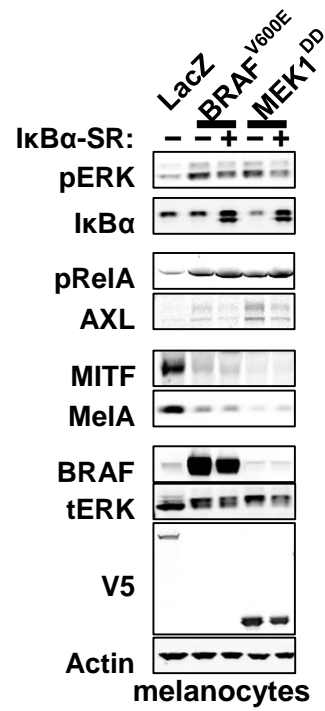
Figure 2.9.
Effect of the IκBα super-repressor on MAPK pathway-mediated AXL induction.

4. <u>Plasticity of two-class dichotomy in melanoma cell lines.</u>

Since MITF and NF-κB can influence the establishment of distinct cell states in melanocytes, we next sought to determine whether these factors could also regulate maintenance of these states in established melanoma cell lines. Therefore, we hypothesized that induction of MITF expression might perturb MITF-low/NF-κB-high cells away from their NF-κB high state. In NF-κB-high/MITF-low cell lines, treatment with cAMP, forskolin, or alpha-melanocyte stimulating hormone (a key regulator of cAMP signaling in melanocytes [104]) induced CREB activity and MITF expression while downregulating markers associated with the NF-κB-high/resistant state (including AXL, NRP1, CDH13, and TPM1). (**Fig. 2.10A, 2.11**) Similarly, ectopic expression of MITF antagonized expression of these markers regardless of MAPK pathway inhibitor treatment (**Fig. 2.10B**).

Conversely, we hypothesized that induction of NF-κB would modulate a cell line from a sensitive, MITF-high state to a resistant, MITF-low state. Consistent with prior work [105], we found that genetic or pharmacological perturbations that activate NF-κB (TNFα stimulus, or expression of IKBKB or TRAF2) also confer resistance to RAF, MEK, RAF+MEK, and ERK inhibition (**Fig. 2.12A**). Although these stimuli robustly activate NF-κB, they do not rescue pERK following RAF inhibitor treatment (**Fig. 2.12B**). Mechanistically, NF-κB activation appears to decrease apoptosis (as measured by Annexin V staining) and cell cycle arrest induced by PLX4720 (**Fig. 2.12C**)—effects consistent with the known role of NF-κB in suppressing apoptosis and driving cell cycle progression. We further predicted that this NF-κB resistance phenotype would be accompanied by a change in transcriptional profile consistent with acquisition of the NF-κB-high/MITF-low state. Indeed, following treatment of sensitive lines with TNFα (an NF-κB agonist), we observed diminished MITF expression and, in some cell

lines, induction of resistance markers including AXL (**Fig. 2.10C, 2.13**), thus linking TNFα-mediated signaling to acquisition of markers of intrinsic resistance. Blockade of NF-κB activity with the IκBα super-repressor abrogated these TNFα-mediated expression changes (**Fig. 2.10C**), confirming the necessity of NF-κB for this effect.

Finally, because MAPK pathway hyperactivation can promote establishment of this high NF-κB/MITF-low state in melanocytes, we wondered whether therapeutic MAPK pathway inhibition in BRAF^{V600}-mutant melanomas would affect maintenance of this state. To test this hypothesis, we cultured four MITF-high, MAPK pathway inhibitor-sensitive melanoma cell lines continuously in PLX4720 until a resistant population emerged (**Fig. 2.14**). Interestingly, resistant clones showed diminished MITF expression (4/4 lines) and gain of AXL expression (2/4 lines, **Fig. 2.10D**). These results suggest that in some contexts, MITF-high/NF-κB-low melanomas can transition towards an NF-κB-high/MITF-low state during acquisition of resistance. These changes were observed even in clones that had also gained other known mechanisms of resistance (**Fig. 2.10D**, e.g., COT expression and p61 BRAF splice variant [90, 92]. This finding implies that transition towards a NF-κB-high/MITF-low state in not mutually exclusive with acquisition of other known resistance effectors—an emerging theme in resistance to targeted therapeutics [106]. Thus, whereas the pre-treatment transcriptional state may influence intrinsic sensitivity to MAPK pathway inhibition, plasticity between states may also contribute to acquired resistance. Cumulatively, these findings demonstrate that, even in melanoma cell lines, the transcriptional states associated with sensitivity and resistance remain plastic; moreover, maintenance of these states in cell lines can be perturbed by the same mediators that govern establishment of these states in melanocytes.

Figure 2.10. Plasticity of two-class dichotomy in melanoma cell lines.
(**a**) Effect of cAMP, forskolin, or αMSH, in combination with IBMX, on expression of MITF and resistance markers.
(**b**) Effect of MITF overexpression on resistance marker expression, in the presence or absence of PLX4720 (2 μM, overnight).
(**c**) Effect of TNFα (25 ng/mL final), with or without concomitant IκBα super-repressor expression, on MITF and resistance markers.
(**d**) Comparison of MITF and AXL expression in parental sensitive and cultured-to-resistant melanoma cell lines, in presence or absence of 2 2 μM PLX4720 (24 hrs). PR1 and PR100 denote independent derivations of a resistant subclone.
(**e**) Model of two-class dichotomy in melanoma.
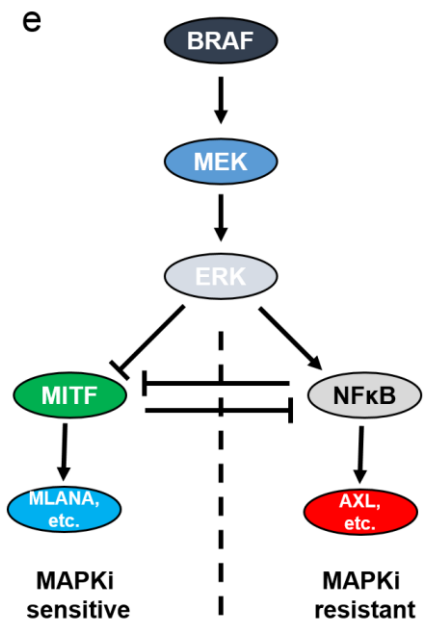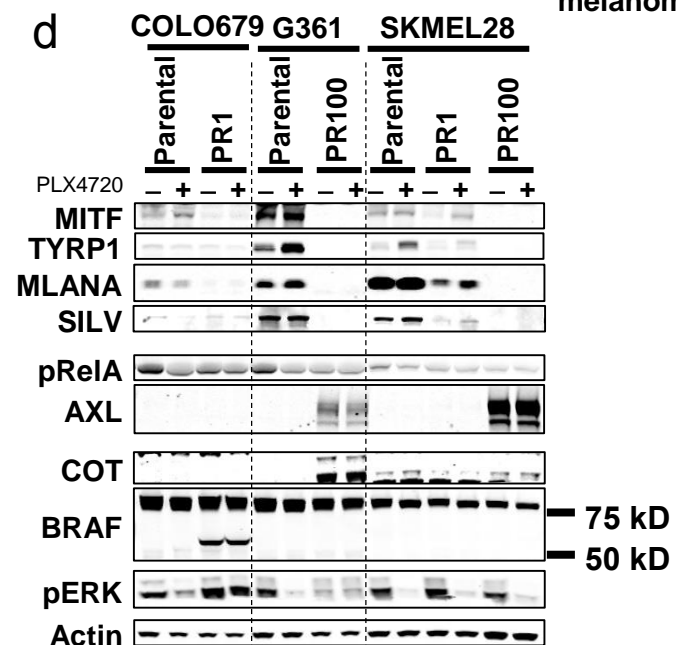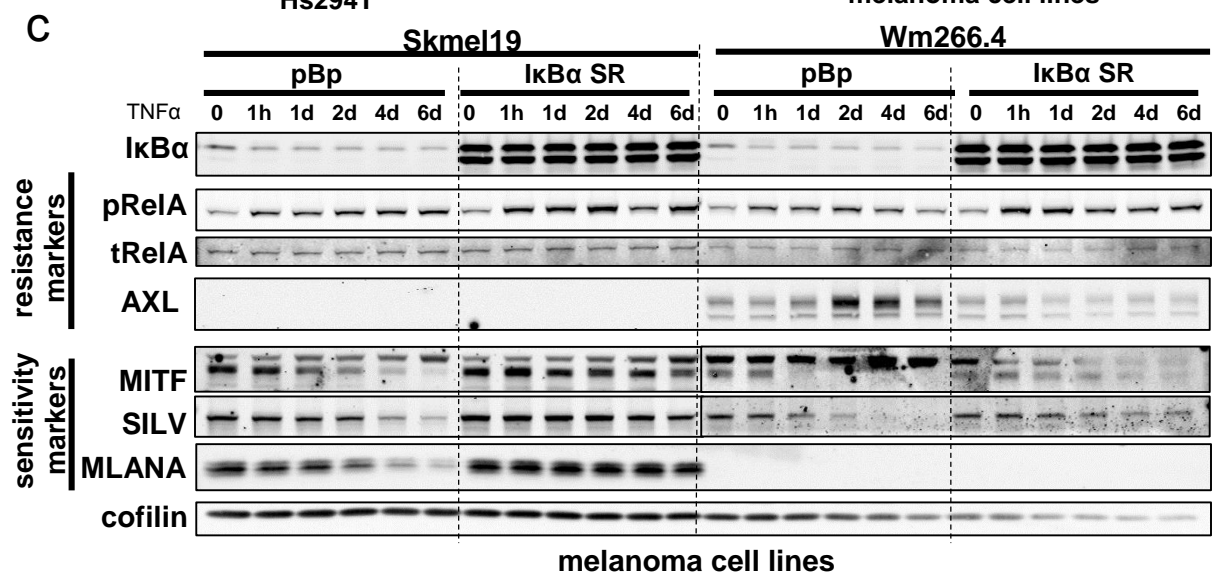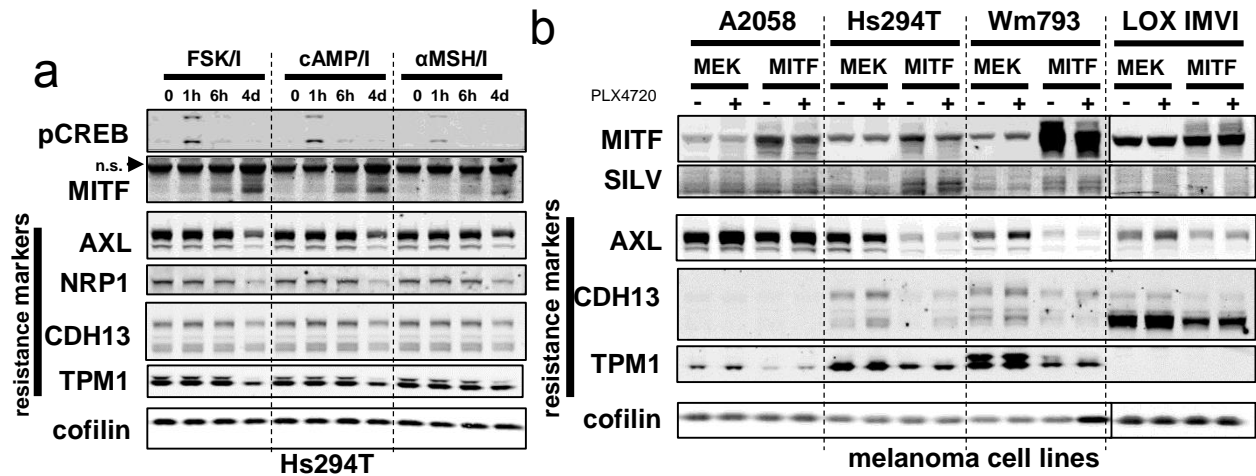
Figure 2.10 (continued)

37
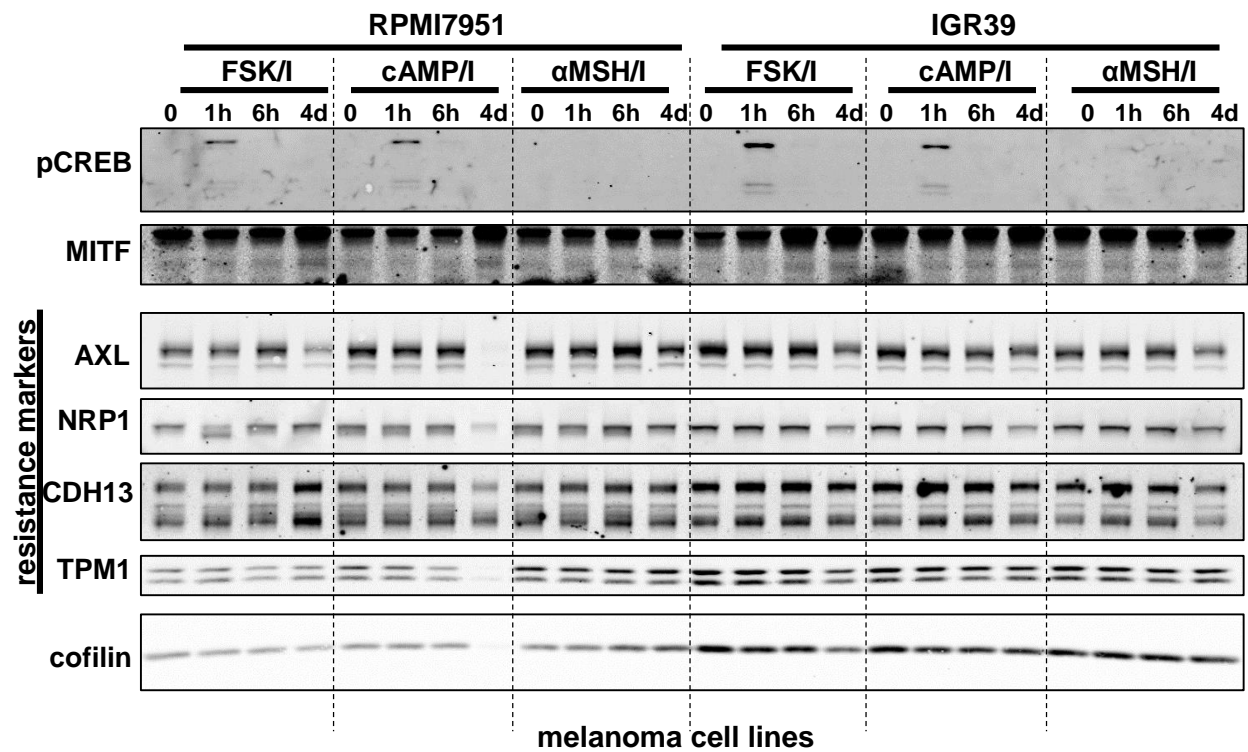
Figure 2.11.
In intrinsically resistant melanoma lines, effect of forskolin, cAMP, and αMSH on expression of MITF, AXL, and other markers of the NF-κB-high/MITF-low state.
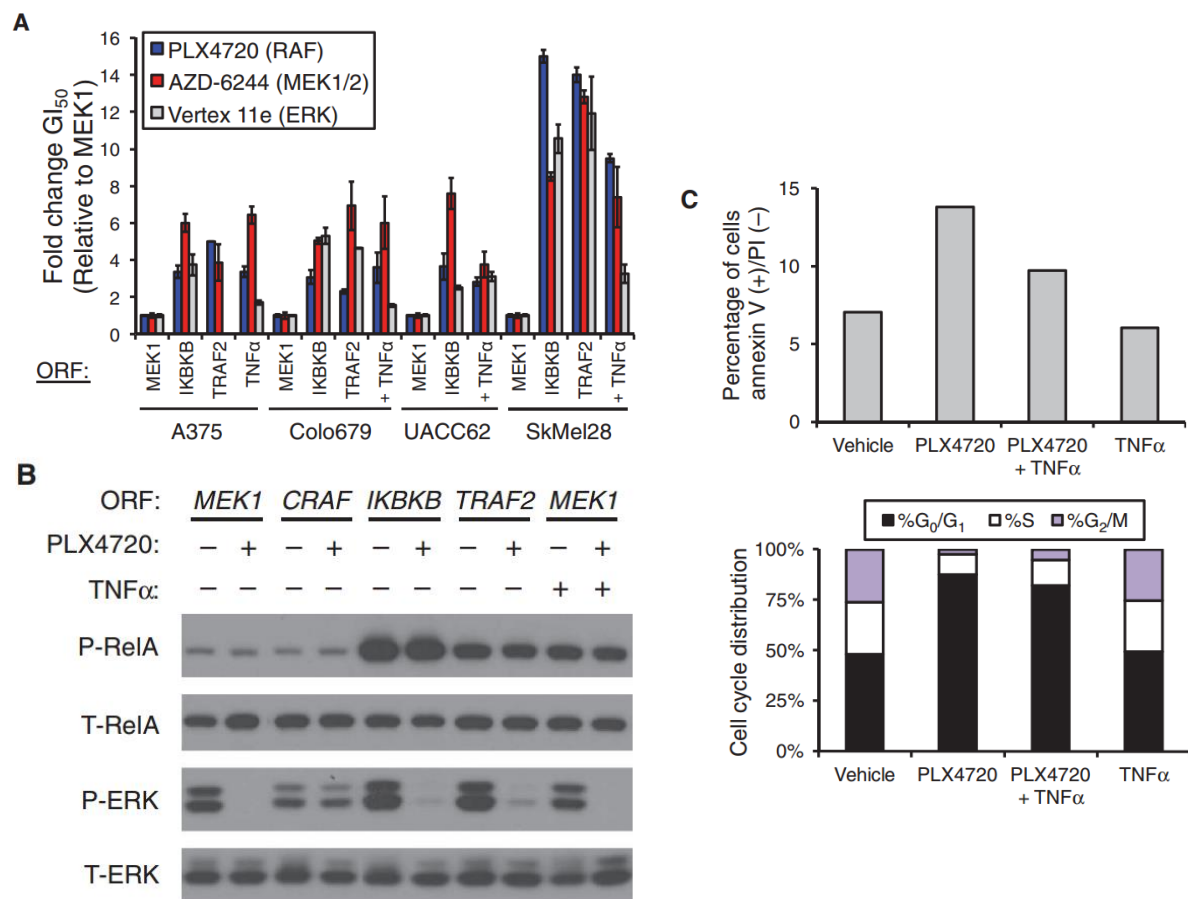
Figure 2.12: **Perturbations activating the NF-κB pathway confer resistance to MAPK pathway inhibition.**
(a) Following expression of the indicated ORFs or stimulus with TNFα (25 ng/mL), GI50 values were calculated for melanoma cells lines following 4d treatment with the indicated MAPK pathway inhibitors. MEK1 is a negative control.
(b) Following the indicated perturbations, cells were assessed for NF-κB pathway activation (as measured by pRelA) and for MAPK pathway activation (as measured by pERK), in the presence or absence of PLX4720. CRAF is a positive control for MAPK pathway re-activation in the presence of PLX4720; MEK1 is a negative control.
(c) Effects of TNFα stimulus on PLX4720-mediated induction of apoptosis (as measured by annexin V (+)/PI (−) staining) and cell cycle arrest. Experiments were conducted in A375 cells.
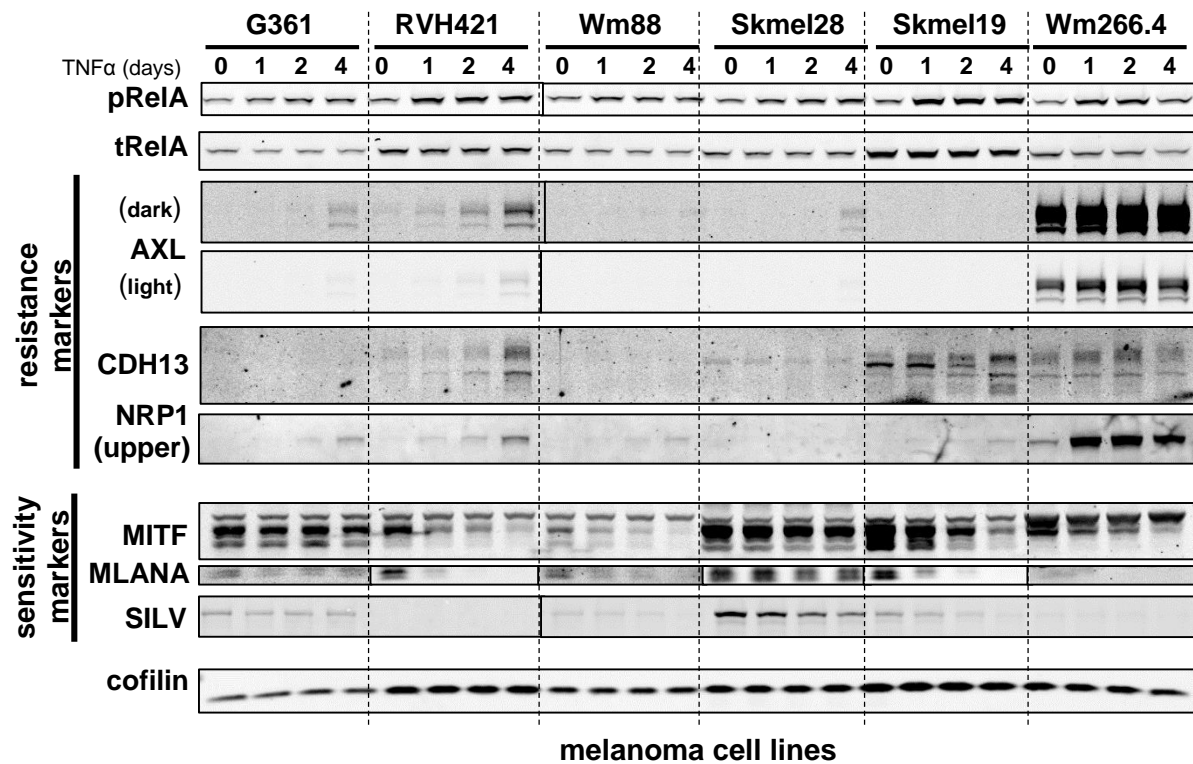
Figure 2.13.
Effect of TNFα (25 ng/mL for indicated time) on expression MITF, MITF target genes, and markers associated with the high-NF-κB/low-MITF class.
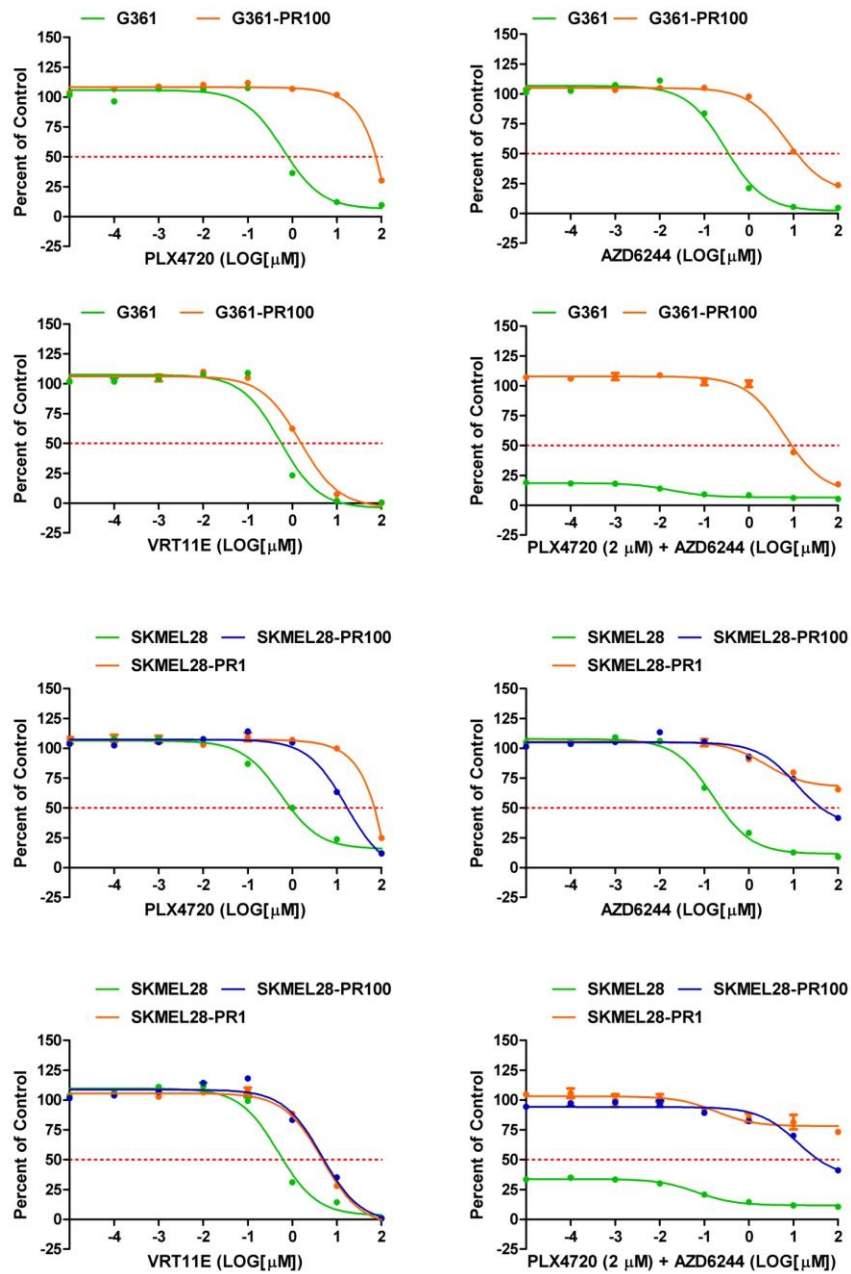
Figure 2.14.
Drug sensitivity characterization of parental and cultured-to-resistant melanoma cell lines.

Discussion and future directions

Cumulatively, the work in this chapter has characterized two cellular states in BRAF^{V600}-mutant melanoma: one characterized by high MITF expression that is sensitive to MAPK pathway inhibition, and another that exhibits low MITF expression, high NF-κB activity, and intrinsic resistance to MAPK pathway inhibition. While this type of transcriptional class distinction has long been recognized in melanoma [101], its possible association with differential response to vemurafenib or dabrafenib/trametinib in BRAF^{V600}-mutant melanoma is novel. The initiation of these states in primary melanocytes can be controlled by the relative balance of aberrant MAPK activation (leading to NF-κB activation) and MITF levels. In melanoma cell lines, these cell states appear to remain plastic in response to perturbations of NF-κB and MITF.

Origin of the low-MITF, high-NF-κB state

These observations raise several fundamental questions worthy of future investigation. First: how does introduction of BRAF^{V600E} into melanocytes induce the low-MITF, high-NF-κB state? We have elucidated certain mechanistic observations that may be pertinent to this process. BRAF^{V600E}, as a constitutively activating mutation, induces aberrant downstream MAPK pathway flux. This altered MAPK flux (rather than some other intrinsic property of mutant BRAF) appears crucial for induction of the low-MITF, high-NF-κB state, because the same phenotype arises when constitutively active MEK (MEK^{DD}) is expressed, and because this transition is attenuated by concomitant treatment with MAPK pathway inhibitors.

One important question is whether the loss of MITF and induction of NF-κB/AXL that we and others[36] have observed following ectopic BRAF^{V600E} expression are artifacts of supra-physiological MAPK pathway flux in this *in vitro* melanocyte model. Conceivably, the natural acquisition of BRAF^{V600E} that occurs in patients might often drive less flux through the MAPK

pathway, permitting maintenance of a MITF-high, NF-κB-low expression phenotype. While we cannot fully exclude this possibility, several lines of evidence suggest that MAPK pathway flux in our experimental system is not abnormally high. First, melanocytes expressing BRAF^{V600E} over a chronic timecourse (8-12 weeks) did not express higher levels of BRAF than BRAF^{WT} parental melanocytes, yet maintained low MITF and robust AXL expression. This observation suggests that even physiological levels of BRAF expression can induce the observed expression changes. Second, melanocytes expressing BRAF^{V600E} over an acute timecourse (3-5 days), although overexpressing BRAF relative to parental cells, displayed pERK levels only moderately above those of parental melanocytes. Thus, at least as measured by pERK, MAPK flux following acute BRAF^{V600E} expression appears to be elevated but not grossly supra-physiological. Moreover, at the level of either pERK or pFRA1, we observe no difference in MAPK pathway activation between sensitive and resistant melanomas, arguing that MAPK pathway flux is not a distinguishing feature between these two classes. Nonetheless, to query more definitively the possibility that differential MAPK pathway flux might contribute to the acquisition of these dichotomous transcriptional states, future investigations could use approaches affording more precise control over BRAF^{V600E} expression levels (e.g., inducible lentiviral systems, or TALEN-mediated genome editing).

Our work shows that, in melanocytes, aberrant MAPK pathway activation (by BRAF^{V600E} or MEK^{DD}) can induce NF-κB pathway activity (as measured by pRelA and gene sets marking NF-κB activation). Furthermore, we have demonstrated in melanoma cell lines that NF-κB activation (e.g., by TNFα) can cause loss of MITF expression. (Abrogation of this effect with the IκBα super-repressor confirms that it requires NF-κB activation.) These findings raise the question of whether NF-κB activation is responsible for loss of MITF expression following

43

acquisition of BRAF^{V600E} in melanocytes. In fact, our data argue that, following BRAF^{V600E} expression, NF-κB activation is not required for loss of MITF, as blockade of the NF-κB pathway with the IκBα super-repressor did not prevent BRAF^{V600E}-mediated loss of MITF expression. This conclusion is consistent with prior evidence that direct phosphorylation of MITF by ERK leads to its proteasomal degradation [107, 108]. Thus, while it is clear that MAPK pathway hyperactivation can cause both activation of NF-κB and loss of MITF expression, it appears that MAPK pathway flux itself rather than subsequent NF-κB induction is the critical factor controlling MITF loss.

The relationship between BRAF^{V600E} and gain of NF-κB activity/resistant state markers also deserves further elucidation. Of note, one such marker, AXL, has been previously characterized as an effector of acquired resistance to MAPK pathway inhibition in BRAF-mutant melanoma. In Chapter 3, we investigate the question of whether AXL, in addition to marking the NF-κB-high state, might also contribute to the phenotype of intrinsic resistance. In melanocytes, BRAF^{V600E} induces NF-κB activation and gain of resistance markers (e.g., AXL) associated with the high NF-κB state. A relevant question is therefore whether NF-κB activation controls acquisition of these resistance markers. Indeed, NF-κB activity is sufficient to induce AXL, as we have shown that NF-κB activation (by TNFα) can induce AXL expression in high-MITF cell lines. Moreover, in melanocytes, co-expression of BRAF^{V600E} with the IκBα super-repressor impaired BRAF^{V600E}-mediated induction of AXL expression, implying that NF-κB transcriptional activity is necessary for maximum AXL induction. However, BRAF^{V600E} induced some AXL expression even in the context of the IκBα super-repressor, suggesting that other, as yet unknown, pathways downstream of MAPK pathway hyperactivation also contribute to the induction of markers of the resistant state. Identifying these other signals transduced secondary

to BRAF^{V600E} is a critical area for future work, since we have shown that induction of this state is a critical determinant of subsequent MAPK pathway inhibitor sensitivity.

Origin of the high-MITF, low-NF-κB state

Given that introduction of BRAF^{V600E} into melanocytes can lead to loss of MITF expression, it may seem surprising that the majority of BRAF^{V600E} melanomas retain MITF expression and low levels of NF-κB activity. At least two potential explanations for this observation may be envisioned. First, it is possible that the majority of BRAF^{V600E} melanomas adaptively dampen MAPK pathway flux following acquisition of BRAF^{V600E} (e.g., by DUSP upregulation or other feedback regulatory mechanisms, [109]). Under this model, melanomas able to moderate the aberrant MAPK pathway flux induced by BRAF^{V600E} might maintain MITF despite acquisition of this mutation. In contrast, those melanomas less able to do so (e.g., because of concomitant loss of negative feedback regulation) would be more likely to lose MITF expression, thus entering the low-MITF/high-NF-κB state. As discussed above, we have to this point not detected any steady-state differences in MAPK pathway flux between the high-MITF and high-NF-κB classes. Nonetheless, explanation remains possible.

An alternative possibility is that many melanocytes may sustain concomitant alterations that preserve an MITF-high/NF-κB-low cellular state despite aberrant MAPK pathway flux following gain of BRAF^{V600E}. Indeed, our data suggests that dysregulation of MITF can impair BRAF^{V600E}-mediated induction of the high-NF-κB state in melanocytes and maintenance of this state in intrinsically resistant cell lines. Moreover, MITF amplification was enriched in the high-MITF cell lines relative to the high-NF-κB cell lines, suggesting that this genomic alteration may explain how some melanomas maintain MITF following acquisition of BRAF^{V600E}. However, MITF amplification is unlikely to be the only—or even the predominant—mechanism by which

45

cells can maintain MITF following introduction of BRAF^{V600E}, as is implied by the fact that most high-MITF BRAF^{V600}-mutant cell lines do not harbor MITF amplification. Further understanding of how BRAF^{V600}-mutant cells maintain MITF expression will be a fruitful area of investigation in light of the importance of MITF expression in determining MAPK pathway inhibitor sensitivity vs. resistance.

While we do not have a complete mechanistic description of why MITF expression marks MAPK pathway dependence, this observation is globally consistent with prior work. In melanocytes, MITF is known to be phosphorylated by the MAPK pathway. While this phosphorylation does decrease MITF protein stability (as previously discussed), it also enhances MITF transcriptional activity.[107] Although BRAF^{V600}-mutant melanoma cells are a notably different cellular context than BRAF^{WT} melanocytes, it appears plausible that MITF marks MAPK pathway inhibitor sensitivity because, in these melanoma cell lines, MITF requires continued MAPK input in order to continue to exert its essential pro-growth, pro-survival oncogenic transcriptional functions.

Mechanistic characterization of the low-MITF, high-NF-κB state

Questions also remain about the high-NF-κB state. For example, if BRAF^{V600E} induces this state in melanocytes, how is it that melanoma cells displaying a similar transcriptional profile demonstrate indifference to MAPK pathway inhibition? In several resistant lines, we have seemingly ruled out the trivial explanation of that resistance is due to inadequate pathway inhibition, as treatment with MAPK pathway inhibitors produces comparable suppression of pERK and pFRA1 in both sensitive and resistant lines. While it remains possible that other markers of MAPK pathway flux would show less inhibition in the resistant lines, data obtained to this point suggest that these lines are fundamentally less dependent on MAPK pathway

activation. In Chapters 3 and 4 we present our efforts to query the role of AXL and COT, respectively, as mechanisms of intrinsic resistance. Even in light of these studies, we still lack a comprehensive mechanistic understanding of why cells in this state are resistant to MAPK pathway inhibitors.

In addition to understanding how MITF-low, NF-κB-high melanomas are resistant to MAPK pathway inhibition, another question involves the effectors of oncogenic transformation operant in this setting. $BRAF^{V600E}$ and MITF amplification are typically considered cooperating oncogenic events. Although $BRAF^{V600E}$ is a melanoma oncogene, it is not individually sufficient for high-efficiency transformation of melanocytes. Rather, it requires cooperation from amplification/overexpression of MITF.[36] Since the high-NF-κB melanomas have $BRAF^{V600}$ mutations but lack MITF, did additional oncogenic alterations (copy number changes, mutations, etc.) contribute to transformation of these cells? To address this question, one could extend the current analyses to query, in an unbiased fashion, what other features—whether mutation, copy number changes, or enrichments of individual genes or signatures—are differentially associated with the intrinsically resistant subtype. Alternatively, one could pursue focused studies to determine whether specific NF-κB effectors (e.g., those induced by $BRAF^{V600E}$ in high-NF-κB/low-MITF lines) can cooperate with $BRAF^{V600E}$ to transform melanocytes. Together, such studies could provide a comprehensive characterization of this alternative cellular state in melanoma, and could nominate additional factors responsible for the initiation and/or maintenance of this state.

Last, it is noteworthy that the transcriptional state observed in the majority of $BRAF^{V600}$-mutant melanomas corresponds to that observed in basal melanocytes (i.e., high MITF and low NF-κB) Therefore, is it possible that the alternative, MITF-low/NF-κB-high state represents an

alternative cellular fate corresponding to a previous developmental state in the natural history of melanocytes or the neural crest? Although highly speculative, this possibility could shed additional light on the transcriptional programs elaborated by this subclass of melanomas.

Therapeutic possibilities in high-NF-κB lines

If most low-MITF/high-NF-κB lines exhibit reduced dependence on MAPK pathway signaling, what treatment strategies might be pursued to kill these melanomas? Here, two conceptual possibilities may be envisioned. On the one hand, the intrinsically resistant lines might in fact retain an underlying dependency on MAPK pathway activation, but that dependency is masked by the expression of one or several resistance effectors. Alternatively, these intrinsically resistant cell lines, despite the presence of $BRAF^{V600E}$, might have no underlying dependency on the MAPK pathway.

In the first case, an interesting strategy could involve searching for perturbations that would render the high NF-κB lines sensitive to MAPK pathway inhibitors. Although not yet comprehensively investigated, this approach has so far proven challenging, as perturbation of individual candidate resistance effectors has not sensitized these lines to MAPK pathway inhibition (cf. COT perturbation in Ch. 3 and AXL perturbation in Ch. 4). This question could also be explored systematically using genome-scale shRNA screens in the presence vs. absence of MAPK pathway inhibitors in one or more intrinsically resistant lines. Of course, it is conceivable that the intrinsic resistance phenotype is multifactorial, meaning that perturbation of single effectors may not exhaustively identify the relevant effectors.

A second approach, particularly appropriate if these lines lack an underlying MAPK pathway dependency, would be to identify novel vulnerabilities through pharmacologic or genetic

screens. Pharmacologically, small molecule screens could identify for novel vulnerabilities in the intrinsically resistant lines. Aside from MAPK pathway inhibitors, we did not note any differential sensitivity or resistance between the two classes of melanoma in the CCLE data set; however, only 26 compounds are currently available for this collection. It is possible, however, that generation of a broader pharmacological profiling dataset across these cell lines (as currently being undertaken by the CTD2 effort at the Broad Institute) might reveal vulnerabilities specific to this class. A complementary approach would be to use shRNA screening data to search for genetic vulnerabilities either shared across all melanomas (regardless of MITF expression) or specific to the low-MITF, high-NF-κB subclass. Indeed, the former approach is detailed in Chapter 5; the latter is planned as part of ongoing systematic shRNA screening efforts at the Broad Institute. Finally, using the computational discovery efforts outline above to identify novel molecular features of the intrinsically resistant melanomas, we may be able to nominate novel candidate dependencies within this subclass.

Conclusion

Together, this work has identified a cell state dichotomy in melanoma as a novel determinant of sensitivity versus resistance to MAPK pathway inhibition. The origin of these states in melanocytes, as well their maintenance in melanoma cell lines, appears to be governed by the balance between MITF and BRAF^{V600E}-induced NF-κB. Although these studies have provided substantial insight, they have also laid the foundation for future questions regarding the mechanistic origin and potential vulnerabilities of these states. These and other questions will provide many fruitful areas of investigation around the starting point described in this chapter.

Methods

Constructs

MEK1, MITF-M, and LacZ were from The RNAi Consortium (Broad Institute). All lentiviral
ORF expression constructs were in vectors pLX304-Blast-V5 or pLX980-Blast-V5. The
retroviral IκBα super-repressor construct has been previously published [61, 110] and was a kind
gift from David Barbie and Jesse Boehm.

Primary melanocytes

Primary melanocytes were grown in TICVA medium (Ham's F-10 (Cellgro), 7% FBS, 1%
penicillin/streptomycin, 2 mM glutamine (Cellgro), 100 µM IBMX, 50 ng ml−1 TPA (12-O-
tetradecanoyl-phorbol-13-acetate), 1 mM 3′,5′-cyclic AMP dibutyrate (dbcAMP; Sigma) and
1 µM sodium vanadate). Following lentiviral introduction of BRAF^{V600E}, cells were switched to
Ham's F10 + 10% FBS.

Melanocyte infections

Following infection, melanocytes chronically expressing BRAF^{V600E} were selected for by
survival in Ham's + 10% FBS (without supplements) as BRAF^{V600E} permits survival in the
absence of TICVA supplements.

Cell culture

All cells were maintained in medium supplemented with 10% FBS (unless otherwise indicated)
and 1% penicillin/streptomycin. The following cell lines were maintained in RPMI-1640: A375,
Colo679, RVH421, Skmel5, Skmel19, Skmel28, UACC62, WM983B, WM793, LOXIMVI, and
all short-term cultures. DMEM: WM88, WM266.4, G361, A2058, Hs294T. MEM: RPMI7951.

DMEM with 15% FBS: IGR39. All cell lines were obtained from in-lab stocks, from ATCC, or from Biological Samples Platform (Broad Institute).

Cultured-to-resistance lines

Colo679, G361, and Skmel28 were serially passaged in PLX4720 until resistance clones emerged. For Skmel28, two separate derivations were performed.

GI50 determination

For drug sensitivity determinations, lines were seeded in 96w format at the following densities:

Cell lines: A375, 3000; Colo679, 8500; Skmel19, 12000; Skmel28, 2000; A2058, 3500; Hs294T, 6000; WM793, 6000; RPMI7951, 4250; IGR39, 3000.

Short-term cultures: Wm1745, 8500; Wm1852, 8500; Wm1930, 8500; Wm1862, 12000; WM1942, 16000; WM1976, 8500; WM3215, 6000; WM3482, 7250; Wm3727, 12000; Wm451Lu, 4500.

The day after plating, if applicable, recombinant human TNFα (CST 8902SC) was added to a final concentration of 25 ng/mL. Cells were then drugged with serial dilutions of indicated inhibitors in medium plus DMSO to give final concentrations ranging from 100 μM to 31.62 nM (PLX4720 and VTX11E) or 31.62 μM to 10 nM (AZD6244), in half-log increments. For combined PLX4720 and AZD6244 treatment, a linear combination of doses was used, starting at 100 μM PLX4720 + 31.62 μM AZD6244. After 4 days of drug treatment, cellular viability was read using CellTiter-Glo and compared to DMSO wells. GI50 calculations were performed in GraphPad Prism; for AZD6244, floor value was set to 0.

Steady-state protein expression

For lysate harvesting, lines were plated in 10 cm dishes at the following densities, to reach equivalent confluence at harvest, and lysed 5 days after plating.

Cell lines: A375, 7.4e5; Colo679, 2.1e6; RVH421, 1e6; Skmel5, 1.5e6; Skmel19, 3e6; Skmel28, 7e5; UACC62, 1.5e6; WM983B, 1.2e6; G361, 2.1e6; Wm88, 1.5e6; Wm266.4, 1.1e6; A2058, 8.61e5; Hs294T, 1.5e6; Wm793, 1.5e6; RPMI7951, 1.1e6; IGR39, 7.4e5; LOXIMVI, 1.3e6.

Short-term cultures: WM1745, 2.1e6; Wm1852, 1.6e6; Wm1930, 2.5e6; WM1862, 3e6; Wm1942, 3.5e6; Wm1976, 2.1e6; Wm3215, 1.5e6; WM3482, 2.1e6; Wm3727, 3e6; Wm451Lu, 1.1e6.

MAPK pathway inhibitor treatment

Cells were seeded in 6-well format at the following densities: RVH421, 1.8e5; Skmel19, 5e5; G361, 3.6e5; A2058, 1.5e5; Hs294T, 2.5e5; WM793, 2.5e5; RPMI7951, 1.8e5; IGR39, 1.25e5.

Forskolin timecourse

Cells were seeded in 12-well plates at the following densities: Hs294T, 1e5; RPMI7951, 7.2e4; IGR39, 5.1e4. The following day, cells were stimulated at the 4 day timepoint with IBMX (100 μM final) plus either forskolin (10 μM final), db-cAMP (1 mM final), or αMSH (1 μM final). Subsequent timepoints were stimulated as indicated.

Ectopic MITF expression

Cells were seeded in 12-well plates at the following densities: A2058, 6.3e4; Hs294T, 1.1e5; Wm793, 1.1e5; LOXIMVI, 1.4e5. The following day, polybrene was added to 4 μg/mL final, 100 μL of the indicated ORF lentivirus was added, and cells were infected 60 minutes at 2250

rpm (1178 x g) at 30 °C. Medium was changed immediately following infection Four days later, medium was changed to fresh medium plus DMSO or 2 μM PLX4720 as indicated.

TNFα timecourse

Cells were seeded in 12-well plates at 7.5e4 cpw, except Skmel19 at 1e5 cpw and treated with TNFα at 25 ng/mL final for the indicated timepoints.

TNFα timecourse with IκBα super-repressor

Cells were seeded in 12w format at 4.1e4 (Skmel19) and 8.1e4 (WM266.4) cpw. The next day, cells were changed to medium plus 4 μg/mL polybrene, then infected with 375 μL retrovirus (60' spin, 2250 rpm (1178 x g), 30 °C). The following morning, cells were changed to fresh medium. In the afternoon, cells were changed again to medium plus 4 μg/mL polybrene, infected again with 375 μL retrovirus. That evening, infection was repeated. The next day, medium was changed to fresh medium plus 1 μg/mL final puromycin, and cells were stimulated for the 6d TNFα timepoint (25 ng/mL final). Subsequent timepoints were stimulated as indicated.

Lysate harvesting

Cells were harvested by washing 1x in PBS, applying sufficient lysis buffer to cover the well (~ 40 uL for 12w plate, ~100 uL for 6w plate, ~250 μL for 10 cm plate), and removing lysis buffer. Plates were not scraped and lysates were not pelleted. Cells were lysed in 1% NP40 buffer (150 mM NaCl, 50 mM Tris pH 7.5, 2 mM EDTA pH 8, 25 mM NaF and 1% NP-40), containing 2x EDTA-free protease inhibitor cocktail (Roche) and 1x phosphatase inhibitors I and II (EMD).

Lysates were quantitated by BCA, normalized, and denatured by boiling in sample buffer plus 20 mM DTT.

Western Blotting

Transfers were on iBlot nitrocellulose membrane using setting P0. Membranes were blocked 1 hour at room temperature in LiCor blocking buffer. Primary antibodies (1:1000 dilution unless otherwise indicated) were incubated overnight at 4°C in LiCor blocking buffer plus 0.1% Tween-20. Secondary antibodies (1:10,000 dilution, LiCor) were incubated at room temperature for 90 minutes in LiCor blocking buffer plus 0.1% Tween-20 and 0.1% SDS. Imaging was on a LiCor Odyssey infrared imager.

Primary antibodies were as follows (CST = Cell Signaling Technology, SCBT = Santa Cruz Biotechnology):

AXL (C44G1, CST 4566; 6C8, Sigma WH0000558M1); MITF (C5, NeoMarkers MS771P, 1:400); SILV (A46. Sigma SAB4100050, 1:500); TYRP1 (G17, SCBT sc-10443, 1:200); MLANA (A103, SCBT, sc-20032, 1:500); pRelA (S536, 93H1, CST 3033); tRelA (L8F6, CST 6956); CDH13 (Sigma SAB1405597, 1:200); NRP1 (D62C6, CST 3725); TPM1 (D12H4, CST 3910); Cofilin (D3F9, CST 5175, 1:20,000); pERK (T202/Y204, D13.14.4E, CST 4370); tERK (L34F12, CST 4696); pFRA1 (S265, D22B1, CST5841); V5 (Invitrogen R960-25) ; BRAF (13, BD Biosciences 612375); pCREB (S133, 87G3, CST 9198); IκBα (L35A5, CST 4814); COT (N17, SCBT sc-1717); pS6 (S235/S236, D57.2.2E, CST 4858); tS6 (54D2, CST 2317)

Gene expression and pharmacological analyses

Gene expression (RMA normalized using ENTREZG v15 CDF), drug sensitivity (IC50 values), and genotyping data for BRAF^{V600}-mutant melanoma cell lines were from the Cancer Cell Line Encyclopedia (CCLE).[100] Pearson correlation coefficients (r) were computed between PLX4720 GI$_{50}$ values and gene expression value. For **Fig. 2.8E**, gene expression, genotyping, and copy number data were from the Wellcome Trust/Sanger COSMIC Cell Lines Project.[111] Gene expression and genotyping data for melanoma short-term cultures (**Fig. 2.3A**) was from Lin et al. [112] and was collapsed to maximum prove value per gene using GSEA Desktop. Genotyping and gene expression data for melanoma tumors in **Fig. 2.1D** was from The Cancer Genome Atlas.

Analysis of CCLE data

The single-sample GSEA enrichment scores used in **Figs. 2.1B, 2.1D, 2.3A, 2.8A, and 2.8E** were obtained as previously described [68, 113]. Briefly, for every gene expression sample profile, the values were first rank-normalized and sorted and then a single-sample enrichment score for each gene set was computed on the basis of the integrated difference between the empirical cumulative distribution functions of the genes in the gene set versus the rest. This procedure is similar to the computation of standard GSEA but is based on absolute rather than differential expression. Published details of this method and other applications are available. [114-116] The full names of gene sets referenced in the text and figures are hinata_nfkb_targets_fibroblast_up ("Hinata_NFKB_FB "), and seki_inflammatory_response_lps_up ("Seki_LPS"), and tian_tnf_signaling_via_nfkb ("Tian_TNF_NFKB"). The "Yokoyama_MITF" signature was derived from Yokoyama et al. [11], Supplementary Tables 5 and 6B (only genes induced/repressed by overexpression of wild-

type MITF were included). Matching scores between index variables other variable were obtained by a normalized and rescaled mutual information estimate.

Briefly, we consider the differential mutual information between two continuous vectors x (target, for example, PLX4720 resistance) and y (feature, for example, an NF-κB gene set): $I(x, y) = \iint P(x, y) \log_2(P(x, y)/(P(x)P(y)))dxdy$ and estimate this quantity with a kernel-density estimate of the joint distribution $P(x,y)$. The discrete data are smoothed with a Gaussian kernel, with width determined by a cross-validation bandwidth estimation at each data point (x_i, y_i), and $P(x,y)$ is found by summing overall densities over a discrete grid (100×100). The resulting estimate of differential mutual information, $I(x,y)$ is then normalized (73, 74) by the joint entropy $H(x,y) = \iint P(x,y) \log_2 P(x,y)dxdy$, to obtain $U(x,y) = I(x,y)/H(x,y)$. Finally, the matching score is obtained by rescaling $U(x, y)$ using the normalized mutual information of x (the target) with itself and adding a "direction" ($\pm$) according to the Pearson correlation $\rho(x, y)$: $S(x, y) = \text{sign}(\rho(x, y))U(x, y)/U(x, x)$. A perfect match (antimatch) corresponds to a score of $+1(-1)$ and a random match to 0. This matching score $S(x, y)$ has advantages over other metrics including increased sensitivity to nonlinear associations and wider dynamic range at the top of the matching scale.

ICC

Five days after seeding in 15 cm plates, cells were rinsed once in cold PBS, scraped in PBS on ice, and pelleted at 1000 x g. Pellets were subsequently formalin-fixed, paraffin-embedded, and processed as below.

Immunohistochemistry

4 µM sections of formalin-fixed, paraffin-embedded specimens were heated at 60°C, deparaffinized in xylene, and hydrated in a series of ethanol dilutions. Epitope retrieval was by microwaving (5 min full power, 15 min reduced power) in 10 mM Tris-EDTA buffer pH 9.0. Slides were blocked 10 minutes in 3% BSA in TBST (Tris pH 7.6 + 0.05% Tween-20). Primary antibodies were as follows: MITF, 1:100 in 3% BSA in TBST, clone D5 (Dako M3621); AXL, 1:100 in 3% BSA in TBST, clone C89E7 (Cell Signaling Technologies 8661). Slides underwent 10 min peroxidase block in 3% H_2O_2. Secondary antibodies were: Goat anti-mouse IgG-HRP (BioRad 170-6516, 1:200 in 3% BSA in TBST; Dako EnVision anti-rabbit (K4003) ready-to-use. Slides were developed with DAB+ (Dako K3468) for 10 min, and counterstained 1 min with hematoxylin (Vector H-3401), prior to dehydration and mounting. Slides were scored for intensity and distribution of AXL and MITF by a dermatopathologist blinded to clinical outcome.

Analysis of cell cycle and apoptosis

Cells were seeded into 10-cm dishes on day 0; treated as indicated with PLX4720 (1 mM), TNFα (25 ng/ml), or vehicle on day 1; and analyzed on day 3. For analysis of cell cycle distributions, cells were fixed with 80% ethanol in water and stained with propidium iodide (PI) (50 mg/ml; BD Pharmingen) containing ribonuclease A (0.1 mg/ml) and 0.05% Triton X-100. For the analysis of annexin V staining, cells were suspended in annexin V binding buffer (10 mM Hepes, 140 mM NaCl, and 2.5 mM $CaCl_2$, pH 7.4) containing annexin V−APC (allophycocyanin) (BD Pharmingen) and PI (50 mg/ml). For both analyses, a minimum of 50,000 events were counted per sample. Cell cycle data were analyzed with ModFit software. Annexin V staining was analyzed with FlowJo software, with annexin V−positive cells defined as those exhibiting annexin V staining intensities exceeding 99.9% of cells in a PI-only control sample.

CHAPTER 3. PERTURBING INTRINSIC MAPK PATHWAY INHIBITOR RESISTANCE: INVESTIGATING AXL AS A CANDIDATE MECHANISM

Abstract

In previous work, we characterized a gene expression signature associated with intrinsic resistance to MAPK pathway inhibitors in BRAF^{V600}-mutant melanoma. We further sought to understand whether any genes within this resistance signature, in addition to being markers of resistance, were also required for maintenance of intrinsic resistance. To nominate such candidate effectors of intrinsic resistance, we intersected our resistance marker gene signature with a validated, near-genome scale list of ORFs sufficient to confer MAPK inhibitor resistance in BRAF^{V600}-mutant melanoma. Only one gene was present in both lists: the receptor tyrosine kinase AXL. AXL was sufficient to confer resistance to inhibition of RAF and MEK (singly or in combination), although cells generally remained sensitive to ERK inhibition. Nonetheless, shRNA knockdown of AXL, and small molecule inhibition of AXL, did not alter MAPK pathway signaling at baseline or following RAF inhibitor treatment, nor did these perturbations reproducibly sensitize intrinsically resistant cells to RAF inhibition. Thus, while AXL is both a marker of intrinsic resistance and sufficient to confer acquired resistance, it is not required for maintenance of the intrinsically resistant state. Nonetheless, these findings suggest that the systematic intersection of gene expression data and the results of genome-scale functional screens may nominate high-priority candidate mediators of drug-resistance phenotypes.

Attributions

All experiments and analyses were performed by David Konieczkowski except as follows:

ORF screens described in **Fig. 3.1** were performed by Cory Johannessen.

Introduction

<u>Background</u>

In the previous chapter, we used gene expression and pharmacologic data to distinguish

BRAF^{V600}-mutant melanoma into two classes: one, with high MITF expression, that was

sensitive to MAPK pathway inhibition, and one with low MITF expression but high NF-κB

activity and expression of other marker genes, that was resistant to MAPK pathway inhibition.

In light of the significant expression differences between the MAPK pathway inhibitor sensitive

and MAPK pathway inhibitor resistant classes, we sought to understand which if any of the

genes overexpressed in the high-NF-κB class might contribute to the phenotype of intrinsic

resistance.

<u>A systematic approach to nominating candidate resistance effectors</u>

In answering this question, we sought to develop an unbiased approach to identifying candidate

mediators of intrinsic resistance to targeted therapeutics. We reasoned that such putative

resistance mediators might be both (1) overexpressed in intrinsically resistant relative to sensitive

cell lines, and (2) individually sufficient to alter drug sensitivity. For a given cancer lineage,

genetic background, and targeted therapeutic intervention (e.g., MAPK pathway inhibition in

BRAF^{V600}-mutant melanoma), such an approach would require two datasets: (1) basal gene

expression and pharmacologic sensitivity profiling across a panel of intrinsically sensitive and

resistant lines and (2) functional genomic screening data for genes able to modify drug

sensitivity/resistance phenotypes. While expression profiling can identify genes associated with

intrinsic resistance or sensitivity, functional screening can identify which if any of those

candidates are necessary or sufficient to effect the phenotype of interest. The intersection of

these datasets, therefore, would nominate high-priority candidate mediators of intrinsic resistance.

Results

1. <u>Intersection of ORF screens and expression profiles identify AXL as a candidate effector of intrinsic MAPK pathway inhibitor resistance.</u>

To comprehensively query what potential effectors of resistance were differentially expressed in $BRAF^{V600}$-mutant melanomas intrinsically resistant to MAPK pathway inhibition, we used two data sources. First, building on prior kinome-scale screening efforts to identify mediators of MAPK pathway inhibitor resistance [92], our lab has recently completed a near-genome-scale screen for human open reading frames (ORFs) sufficient to confer resistance to MAPK pathway inhibition in $BRAF^{V600}$-mutant melanoma (C. Johannessen, unpublished). This screen encompasses ~13,000 ORFs; although not fully comprehensive, it provides a broad survey of effectors sufficient to confer MAPK pathway inhibitor resistance in melanoma.

Second, as a comprehensive query of single genes whose expression was associated with intrinsic resistance, we used the Cancer Cell Line Encyclopedia dataset, as described in Chapter 2. For this analysis, we considered a panel of 29 $BRAF^{V600}$-mutant melanoma cell lines for which both gene expression profiles and pharmacological sensitivity data was available. We calculated the correlation coefficient (r) between the expression levels of each gene and the measured PLX4720 GI50 concentration across the cell line panel. As a result, genes with higher expression in lines intrinsically resistant to PLX4720 had positive correlation coefficients; genes with lower expression in intrinsically resistant lines had negative correlation coefficients.

Intersecting these two data sources (**Fig. 3.1**) yielded a total of 11,334 ORFs that could be subjected to our integrated analysis (e.g., they contained both ORF screening results and gene expression profiling annotation across the panel). In secondary functional assays performed in the Garraway lab, 107/11334 ORFs were validated to confer MAPK pathway inhibitor resistance with a z score > 4.0. Conversely, 77/11334 tested genes displayed strong (r>0.6) correlation with PLX4720 GI_{50}, meaning that they were overexpressed in PLX4720 resistant lines relative to sensitive lines. Intersecting those lists, we found that only one gene, the receptor tyrosine kinase AXL, was common to both categories. This finding led us to hypothesize that AXL might be an effector of innate resistance to MAPK pathway inhibitors in $BRAF^{V600}$-mutant melanoma cells.
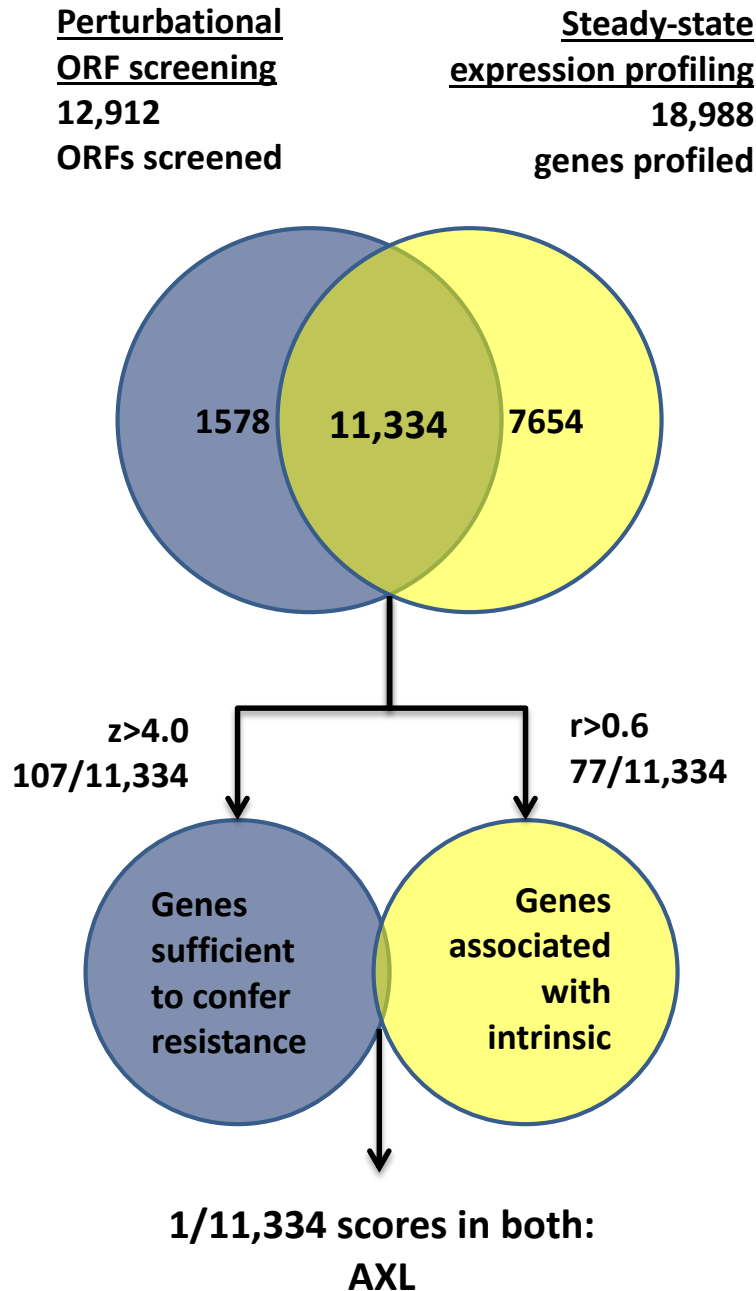
Figure 3.1: **Intersection of ORF screens and expression profiles identify AXL as a candidate effector of intrinsic MAPK pathway inhibitor resistance.**
Left: 12,912 human ORFs were screened in A375 for ability to confer resistance to MAPK pathway inhibition. 107 ORFs subsequently validated with z score >4.0.
Right: Expression of 18,988 genes was profiled in the Cancer Cell Line Encyclopedia across a collection of BRAF_V600-mutant melanoma cell lines for correlation between gene expression and intrinsic MAPK pathway inhibitor resistance. 77 genes were correlated with r>0.6.
Bottom: Of the 107 candidate resistance ORFs and 77 genes associated with intrinsic resistance, only one, AXL, was present in both lists.

2. <u>Overexpression of AXL confers resistance to RAF, MEK, and RAF+MEK, but not ERK, inhibition</u>

Next, we validated the ability of AXL to confer resistance to a spectrum of MAPK pathway inhibitors. (Expression of AXL in the resistant class was described in the previous chapter.) We lentivirally expressed AXL in three cell lines (A375, Skmel28, UACC62) and treated them with inhibitors of RAF (PLX4720, 2 μM), MEK (AZD6244, 200 nM), RAF and MEK in combination, or ERK (VTX11E, 2 μM). Growth was then assessed after 4 days drug treatment. MEK1 was used as a negative control; RAF1 was used as a positive control for MEK-dependent RAF inhibitor rescue; MITF was used as a positive control for MAPK-independent rescue. Consistent with the screening identification of AXL, we found that AXL was able to confer resistance to RAF, MEK, and RAF+MEK inhibition. (**Fig. 3.2**) Notably, AXL did not confer robust ERK inhibitor resistance, a finding that stands in contrast to the ERK inhibitor resistance observed in MAPK pathway inhibitor resistant cell lines. Nonetheless, these validation assays confirm the screening phenotype that AXL is sufficient to confer resistance to RAF and MEK inhibition.
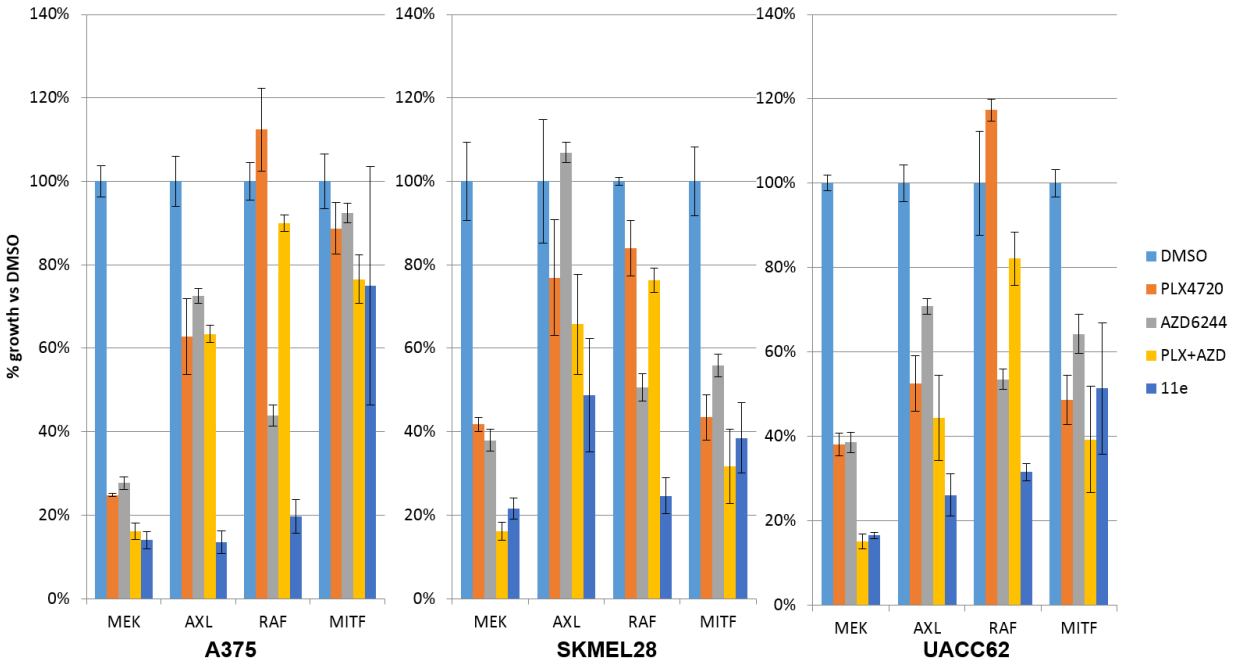
Figure 3.2: **Overexpression of AXL confers resistance to RAF, MEK, and RAF+MEK, but not ERK, inhibition.**
Following expression of indicated ORFs, viability was measured after 4 days of treatment with 2 μM PLX4720 (RAFi), 200 nM AZD6244 (MEKi), 2 μM PLX4720 + 200 nM AZD6244, or 2 μM 11e (ERKi). MEK is a negative control; RAF is a positive control for MAPK-dependent rescue; MITF is a positive control for MAPK-independent rescue.

3. Overexpression of AXL confers Akt activation and rescue of pERK following MAPK pathway inhibitor treatment.

To elucidate the mechanism of AXL-mediated resistance to MAPKi, we overexpressed AXL in sensitive cell lines (**Fig. 3.3**; MEK is a negative control, RAF1 a positive control for MAPK pathway reactivation in the presence of RAF inhibition). We observed that AXL has little effect on ERK phosphorylation at baseline; however, upon treatment with RAF, MEK, or RAF+MEK inhibitors, AXL expression preserved both ERK phosphorylation and Cyclin D1 expression. The strength of pERK rescue was comparable to that effected by RAF1 following PLX4720 treatment. (Enhanced ERK phosphorylation following ERK inhibition is a putative feedback effect we have commonly observed.) We also noted that AXL expression induces Akt phosphorylation, which is further augmented by MAPK pathway inhibitor treatment. Unlike pERK reactivation, Akt activation is not commonly observed following expression of resistance effectors (e.g., no increase in pAkt following RAF1 expression, right lanes), although there is some evidence that PI3 kinase pathway dysregulation may promote melanoma cell survival following RAF inhibition *in vivo* [117]. Thus, ectopic AXL expression conferred two distinct phenotypes: activation of Akt, and rescue of ERK phosphorylation following MAPK pathway inhibitor treatment.
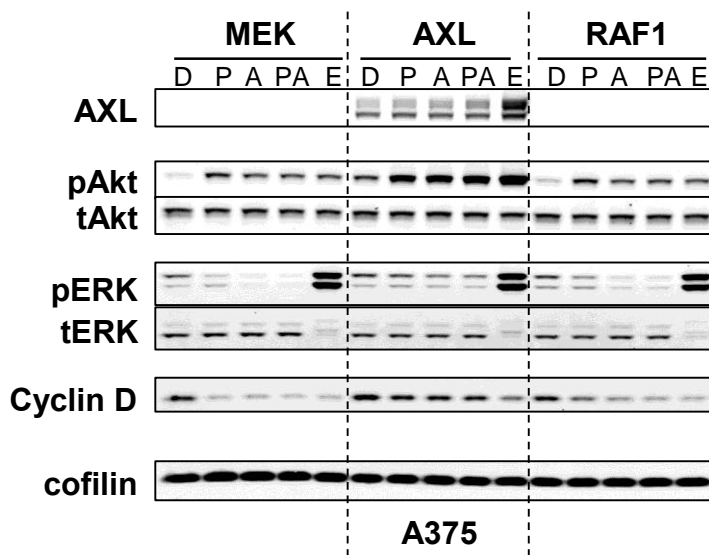
Figure 3.3: **Overexpression of AXL confers Akt activation and rescue of pERK following MAPK pathway inhibitor treatment.**
Following expression of indicated ORFs in A375 cells, lysates were harvested following overnight treatment with 2 μM PLX4720 (RAFi), 200 nM AZD6244 (MEKi), 2 μM PLX4720 + 200 nM AZD6244, or 2 μM 11e (ERKi). MEK is a negative control; RAF is a positive control for MAPK pathway reactivation.

4. Stimulation with AXL ligand GAS6 confers Akt activation and, upon MAPK inhibitor treatment, rescue of ERK phosphorylation.

To confirm that pAkt induction and pERK rescue are not artifacts of ectopic AXL overexpression, we also assessed whether endogenous AXL could mediate these responses. We used A375, a MAPK pathway inhibitor sensitive cell line that, unusually, expresses AXL (but not it ligand, GAS6 ligand (thus, AXL is inactive in these cells at baseline). Upon stimulation with recombinant GAS6 (1000 ng/mL), we observed induction of pAkt, which was further potentiated by the RAF inhibitor PLX4720. We also observed an increase in pERK following GAS6 stimulus (DMSO wells). Moreover, in the context of PLX4720 treatment, GAS6 effected a complete rescue of pERK levels. (**Fig. 3.4**). Whereas AXL overexpression produced sustained pAkt phosphorylation, GAS6 stimulus caused transient pAkt activation and pERK rescue; the levels returned to baseline within 2 hrs. after stimulus. At later timepoints, AXL expression levels also decreased, an observation consistent with stimulus-dependent receptor internalization and degradation. Although the kinetics differed between ectopic AXL expression and GAS6 ligand exposure, these experiments confirm that endogenous AXL is able to mediate activation of both Akt and ERK.
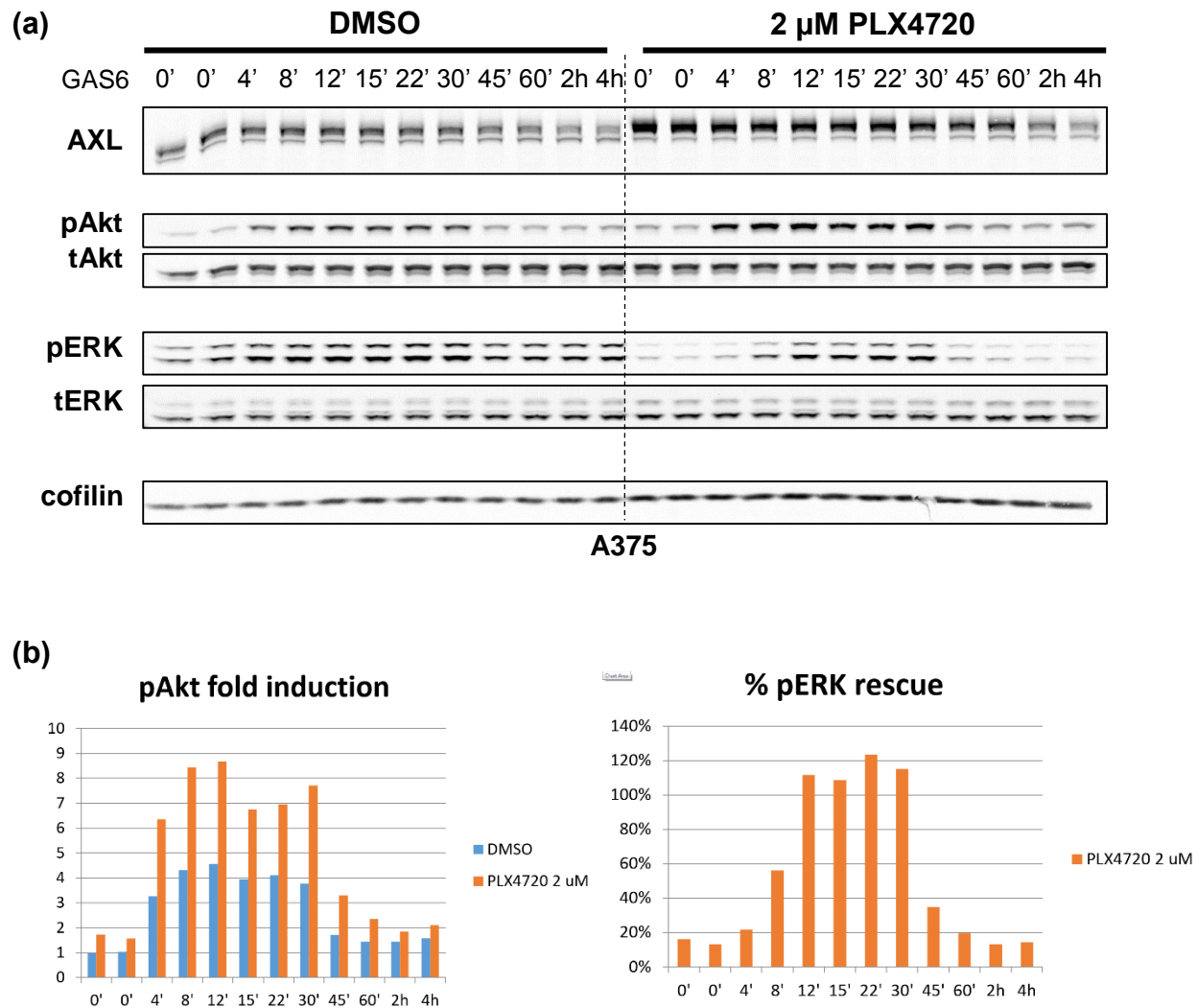
Figure 3.4: **Stimulation with AXL ligand GAS6 confers Akt activation and, upon MAPK pathway inhibitor treatment, rescue of ERK phosphorylation.**
A375 cells, endogenously expressing AXL, were stimulated with the AXL ligand GAS6 (1000 ng/mL) for the indicated length of time before harvest. **(a)** Western blot. **(b)** quantification of Western blot.

5. Re-activation of pERK, but not activation of Akt, confers resistance to MAPK pathway inhibitors.

Prior experiments demonstrated that AXL can activate both MAPK and Akt pathways. MAPK pathway reactivation is a known mechanism of resistance to RAF/MEK inhibition. We sought to query whether Akt activation could also contribute to the observed AXL-mediated resistance. To this end, we expressed MEK1^{WT} (negative control), constitutively active MEK1 (MEK1^{DD}) or KRAS^{G12V} (positive controls), or constitutively active myristoylated Akt. By western blot, we confirmed that myrAkt displayed robust Akt phosphorylation (**Fig. 3.5A**). We then assessed the effects of each construct on MAPK pathway inhibitor resistance (**Fig. 3.5B**). We found that, unlike MEK1^{DD} and KRAS^{G12V}, myrAkt conferred no resistance to any tested inhibitor. While this finding does not rule out the possible contribution of Akt in enhancing resistance mediated by other pathways, it does argue that Akt activation is not individually sufficient *in vitro* to confer resistance to MAPK pathway inhibition. This conclusion is also consistent with the enhanced Akt phosphorylation seen after MAPK pathway inhibitor treatment; if pAkt were sufficient to cause resistance, it would be unclear why cells that experienced high pAkt following drug treatment would still be sensitive to drug. We therefore conclude that AXL mediates resistance to MAPK pathway inhibitors via re-activation of ERK phosphorylation.
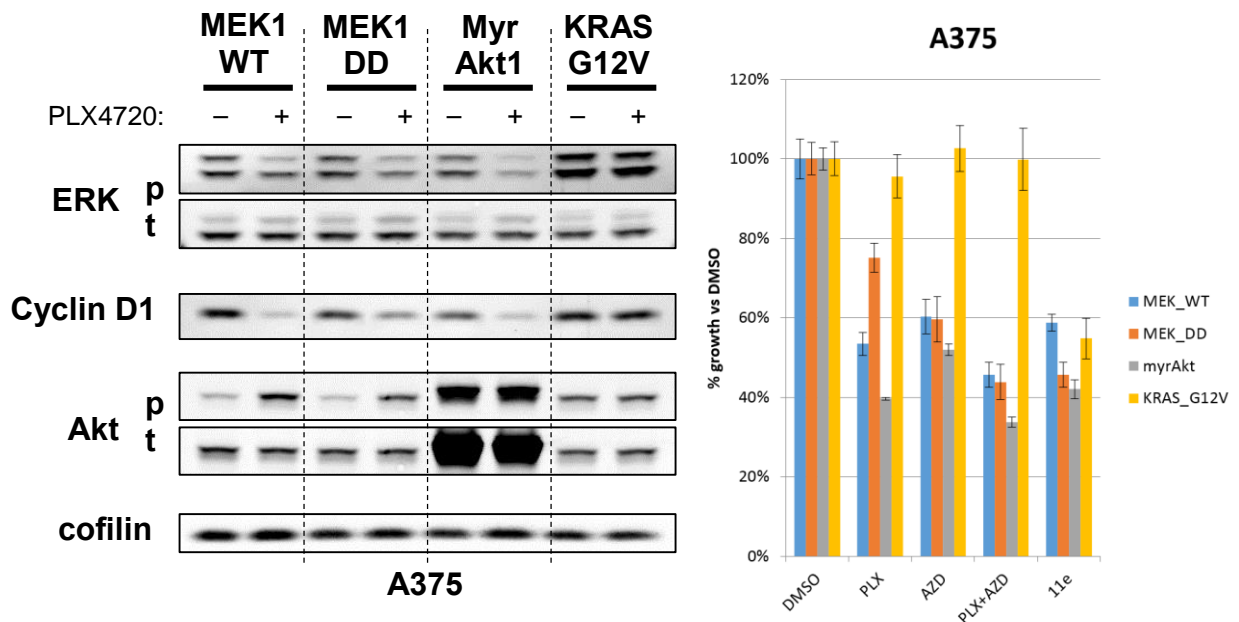
Figure 3.5: **Re-activation of pERK, but not activation of Akt, confers resistance to MAPK pathway inhibitors.**

(a) A375 cells expressing MEK1 (negative control), MEK1^{DD} (control for MAPK re-activation without Akt activation), myrisoylated Akt (control for Akt activation without MAPK re-activation), or KRAS^{G12V} (control for MAPK re-activation and Akt activation) were treated overnight with 2 μM PLX4720.

(b) In parallel, effects of constructs in (a) on viability in the presence of indicated MAPK inhibitors was assessed after 4d drug treatment. PLX = 2 μM PLX4720 (RAFi); AZD = 200 nM AZD6244 (MEKi), 11e = 2 μM VTX11E (ERKi).

70

6. <u>In intrinsically resistant cell lines, AXL knockdown does not alter pERK signaling at baseline or following RAF inhibitor treatment.</u>

Having established the sufficiency of AXL to effect resistance to RAF/MEK inhibition, we next asked whether AXL expression was necessary for maintenance of intrinsic resistance. To do so, we leveraged both shRNA knockdown and small molecule AXL inhibition. First, we noted that despite robust knockdown, AXL shRNAs did not alter ERK phosphorylation either at baseline, or following PLX4720 treatment (**Fig. 3.6**). Although we cannot exclude the possibility that residual AXL expression following knockdown continues to mediate ERK signaling in these cells, the highly efficient knockdown suggests that this explanation is unlikely. Rather, this finding suggests that, although overexpressed AXL is sufficient to reactivate the MAPK pathway, endogenous AXL may not directly influence MAPK pathway signaling levels at baseline or in the context of RAF inhibition.

Figure 3.6: **In intrinsically resistant cell lines, AXL knockdown does not alter pERK signaling at baseline or following RAF inhibitor treatment.**
Indicated cell lines were infected with indicated shRNAs targeting AXL or control hairpin, selected, and treated overnight with or without 2 μM PLX4720 (RAFi). Effects on MAPK signaling were assessed by Western blot.

7. <u>In intrinsically resistant cell lines, AXL knockdown does not reproducibly sensitize to RAF inhibition.</u>

Next, we queried whether AXL knockdown could re-sensitize intrinsically resistant cells to MAPK pathway inhibition. Following infection with either control or AXL shRNAs, cells were re-seeded for pharmacologic growth inhibition assays (**Fig. 3.7**). One shRNA targeting AXL (shAXL.575) did confer a left shift in GI50 in some lines (RPMI7951 and Wm793), indicating sensitization. However, this shRNA had a more modest in other intrinsically resistant lines (Hs294T and IGR39). Moreover, this shRNA also shifted the GI50 value for the negative control sensitive cell line tested (A375). Finally, this effect was not phenocopied in any line by a second shRNA displaying almost equivalent knockdown (shAXL.5353). In aggregate, these findings suggest that AXL knockdown may have minimal effects on sensitivity to RAF inhibition and raise the possibility that left-shift observed with shAXL.575 in some cell lines was an off-target effect.
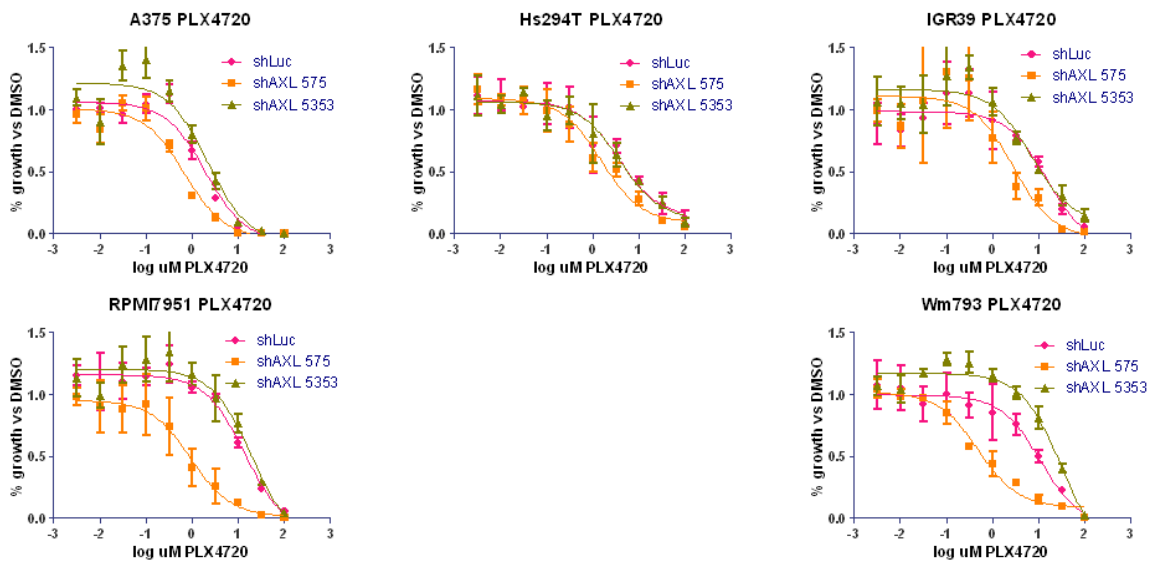
Figure 3.7: **AXL knockdown does not reproducibly sensitize intrinsically resistant lines to RAF inhibition.**
Indicated cell lines were infected with indicated shRNAs targeting AXL or control hairpin, selected, reseeded, and viability measured following 4 days of PLX4720 20 treatment at the indicated doses.

8. Following ectopic AXL expression, AXL inhibitors abrogate AXL-mediated pAkt induction and pERK rescue.

To determine if pharmacologic inhibition of AXL might sensitize intrinsically resistant melanoma cells to RAF/MEK inhibition, we used three small-molecule AXL inhibitors: R428, XL184, and XL880. Here, we used drug concentrations that achieved maximum inhibition of phosphorylation of ectopic AXL while minimizing cellular toxicity (data not shown). To confirm the efficacy of the selected doses, we overexpressed either MEK1 (negative control) or AXL in A375 and treated cells with each AXL inhibitor alone or in combination with PLX4720. As expected, we saw that ectopic AXL expression led to AXL autophosphorylation, increased basal Akt phosphorylation, and rescued pERK and Cyclin D1 levels following PLX4720 treatment. However, co-treatment with the AXL inhibitors at the optimized doses diminished or abrogated AXL autophosphorylation, induction of pAkt, and rescue of pERK and Cyclin D1 levels following RAF inhibitor treatment (**Fig. 3.8**). These effects were similar to those observed following concomitant knockdown of overexpressed AXL (right lanes). Thus, the AXL inhibitors restored signaling, both at baseline and following RAF inhibition, to that observed in the MEK1-expressing negative controls (left lanes). We therefore concluded that these AXL inhibitors, at the concentrations tested, are effective loss-of-function reagents for AXL.
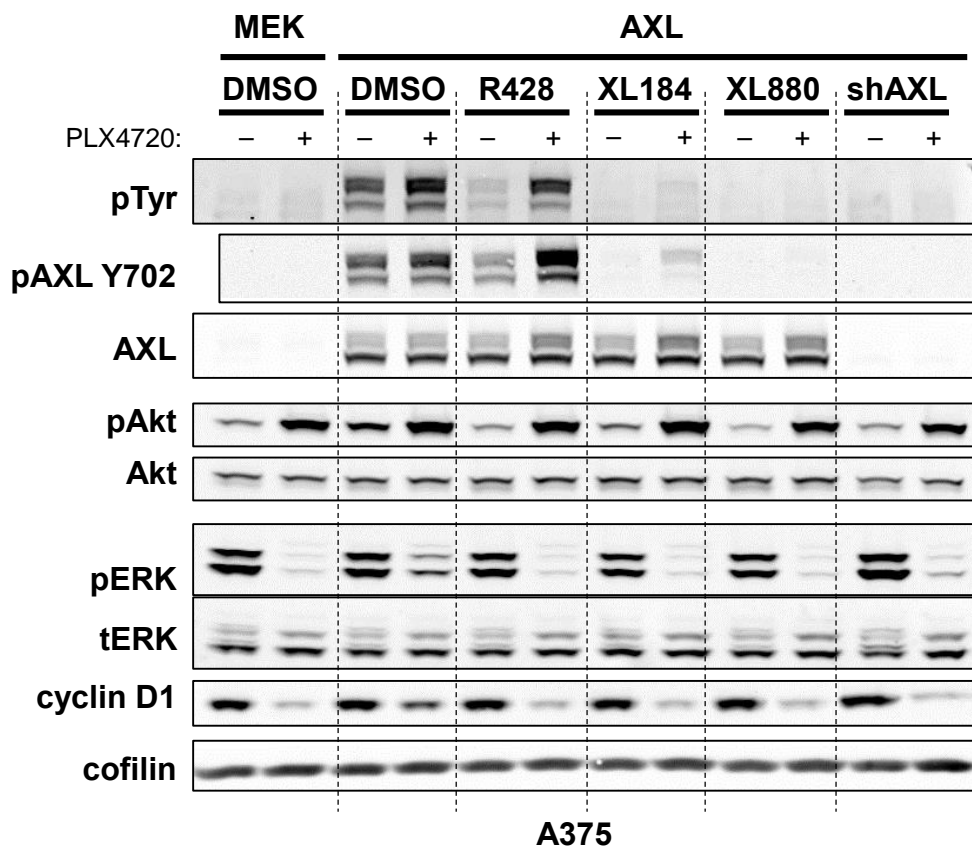
Figure 3.8: **Following ectopic AXL expression, AXL inhibitors abrogate AXL-mediated pAkt induction and pERK rescue.**
Following expression of indicated ORFs (MEK = negative control), A375 cells were treated with AXL inhibitors R428 (500 nM), XL184 (3 µM), or XL880 (100 nM), in the presence or absence of 2 µM PLX4720 (RAFi). Effects of the AXL inhibitors on AXL-mediated pAkt induction and pERK rescue were assessed by Western blot.

9. <u>In intrinsically resistant lines, AXL inhibitors do not alter pAkt or pERK levels at baseline or following RAF inhibitor treatment.</u>

Having validated the utility of small molecule AXL inhibitors for pharmacologic blockade of AXL function, we then queried their signaling effects on cell lines endogenously expressing AXL. In three intrinsically resistant lines (Hs294T, RPMI7951, and IGR39), we found that treatment with the AXL inhibitors had no effect on basal ERK phosphorylation, residual pERK levels following PLX4720 treatment, or pAkt levels (**Fig. 3.9**). Because basal AXL autophosphorylation was not detectable in these cells, we cannot exclude the possibility that these inhibitors are not effectually inhibiting putative signaling from endogenous AXL. Nonetheless, finding is consistent with the lack of effect of AXL shRNAs on these signaling mediators. Cumulatively, this loss-of-function evidence suggests that, in intrinsically resistant lines, AXL signaling does not contribute substantially to basal pAkt levels, pERK levels, or residual pERK levels following RAF inhibitor treatment.
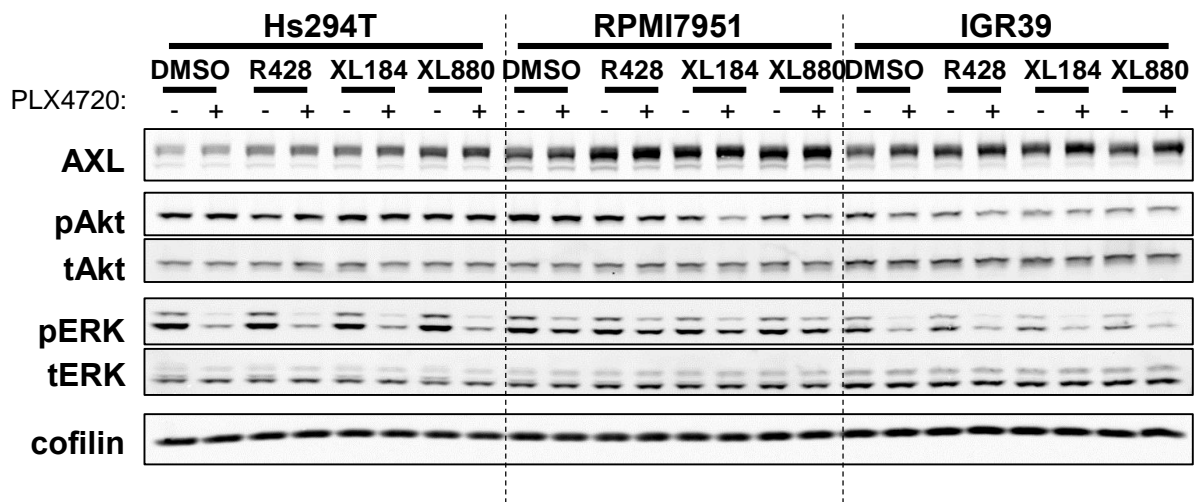
Figure 3.9: **In intrinsically resistant lines, AXL inhibitors do not alter pAkt or pERK levels at baseline or following RAF inhibitor treatment.**
Intrinsically resistant lines were treated overnight with AXL inhibitors R428 (500 nM), XL184 (3 μM), and XL880 (100 nM), in the presence or absence of 2 μM PLX4720. Lysates were harvested an assessed for pAkt and pERK by Western blot.

10. <u>AXL inhibitors do not sensitize intrinsically resistant lines to RAF inhibition.</u>

As an additional test of whether AXL is required for maintenance of the intrinsic resistance

phenotype, we measured PLX4720 GI50 values, across multiple intrinsically resistant lines in the

presence or absence of each AXL inhibitor. We consistently observed minimal if any shift in the

PLX4720 GI50 following AXL inhibition (**Fig. 3.10**). This data, which is consistent with the

aggregate interpretation of the shRNA knockdown data (**Fig. 3.7**) as well as with the lack of

measurable signaling effects of AXL inhibitors in these cell lines, suggests that AXL is not

required for maintenance of intrinsic resistance to MAPK pathway inhibition in BRAF^{V600}-

mutant melanoma.
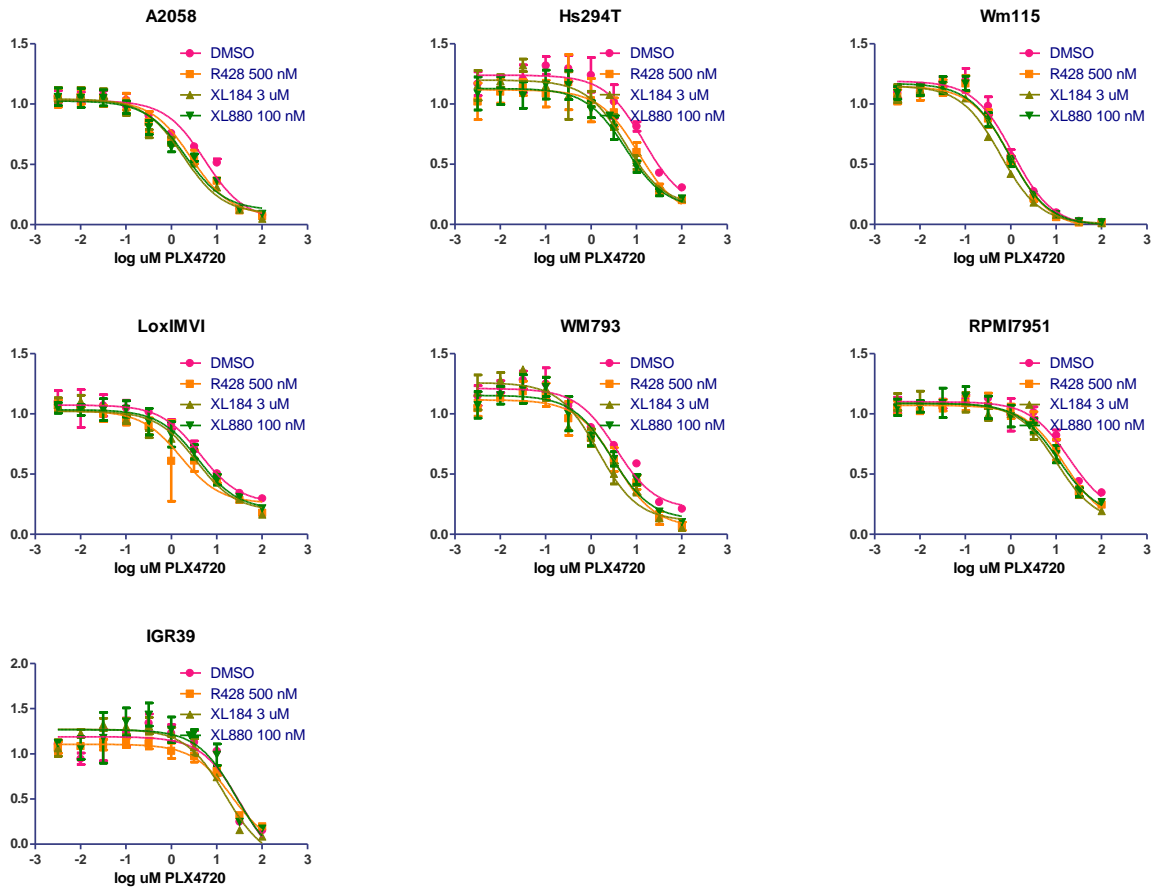
Figure 3.10: **AXL inhibitors do not sensitize intrinsically resistant lines to RAF inhibition.**
Melanoma cell lines intrinsically resistant to MAPK pathway inhibitors, treated with or without a fixed dose of the indicated AXL inhibitors, were assayed for sensitivity to PLX4720 (RAFi).

Discussion and future directions

Together, the work presented in this chapter has used the intersection of functional resistance screens and expression profiling data to nominate AXL as a candidate effector of intrinsic resistance to MAPK pathway inhibition in $BRAF^{V600}$-mutant melanoma. Subsequent functional validation work has revealed that, while AXL is sufficient to confer resistance to MAPK pathway inhibition, likely by re-activation of pERK, it is not required for maintenance of intrinsic resistance.

<u>A framework for querying targeted therapeutic resistance in cancer</u>

Together, these experiments have delineated several important observations. First, they have nominated a framework for identifying candidate mediators of drug resistance. For a given cancer lineage, genetic background, and targeted therapeutic intervention (e.g., MAPK pathway inhibition in $BRAF^{V600}$-mutant melanoma), the paired availability of (1) steady-state gene expression profiling across a panel of sensitive and resistant lines and (2) functional genomic screening data is a potentially powerful combination. While expression profiling can identify genes associated with intrinsic resistance or sensitivity, functional screening can identify which if any of those candidates are necessary or sufficient to effect the phenotype of interest. In the particular case tested here, the intersection of ORF screens for acquisition of resistance with gene expression markers of innate resistance means that a candidate gene belonging to both lists is both expressed in resistant lines and sufficient to confer resistance; these two findings suggest that it is therefore a high-priority candidate mediator of intrinsic resistance. It is important to point out, though, that many other possible variations exist: for example, an shRNA screen identifying genes whose loss confers resistance could similarly be intersected with expression profiles to query whether any of the hits are over-expressed at baseline in sensitive cells relative

to resistant cells. To our knowledge, the systematic intersection of two such datasets, as performed here, constitutes a novel approach to understanding targeted therapeutic resistance in cancer.

AXL biology

In the particular case tested here, we identified AXL as associated with intrinsic resistance and sufficient to cause acquired resistance to MAPK pathway inhibition in BRAF^{V600}-mutant melanoma. AXL is a receptor tyrosine kinase belonging to the TAM family (TYRO3, AXL, MERTK). AXL is widely expressed in normal tissues. Like other RTKs, it undergoes heterodimerization and trans-phosphorylation upon binding its ligand, GAS6. [118] AXL has been shown to activate diverse downstream signaling pathways including Akt, MAPK, and NF-κB [119, 120], although we observed activation only of Akt and MAPK. While AXL was initially isolated from chronic myelogenous leukemia as a cDNA clone with transforming ability [121], few studies have specifically addressed it melanoma; those that have done so have noted (a) its expression in a subset of melanomas, with a possible link to enhanced invasive behavior [122], and (b) its expression in uveal melanoma, where stimulation with GAS6 was shown to be mitogenic [123].

AXL in other resistance contexts

Intriguingly, AXL has also been linked to acquired resistance to targeted therapeutics in other cancer contexts. In EGFR-mutant non-small cell lung cancer (NSCLC), acquisition of erlotinib has been linked to gain of AXL expression as part of a broader program of epithelial-to-mesenchymal cell state change. [124] AXL was shown to be individually sufficient to confer resistance to erlotinib when overexpressed. After long-term exposure of an initially erlotinib-sensitive NSCLC to erlotinib, outgrowing subclones that had acquired erlotinib resistance had

82

also acquired AXL. Moreover, AXL was required for maintenance of this acquired erlotinib resistance. Separately, in *in vitro* cultured-to-resistance experiments, AXL has also been shown to associated with the development of lapatinib resistance in ERBB2-expressing breast cancer [125] and to imatinib in KIT-mutant gastrointestinal stromal tumor [126].

AXL is not required for maintenance of intrinsic resistance

In specific context of MAPK pathway inhibitor resistance in $BRAF^{V600}$-mutant melanoma, we identified AXL as both overexpressed in intrinsically resistant lines and sufficient to confer resistance. Both of these index findings validated robustly in secondary assays, with AXL strongly expressed in resistant lines and both conferring resistance to and rescuing loss of pERK following inhibition of RAF, MEK, or RAF+MEK. On the basis of this data, and building on our analysis framework, we queried a further hypothesis: that AXL was also required for the intrinsic resistance phenotype. Through shRNA and small molecule inhibition studies, we demonstrated that AXL is in fact not required for the maintenance of intrinsic resistance.

These results suggest several observations. Most fundamentally, the finding that AXL is not necessary for intrinsic resistance is not inconsistent with the data that led us to formulate this hypothesis. We selected genes that could confer resistance and that were expressed in resistant lines—not genes that were necessary for resistance. To address that question directly, a potentially powerful approach would be an shRNA screen in an intrinsically resistant line, to identify genes whose loss enhanced sensitivity to RAF inhibition. Indeed, such a screen could become another variation on the theme here established of intersecting functional screens with expression data, as it would be reasonable to query whether any hits were expressed more strongly at baseline in the resistant lines. Thus, although AXL did not prove essential for maintenance of intrinsic resistance, this result it not inconsistent with the analytic framework that

nominated it; rather, it suggest future applications of this framework for continuing to query the phenomenon of intrinsic resistance.

Moreover, the fact that AXL is not the sole and necessary effector of intrinsic resistance does not mean that it makes no contribution to intrinsic resistance. Conceptually, this is consistent with our prior knowledge: RPMI-7951, for example, one of the intrinsically resistant, AXL-expressing lines, is known to also harbor amplification of COT, another known resistance effector. It would therefore be surprising if, in this context, abrogation of AXL alone were able to abrogate resistance, since COT would presumably still be active as an additional resistance mediator. Thus, it remains eminently possible that AXL is one of multiple resistance effectors operant in the setting of intrinsic resistance, and that for that reason, inhibition of it alone does not restore sensitivity.

Indeed, the data presented in this and the prior chapter suggest that intrinsic resistance is not a function of expression of a single resistance effector, but rather a broader question of cellular state. The gene expression differences between sensitive and resistant classes are profound, and by no means confined to differential expression of AXL. Gain or loss of many different mediators of resistance and sensitivity might therefore be at work in these lines; indeed, it is an open question whether the intrinsic resistant lines even have an underlying dependency on the MAPK pathway. Moreover, we know that NF-κB activation is a master regulator of the transition between high-MITF/sensitive and low-MITF/resistant states. We have shown that expression of AXL is induced by NF-κB activation, positioning AXL as a marker or downstream effector of the high-NF-κB intrinsic resistance state (perhaps one of many) rather than an upstream, essential master regulator.

Last, it is noteworthy that AXL confers resistance to inhibition of RAF, MEK, and RAF+MEK, but not to inhibition of ERK. This phenomenon does not match the phenotype observed in intrinsically resistant lines, which are also resistant to ERK inhibition. This discrepancy is highly consistent with the hypothesis that other resistance mediators, in addition to AXL, are at work in intrinsic resistance.

In addition to our framework nominating AXL, another reason for interest in AXL was that it had been shown to be involved in resistance to targeted therapeutics in other contexts[124-126]. Intriguingly, all of the therapeutics in question impinge on some way on the MAPK pathway: lapatinib in breast cancer, imatinib in GIST, and erlotinib in NSCLC. Although none of these investigations queried the setting of intrinsic resistance, all showed that, following long-term exposure of sensitive parental cell lines to the drug in question, outgrowing subclones that had acquired inhibitor resistance had also acquired AXL expression. In two cases, the authors showed that inhibition of AXL restored sensitivity to the drug in question. [124, 125] And in one case, the authors demonstrated both that AXL was sufficient to cause inhibitor resistance, and that acquisition of its expression was associated with a broader program of gene expression changes (in that case, epithelial-to-mesenchymal transition in NSCLC). [124] Although the NSCLC study concerned itself with acquired, rather than intrinsic, resistance, it is intriguing to note that, in their cellular context, an analysis analogous to ours would likely have identified AXL as well, as they found AXL to be both sufficient to confer resistance and differentially expressed between sensitive and resistant lines. Yet they, unlike we, found that AXL was required for maintenance of the resistant phenotype. A relevant question, therefore, since AXL has emerged in several resistance contexts, is whether these high-AXL, inhibitor resistant states share fundamental biological similarities, or whether AXL simply happens to be a pleiotropic

RTK capable of overcoming many inhibitors, or at least marking resistant states, in a relatively non-specific fashion.

Conclusion

Taken together, the results in this section offer a framework—intersection of functional genomic screens with steady-state expression profiling—for identifying high-priority candidate mediators of resistance. In this case, we have nominated AXL as such a potential mediator but demonstrated that it is not required for sustaining intrinsic MAPK pathway inhibitor resistance in BRAF^{V600}-mutant melanoma. Overall, this result is consistent both with the phenotypic effects of AXL overexpression and with the profound expression differences between intrinsic sensitivity and resistance. Nonetheless, the analytical method we present here may have broad future utility in nominating other genes whose expression patterns and functional properties make them compelling candidate effectors of drug resistance.

Methods

Cell culture

All cells were maintained in medium supplemented with 10% FBS (unless otherwise indicated) and 1% penicillin/streptomycin. The following cell lines were maintained in RPMI-1640: A375, Skmel28, UACC62, WM793, LOXIMVI,. DMEM: A2058, Hs294T. MEM: RPMI7951, Wm115. DMEM with 15% FBS: IGR39. All cell lines were obtained from in-lab stocks, from ATCC, or from Biological Samples Platform (Broad Institute).

Gene expression and pharmacological analyses

Gene expression (RMA normalized using ENTREZG v15 CDF), drug sensitivity (IC50 values), and genotyping data for BRAF^{V600}-mutant melanoma cell lines were from the Cancer Cell Line

Encyclopedia (CCLE). [100] Pearson correlation coefficients (r) were computed between PLX4720 GI_{50} values and gene expression value.

Candidate resistance ORFs were nominated on the basis of their ability to confer rescue to RAF, MEK, RAF+MEK, or ERK inhibition, in A375 cells, over a 4-day drug treatment. Subsequently, ORFs were validated in 9 additional melanoma cell lines; only the 107 ORFs with a validation Z score of >4.0 were considered for subsequent analyses.

Constructs

Lentiviral MEK1, RAF1, MITF-M, and AXL (clone 7F12), in vectors pLX980-Blast-V5 or pLX304-Blast-V5, were from The RNAi Consortium (Broad Institute). Retroviral pBABE-Puro-MEK1_WT, pBABE-Puro-MEK1_DD, pWZL-Blast-myrAkt1, and pWZL-Blast-KRAS_G12V constructs were from Cory Johannessen.

shRNAs

All shRNAs were in pLKO.1 vector.

target	name	TRC identifier	target sequence
Luciferase	shLuc	TRCN0000072243	CTTCGAAATGTCCGTTCGGTT
AXL	575	TRCN0000000575	CGAAATCCTCTATGTCAACAT
AXL	5313	TRCN0000195353	CGTGGAGAACAGCGAGATTTA
AXL	574	TRCN0000000574	CGAAAGAAGGAGACCCGTTAT

Lentiviral infections

For validation of AXL rescue of MAPK pathway inhibitors, cells were seeded in 96-well plates and the following day were spin infected at 2250 rpm (1178 x g) for 1 hour at 30 °C using a 1:10 dilution of ORF lentivirus. Medium was changed immediately following infection. After 3d, wells were drugged with MAPK pathway inhibitors at the indicated concentrations. 4 days later, cellular viability was read out by CellTiter-Glo.

For myrAkt resistance experiments, A375 cells were seeded in 96w format (900 cpw) in 100 µL. The next day, polybrene was added to wells to 4 µg/mL final, 50 µL medium was removed, and 50 µL retrovirus was added. Remaining steps were performed as described above.

For western blot studies, infections were performed in 12-well plates at the following densities: A375, 6e4; Wm793, 1.5e5; RPMI-7951, 1.25e5; IGR39, 6e4. The next day, cells were changed to medium plus 4 µg/mL polybrene, virus was added (1:10 dilution for ORF lentiviruses, 1:50-1:100 dilution for shRNA lentiviruses, 1:2 for retroviruses) and cells were spin infected at 2250 rpm (1178 x g) for 30 minutes at 30 °C. The following day, medium was changed to fresh medium plus puromycin (1 µg/mL final) or blasticidin (10 µg/mL final). Following 3-5 days of selection, cells were changed again to fresh medium plus DMSO or indicated small molecule inhibitors.

AXL inhibitors

R428 was purchased from Symansis. XL184 and XL880 were purchased from Selleck. All compounds were resuspended in DMSO.

AXL inhibitor treatment

For western blots and GI50 curves, cells were drugged first with PLX4720 (at serial dilutions for GI50 curves or at fixed 2 µM for western blots), then immediately drugged again with AXL inhibitors to the indicated final concentrations.

Drug sensitivity assays

For GI50 determinations following AXL knockdown, cells were re-seeded following selection to 96-well plates at 1500-3000 cpw. For GI50 determinations in the presence of AXL inhibitor, cells were seeded at the following densities: Cell lines: A2058, 3500; Hs294T, 6000; WM793, 6000; RPMI7951, 4250; IGR39, 3000. The day after plating, cells were drugged with AXL inhibitor (if indicated), then with serial dilutions of PLX4720 in medium DMSO to give final concentrations ranging from 100 µM to 31.62 nM, in half-log increments. After 4 days of drug treatment, cellular viability was read using CellTiter-Glo and compared to DMSO wells. GI50 calculations were performed in GraphPad Prism.

GAS6 stimulation

Recombinant human GAS6, without carrier protein, was purchased from RND (885-GS-050), resuspended, aliquotted, and stored according to manufacturer's instructions. Prior to GAS6 stimulation, cells were plated in full serum at 2e5 cpw in 12w plates. The next day, cells were washed 1x in PBS, changed to fresh full-serum medium with DMSO or 2 µM PLX4720, and stimulated with GAS6 (1000 ng/mL final) over the indicated timecourse.

Lysate harvesting

Cells were harvested by washing 1x in PBS, applying sufficient lysis buffer to cover the well (~ 40 uL for 12w plate, ~100 uL for 6w plate, ~250 µL for 10 cm plate), and removing lysis buffer.

Plates were not scraped and lysates were not pelleted. Cells were lysed in 1% NP40 buffer (150 mM NaCl, 50 mM Tris pH 7.5, 2 mM EDTA pH 8, 25 mM NaF and 1% NP-40), containing 2x EDTA-free protease inhibitor cocktail (Roche) and 1x phosphatase inhibitors I and II (EMD). Lysates were quantitated by BCA, normalized, and denatured by boiling in sample buffer plus 20 mM DTT.

<u>Western Blotting</u>

Transfers were on iBlot nitrocellulose membrane using setting P0. Membranes were blocked 1 hour at room temperature in LiCor blocking buffer. Primary antibodies (1:1000 dilution unless otherwise indicated) were incubated overnight at 4°C in LiCor blocking buffer plus 0.1% Tween-20. Secondary antibodies (1:10,000 dilution, LiCor) were incubated at room temperature for 90 minutes in LiCor blocking buffer plus 0.1% Tween-20 and 0.1% SDS. Imaging was on a LiCor Odyssey infrared imager.

The following primary antibodies were used at 1:1000 unless otherwise indicated. CST = Cell Signaling Technology. AXL (C44G1, CST 4566; 6C8, Sigma WH0000558M1); Cofilin (D3F9, CST 5175, 1:20,000); pERK (T202/Y204, D13.14.4E, CST 4370); tERK (L34F12, CST 4696); pAkt (S473, D9E, CST 4060); Akt (40D4, CST 2920); Cyclin D1 (NeoMarkers Ab-3 Rb-010-P, 1:400); pTyr (4G10, Millipore); pAXL (Y702, D12B2, CST 5724).

CHAPTER 4. MODULATING ACQUIRED MAPK PATHWAY INHIBITOR RESISTANCE: PERTURBING COT BY MODULATING NF-κB.

Abstract

Although the BRAF inhibitor vemurafenib has shown dramatic efficacy in BRAF^{V600}-mutant melanoma, relapse (acquired resistance) is universal. Prior work has elucidated overexpression of the kinase COT/MAP3K8 as a mechanism of acquired resistance to vemurafenib/PLX4720. COT is also expressed at baseline in some BRAF^{V600}-mutant cell lines intrinsically resistant to PLX4720. However, the prospects for COT as a therapeutic target are tempered by the lack of effective small molecule COT inhibitors. For this reason, we sought to determine whether alternative avenues might exist to perturb COT expression and/or stability. Of note, COT protein is highly labile and requires binding to NFKB1 p105 for stability. We reasoned that targeting p105 might destabilize COT and impair COT-mediated resistance. Indeed, shRNA knockdown of p105 was highly effective in decreasing both ectopic and endogenously expressed COT. In ectopic contexts, p105 knockdown also decreased COT-mediated rescue of pERK following PLX4720 treatment and partially reversed COT-mediated PLX4720 resistance. In cell lines endogenously expressing COT, however, knockdown of p105 or COT affected neither residual pERK following PLX4720 treatment nor resistance to PLX4720. This finding suggests that COT, although sufficient to confer acquired resistance to MAPK pathway inhibitors, is not required for the maintenance of intrinsic resistance. Cumulatively, this work provides a proof of principle that targeting binding partners can perturb resistance effectors but suggests that indirect targeting of COT may not be sufficient to overcome intrinsic resistance.

Attributions

All experiments and analyses were performed by David Konieczkowski except as follows:

Experiments in **Fig. 4.1** were performed by Jean-Philippe Theurillat.

Experiments in **Fig. 4.2** were performed by Laura Johnson.

Introduction

Background

The impressive therapeutic responses associated with vemurafenib treatment in $BRAF^{V600}$-mutant melanoma have been tempered by the observation that all patients eventually relapse. [87] This phenomenon, in which an initially sensitive melanoma transitions to a resistant phenotype, is referred to as "acquired resistance." Prior work in the Garraway lab and elsewhere has sought to elucidate mechanisms of acquired resistance, chiefly by searching for perturbations able to confer MAPK pathway inhibitor resistance on an otherwise sensitive cell line.

One example of this approach was a genetic screen published from our lab. [92] In this screen, a collection of ~600 kinases was screened for the ability to rescue viability in the A375 melanoma cell line following treatment with PLX4720 (the preclinical of vemurafenib). Of the 9 kinases validated to confer statistically significant rescue, COT/MAP3K8 was nominated for further investigation as having the strongest resistance phenotype across multiple cell lines.

COT: an effector of PLX4720 resistance

COT/MAP3K8/TPL2 was originally identified as a transforming cDNA clone [127] that was subsequently shown to activate the MAPK pathway through its function as a MAP3K [128].

Since its initial discovery, COT has been shown to be of critical importance in the context of immune signaling. COT is required for signaling cross-talk from inflammatory pathways to the MAPK pathway; it is also required for normal transcriptional response to innate immune stimuli such as LPS or other Toll-like receptor ligands. [129-131]

Consistent with its annotation as a MAP3K, COT was found to confer resistance to PLX4720 through reactivation of ERK phosphorylation. In addition, two BRAF^{V600E} cell lines, one melanoma and one colon, harbored copy number gains spanning the *MAP3K8* locus; both lines were profoundly resistant to PLX4720. Intriguingly, in melanocytes and in cell lines, COT displayed a reciprocal expression pattern with BRAF. BRAF^{WT} melanocytes express endogenous COT, but ectopic expression of BRAF^{V600E} causes loss of COT. Conversely, in A375 (a BRAF^{V600E} melanoma cell line), ectopic COT was only moderately expressed from a CMV promoter; following knockdown of endogenous BRAF or treatment with PLX4720, however, ectopic COT expression was strongly potentiated. [92]

Cumulatively, these findings nominate COT as a putative target for overcoming acquired resistance. Conceivably, COT inhibition could be administered concomitantly with vemurafenib or other MAPK inhibitors to forestall COT-mediated resistance or as salvage therapy following COT-driven relapse. Unfortunately, COT inhibitors have yet to be deployed in the clinical arena [132-136], reviewed in [137].

NFKB1 p105 binds and stabilizes COT

In light of our interest in NF-κB signaling in melanoma (detailed in other chapters), we considered the established links between COT function and NF-κB activity in inflammatory and immune-related signal transduction. In particular, its link to the NF-κB pathway suggested a

potential means to perturb COT function. NFKB1, one of the NF-κB family of transcription factors, is transcribed as a 105 kD inactive precursor (p105), containing both an N-terminal, transcriptionally active Rel homology domain, and a C-terminal inhibitory ankyrin repeat domain. At baseline, the presence of the ankyrin repeat domain sequesters full-length p105 in the cytoplasm, where it is transcriptionally inactive. Following stimulus, p105 is cleaved between the N-terminal and C-terminal domains, liberating the C-terminal ankyrin repeats for degradation and the N-terminal Rel homology domain (referred to as p50) for transcriptional activity.

Notably, full-length, inactive NFKB1 p105 both stabilizes and sequesters COT through COT's interaction with the C-terminal ankyrin repeats of p105; thus, p105 and COT reciprocally bind and stabilize each other. [138-141] The consequences of this binding are twofold: p105 is absolutely required for COT protein stability and expression, but binding to p105 blocks COT from accessing its downstream substrates [140-142]. Thus, p105-bound COT forms a latent reservoir of sequestered, inactive COT that can be liberated following stimulus-directed p105 cleavage. Once p105 cleavage—a feature of NF-κB pathway activation—liberates COT, COT is able to exercise its MAP3K functions before being rapidly degraded.

The key role of p105 in COT stability and activity led us to hypothesize that targeting p105 could provide an alternative means of COT perturbation, with possible therapeutic implications. To this end, we formulated two hypotheses. First, we hypothesized that differences in p105 levels or binding to COT might explain the reciprocal relationship of COT and BRAF observed in primary melanocytes and in A375 cells. Second, we hypothesized that by perturbing p105, we could in turn perturb COT and COT-mediated rescue of pERK and resistance following PLX4720 treatment.

94

Results

1. <u>In melanocytes, introduction of BRAF^{V600E} leads to loss of COT expression without accompanying decrease in p105 levels.</u>

To test the hypothesis that endogenous p105 is involved in reciprocal regulation of BRAF and COT levels, we considered two contexts in which this phenomenon has been demonstrated: melanocytes and melanoma cell lines. BRAF^{WT} melanocytes express COT at baseline, expression that was abrogated by the introduction of BRAF^{V600E} (**Fig. 4.1**). In light of the role of p105 in stabilizing COT, we predicted that loss of COT expression might be due, at least in part, to lower levels of p105 following introduction of BRAF^{V600E}. Surprisingly, however, we found that p105 levels increased following BRAF^{V600E} introduction (**Fig. 4.1**). The mechanistic basis of this observation is unknown, but it is inconsistent with the idea that the balance between COT and BRAF in melanocytes is controlled primarily by p105 levels. Moreover, it has previously been shown that COT mRNA levels decrease following introduction of BRAF^{V600E}. [92] Together, these data suggest that reciprocal regulation of COT and BRAF does not depend on p105 but rather may operate through either transcriptional or other post-translational regulatory mechanisms.
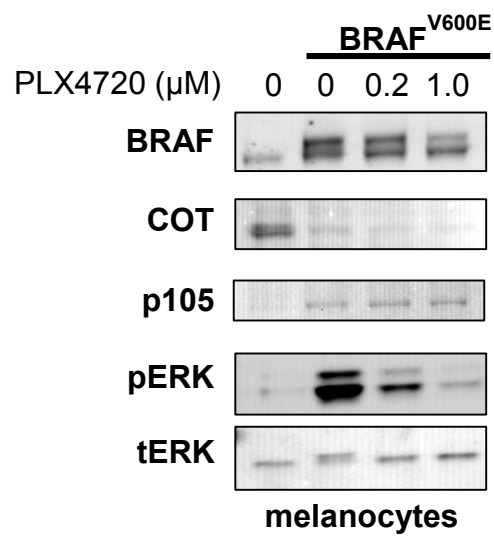
Figure 4.1: **In melanocytes, introduction of BRAF^{V600E} leads to loss of COT expression without accompanying decrease in p105 levels.**
Expression of COT and p105 in melanocytes at baseline (L), or following introduction of BRAF^{V600E} with or without co-treatment with the BRAF inhibitor PLX4720.

2. <u>In melanoma cells, BRAF knockdown leads to enhanced expression of ectopic COT without accompanying increase in p105 levels.</u>

We next turned our attention to melanoma cell lines to query the possible role of endogenous p105 in modulating expression of ectopic COT. We used the A375 melanoma cell line, which endogenously express BRAF^{V600E} but not COT. COT is detectable following lentiviral expression and is further upregulated upon concomitant knockdown of BRAF. (**Fig. 4.2**) Because expression of COT in this context is driven by a constitutive CMV promoter, regulation of COT in this context is likely to be at the level of protein stability rather than transcription. Since p105 is a key regulator of COT protein stability, we predicted that enhanced COT expression following BRAF knockdown would be accompanied by either (a) increased p105 levels or (b) constant total p105 levels but increased association between COT and p105. To test the first possibility, we blotted whole-cell lysates (left panel) for p105 following introduction of COT, with or without knockdown of BRAF. Knockdown of BRAF had no effect on p105 levels. We reasoned that even if total p105 levels remained constant, enhanced COT expression might be due to an increase in COT-p105 association. To query this possibility, we immunoprecipitated COT (right panel) from the same lysates and then probed for p105. Here, too, we observed no differences in COT-bound p105. Thus, although the mechanism underlying reciprocity of BRAF^{V600E} expression and COT expression and/or protein stability remains unknown, the preceding experiments argue that p105 is not the key mediator of this regulation either in melanocytes or in melanoma cells.
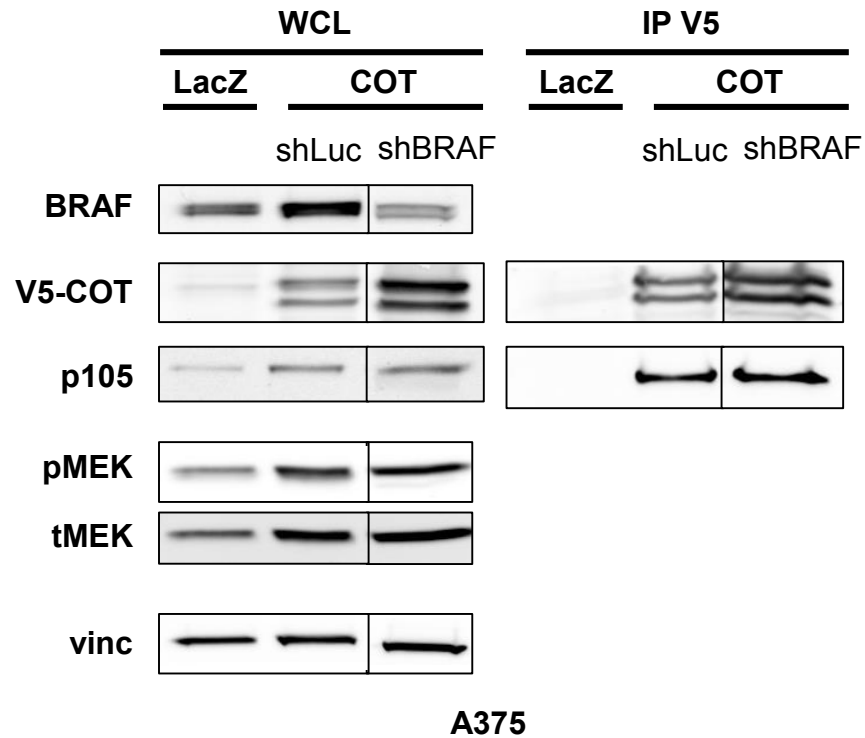
Figure 4.2: **In melanoma cells, BRAF knockdown leads to enhanced expression of ectopic COT without accompanying increase in p105 levels.**
In A375 melanoma cells expressing negative control (LacZ) or V5-tagged COT, levels of total p105 were measured in whole-cell lysates (WCL) following knockdown of BRAF. Additionally, levels of COT-bound p105 were measured by immunopreciptiation with V5 (IP V5).

3. p105 super-repressor enhances ectopic COT expression but does not impair COT-mediated rescue of pERK.

Having determined that differential expression of endogenous p105, or altered interaction between COT and endogenous p105, might not be a primary determinant of the balance between COT and BRAF expression in melanocytes or melanoma cells, we turned to our second hypothesis: that perturbation of p105 could modulate COT function. In particular, we hypothesized that sequestration of COT by p105 might prevent its ability to re-activate MAPK and/or drive PLX4720 resistance. [141] To this end, we used a p105 super-repressor construct (p105 SR). This construct is N-terminally deleted, encoding only the inhibitory C-terminal ankyrin repeat domains, and it carries a S930A mutation, which prevents its phosphorylation and degradation. [143] Because this super-repressor can neither be phosphorylated nor targeted for degradation, it should permanently sequester COT. As negative controls, we used an empty vector and an IκBα super-repressor; IκBα is structurally and functionally homologous to the inhibitory C terminal ankyrin repeats of p105, but has not been shown to interact with COT. We found that expression of the p105 super-repressor led to strongly increased levels of COT (**Fig. 4.3**, lanes 4 vs. 6 and 10 vs. 12). Conversely, expression of COT also led to increased expression of p105, whether endogenous (lanes 1 vs. 4 or 7 vs. 10) or from the super-repressor construct (lanes 3 vs. 6 and 9 vs. 12). These results imply a mutual stabilization between p105 and COT. Moreover, expression of the super-repressor had no effect on pERK of pMEK levels following PLX4720 treatment (1 μM, 18 hrs.; lanes 10 vs. 12). These results suggest that, while p105 SR may sequester COT, sufficient free COT remains to activate pERK in the presence of PLX4720. We therefore concluded that sequestration of COT by p105 is insufficient to abrogate COT-mediated resistance.
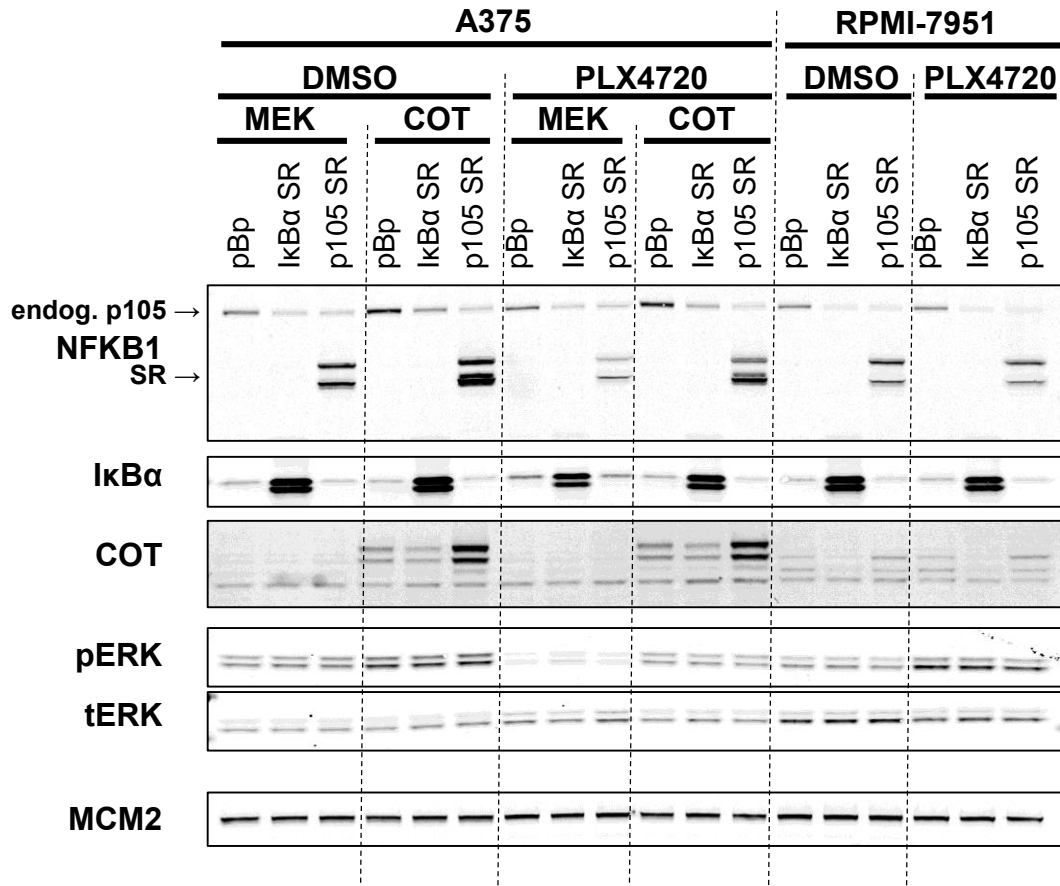
Figure 4.3: **p105 super-repressor enhances ectopic COT expression but does not impair COT-mediated rescue of pERK**.
In A375 cells (L) expressing negative control (MEK) or COT, effects of expression of a non-cleavable, constitutively COT-bound p105 super-repressor (p105 SR) on ectopic COT levels and COT-mediated rescue of pERK following PLX4720 treatment. pBp (empty vector) and IκBα SR are negative controls. RPMI-7951 (R) expresses endogenous COT.

4. NFKB1 knockdown decreases p105 levels more effectively than does IL-1β-mediated p105 cleavage.

Since increased levels of p105 led to increased levels of COT, we reasoned that decreasing levels of p105 might inhibit COT function by decreasing COT levels. We compared two strategies for decreasing p105 levels: stimulus-driven p105 cleavage using IL-1β, and shRNA knockdown of NFKB1. We compared several doses and timepoints against five p105 shRNAs. (**Fig. 4.4**) We found that IL-1β achieved a maximum of ~50% reduction in p105 levels, and that this effect was largely durable up to 5 days. In contrast, NFKB1 shRNAs achieved a ~90% reduction in p105 levels. Since shRNAs were significantly more effective than IL-1β at depleting p105, three p105 shRNAs (6517, 6518, 6520) displaying excellent knockdown and minimal toxicity were selected for future studies. Notably, one selected shRNA, 6517, targets the 3' UTR of the NFKB1 transcript and therefore can be used in combination with the p105 SR construct.
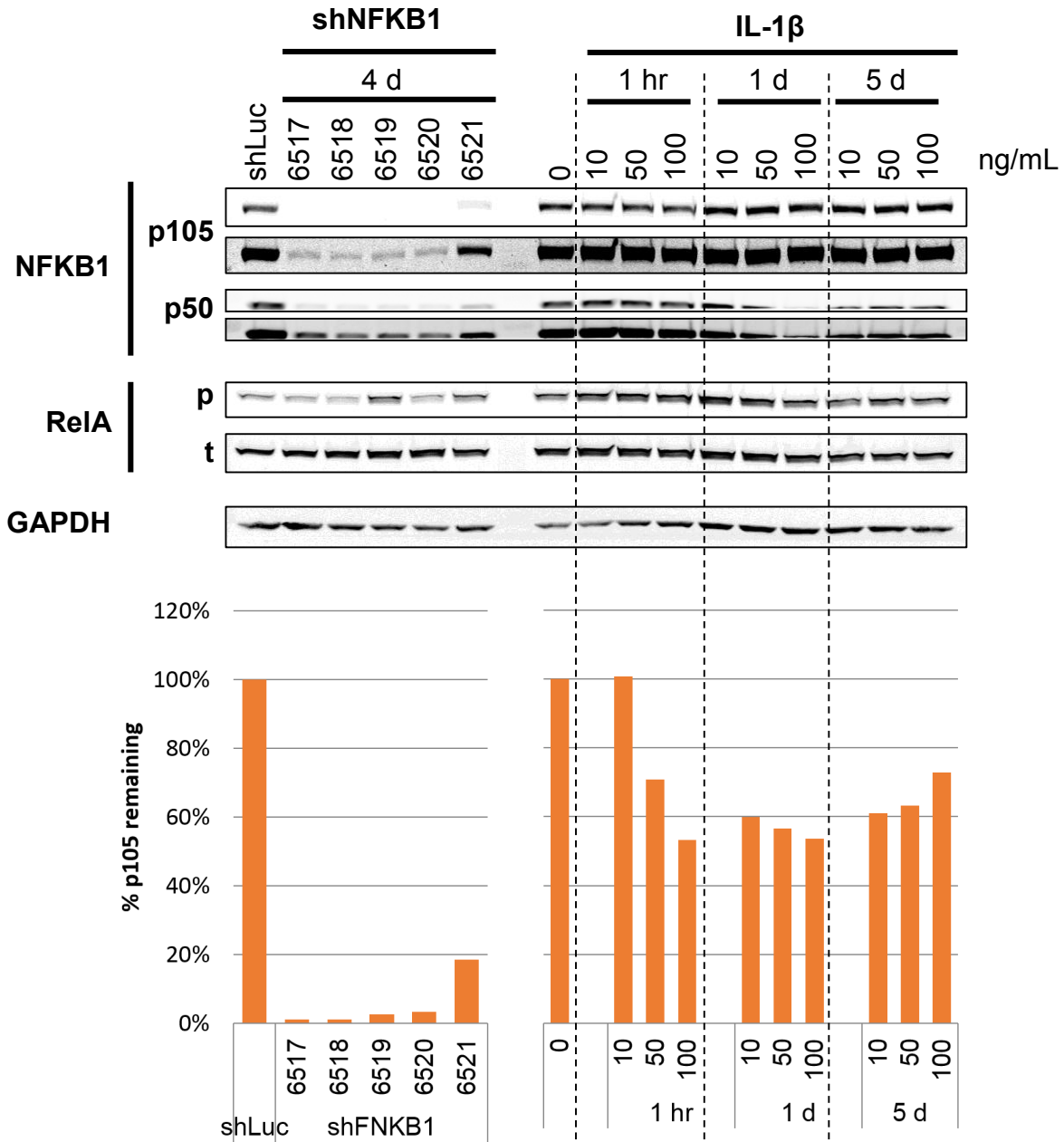
Figure 4.4: **NFKB1 knockdown decreases p105 levels more effectively than does IL-1β-mediated p105 cleavage.**
In A375 cells, p105 levels were measured following NFKB1 knockdown (L) or IL-1β-mediated cleavage (R) at various IL-1β doses/timepoints.   Top: western blot. Bottom: quantification of western blot.

102

5. <u>Knockdown of p105 NFKB1 decreases ectopic and endogenous COT expression.</u>

To query the reciprocal effects of modulation of p105 or COT on each other, we examined two

contexts: A375 cells expressing exogenous COT (**Fig. 4.5A**), and endogenously COT-amplified

BRAF^{V600E} cell lines (RPMI-7951 and OUMS23). (**Fig. 4.5B** and **Fig. 4.5C**) (Western blots for

these experiments, by cell line, are presented in **Fig. 4.5A-C**; quantification of these experiments,

by target, is presented in **Fig. 4.6-4.8**.) First, we examined how perturbation of COT altered p105

levels. Consistent with prior findings, introduction of COT into A375 led to increased p105

levels (**Fig. 4.5A**), presumably through reciprocal p105/COT stabilization. Conversely, in all

cell lines, shCOT led to modest decreases in p105 expression (**Fig. 4.5A-C**). shCOT also

provided a positive control for loss of COT following subsequent perturbations.

Figure 4.5: **Knockdown of p105 NFKB1 decreases ectopic and endogenous COT expression.**
In **(a)** A375 cells ectopically expressing MEK (negative control) or COT, **(b)** RPMI-7951 cells endogenously expressing COT, or **(c)** OUMS23 cells endogenously expressing COT, effect of shNFKB1 or p105 super-repressor on levels of p105, COT, and pERK with or without PLX4720 treatment (1 µM overnight). shCOT is a positive control for loss of COT; shLuc and pBp are negative controls.
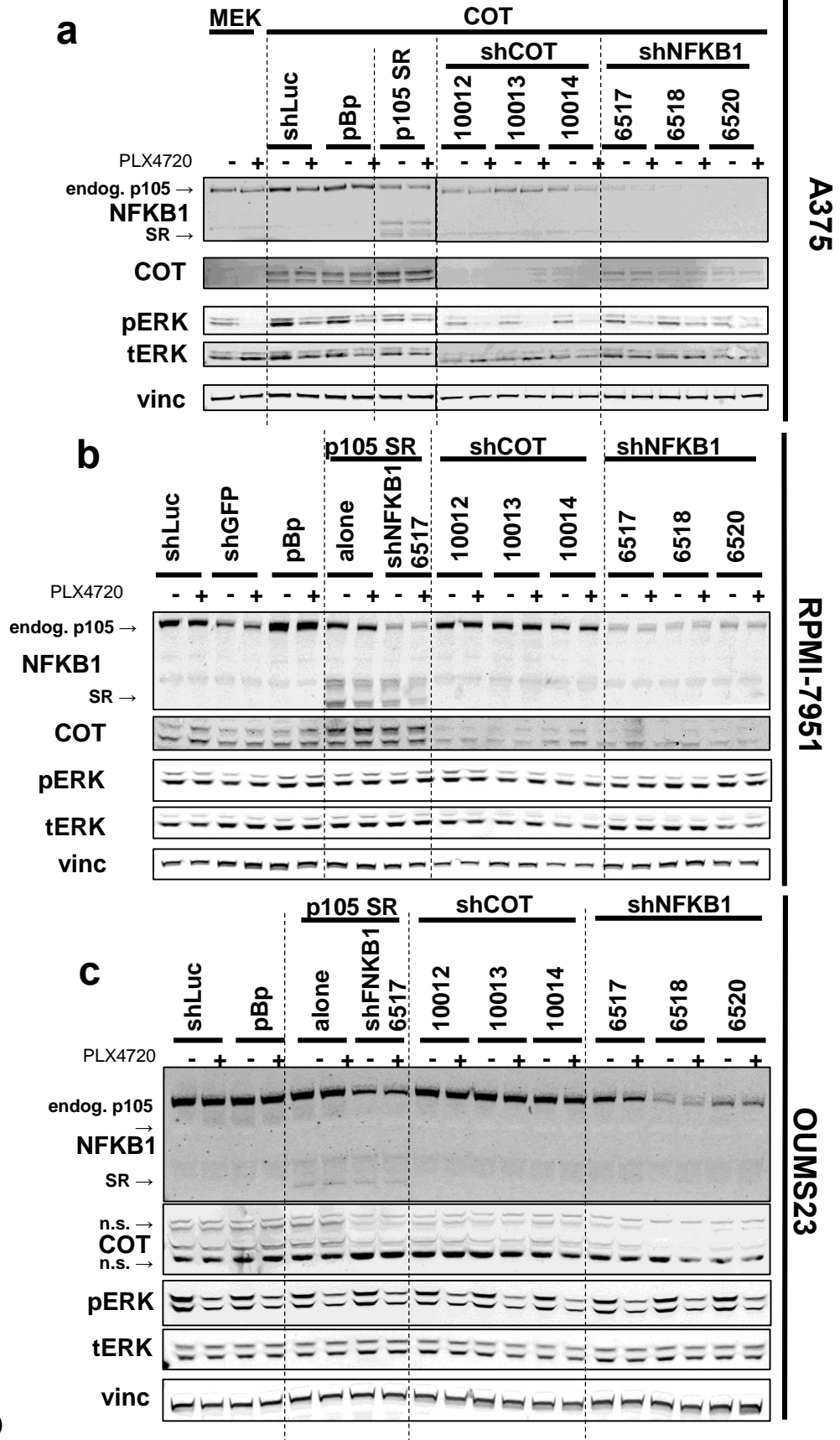
Figure 4.5 (continued)

105

6. <u>Knockdown of NFKB1 decreases p105 levels.</u>

To understand how perturbing p105 affected COT, we used shRNAs targeting NFKB1. These shRNAs were highly effective in all cellular contexts (typically >80% knockdown, **Fig. 4.6**). We also, however, considered the effect of the p105 SR. As observed previously (**Fig. 4.3**), p105 SR increased COT protein levels in both exogenous (**Fig. 4.5A**) and endogenous (**Fig. 4.5B** and **Fig. 4.5C**) contexts, suggesting that COT was binding to and being stabilized by the p105 SR. The p105 SR did not, however, impair COT-mediated pERK rescue following PLX4720 treatment. We reasoned that this might be due to competition between the p105 SR, which permanently sequesters COT, and endogenous p105, from which COT could still be liberated to effect pERK rescue. Conversely, it is possible that, in the setting of shNFKB1, residual p105 might still suffice to stabilize COT and allow its activity. In this context, addition of p105 SR should compete COT away from the small amount of remaining endogenous p105, permanently sequestering and inactivating it. To address these two questions, we simultaneously expressed the p105 SR while using a 3' UTR-targeted shRNA to abrogate endogenous p105. This condition was not tested in A375+COT; in OUMS23, inadequate p105 SR expression was achieved. In RPMI-7951, however, p105SR was adequately expressed such that approximately 75% of expressed p105 was in fact p105SR.
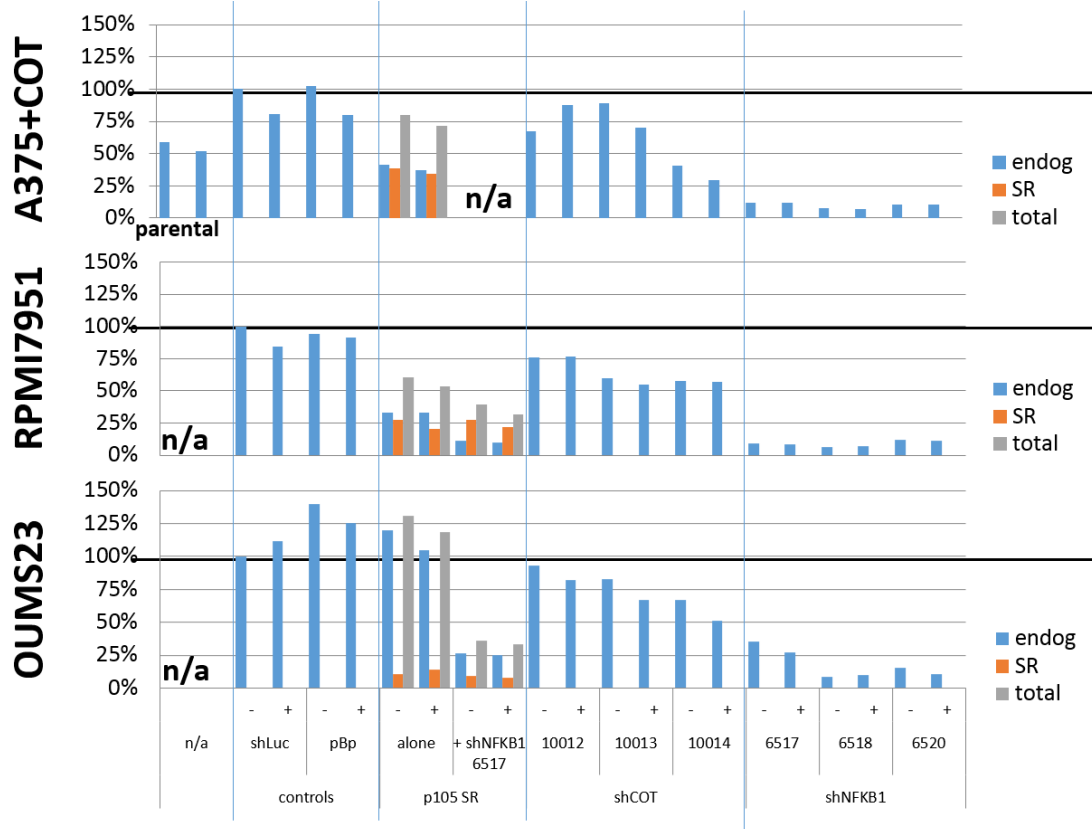
Figure 4.6: **Knockdown of NFKB1 decreases p105 levels.**
p105 levels in A375 (exogenously expressing COT), RPMI7951, and OUMS23
(endogenously expressing COT), following NFKB1 knockdown (R) or other indicated
perturbations, with or without 1 μM overnight PLX4720 treatment (-/+). Percentage is
relative to negative control shLuc + DMSO (black line). Where expressed, p105 super-
repressor is quantified separately. Quantification is from Figure 4.5A-C.

7. Knockdown of p105 NFKB1 decreases COT expression in exogenous and endogenous contexts.

Following these perturbations—shCOT, shNFKB1, p105 SR, and the combination of shNFKB1 and p105 SR—COT levels were quantified (**Fig. 4.7**). As expected, COT levels increased robustly upon expression p105 SR alone; conversely, shCOT suppressed COT levels. We then assessed the effect of p105 knockdown on COT levels. Strikingly, we found robust suppression of COT expression following shNFKB1 (~50% in A375, ~80% in RPMI-7951 and OUMS23). In many cases, the effect of shNFKB1 on COT levels was actually greater than the effect of shCOT itself. This finding seemingly endorsed our core hypothesis that COT and p105 levels reciprocally regulate each other, and that perturbing one is a potentially useful means to altering levels of the other. With respect to the p105 SR construct, in RPMI-7951, the majority of p105 was successfully replaced by p105 SR (**Fig. 4.6**), leading to a full restoration of COT levels and demonstrating that the effects of shNFKB1 on COT levels are not due to off-target effects.
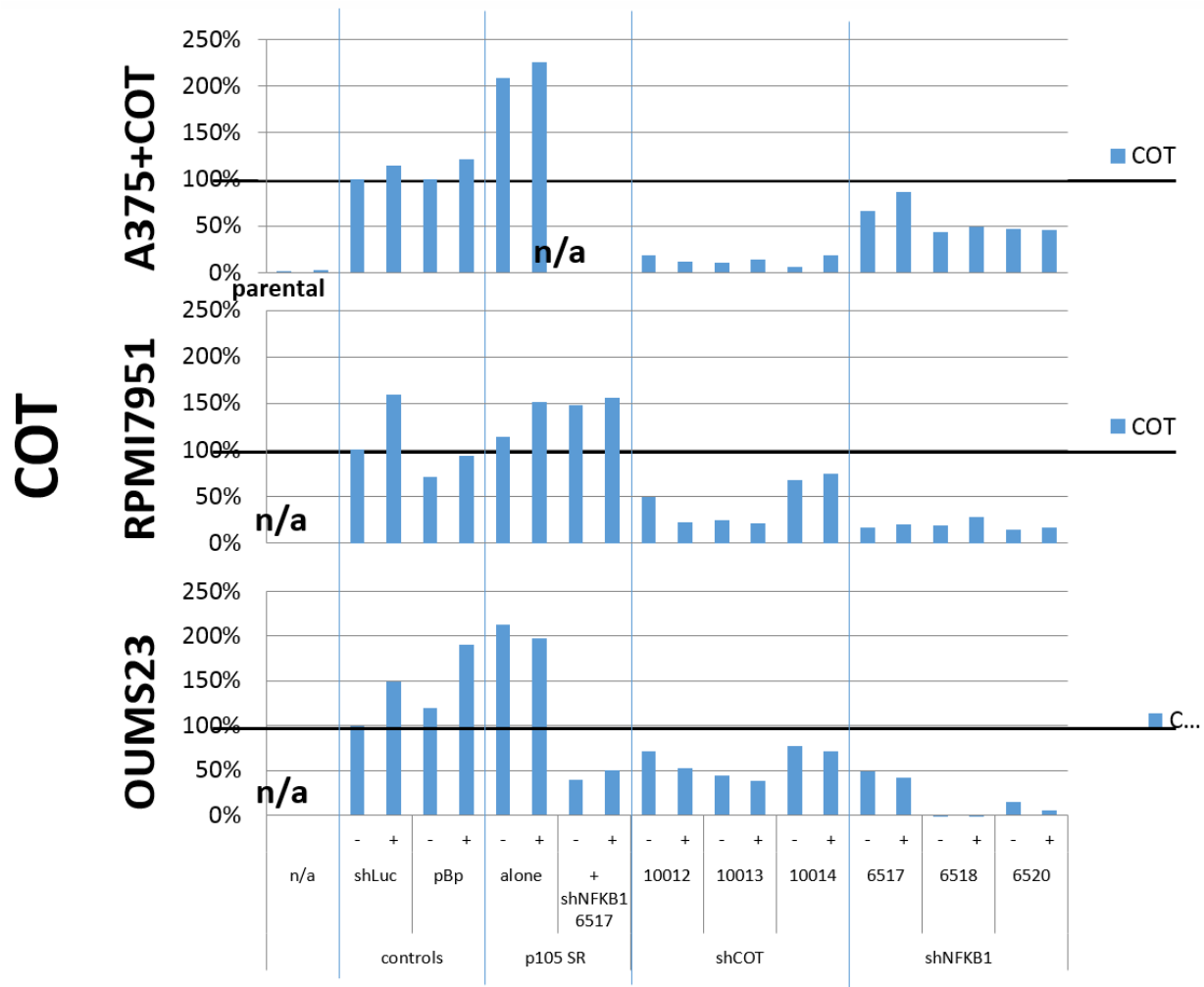
Figure 4.7: **Knockdown of p105 NFKB1 decreases COT expression in exogenous and endogenous contexts.**

COT levels in A375 (exogenously expressing COT), RPMI7951, and OUMS23 (endogenously expressing COT), following NFKB1 knockdown (R) or other indicated perturbations, with or without 1 μM overnight PLX4720 treatment (-/+). Percentage is relative to negative control shLuc + DMSO (black line). Quantification is from Figure 4.5A-C.

8. <u>Knockdown of p105 NFKB1 decreases residual pERK following PLX4720 treatment in the setting of exogenous, but not endogenous, COT expression.</u>

Next, we assessed the effect of these perturbations of COT levels on its ability to reactivate the MAPK pathway, as measured by pERK, in the presence of the BRAF inhibitor PLX4720 (**Fig. 4.8**). Results are presented normalized to the amount of pERK rescue achieved at baseline. (E.g., if A375+COT+shLuc has 40% of basal pERK remaining after PLX4720 treatment, and A375+COT+shCOT has 20% of basal of pERK remaining after PLX4720 treatment, the normalized value for A375+COT+shCOT is 50% of rescue remaining.) As expected, parental A375 cells show total loss of pERK upon PLX4720 treatment; shCOT abrogated the majority of COT-mediated pERK rescue (~20% rescue remaining for 2/3 shRNAs), providing a technical positive control. We next considered the effects of shNFKB1. Although its effects were more modest than shCOT, shNFKB1 was able measurably to suppress COT-mediated rescue of pERK in the setting of A375+COT (~75% rescue remaining for 2/3 shRNAs). This finding provides a key confirmation of our hypothesis that perturbations of p105 could perturb COT-mediated MAPK pathway reactivation.

We then turned our attention to residual pERK in the setting of endogenous COT expression. Of note, RPMI7951 is the only intrinsically resistant melanoma line with amplified COT; moreover, it is the only intrinsically resistant melanoma line that maintains pERK following MAPK pathway inhibitor treatment (cf. **Fig. 2.3C**). We therefore hypothesized that suppression of COT might suppress this residual pERK. In RPMI-7951 and OUMS23, shCOT, the positive control in this experiment, achieved measurable COT suppression (~50% remaining) yet did not alter pERK rescue. Moreover, shNFKB1—despite suppressing COT more profoundly than shCOT itself (~25% remaining, **Fig. 4.7**)—did not alter residual pERK following PLX4720 treatment

(**Fig. 4.8**) Even in the context of the p105 SR, where any wild-type p105 enduring after knock-down would have to compete with an excess of p105 SR, we saw no effect on pERK rescue (**Fig. 4.8**). These findings suggest that, in cell lines that endogenously express COT and are intrinsically resistant to PLX4720, perturbation of COT directly or by shNFKB1 is unable to modulate residual pERK following PLX4720 treatment.
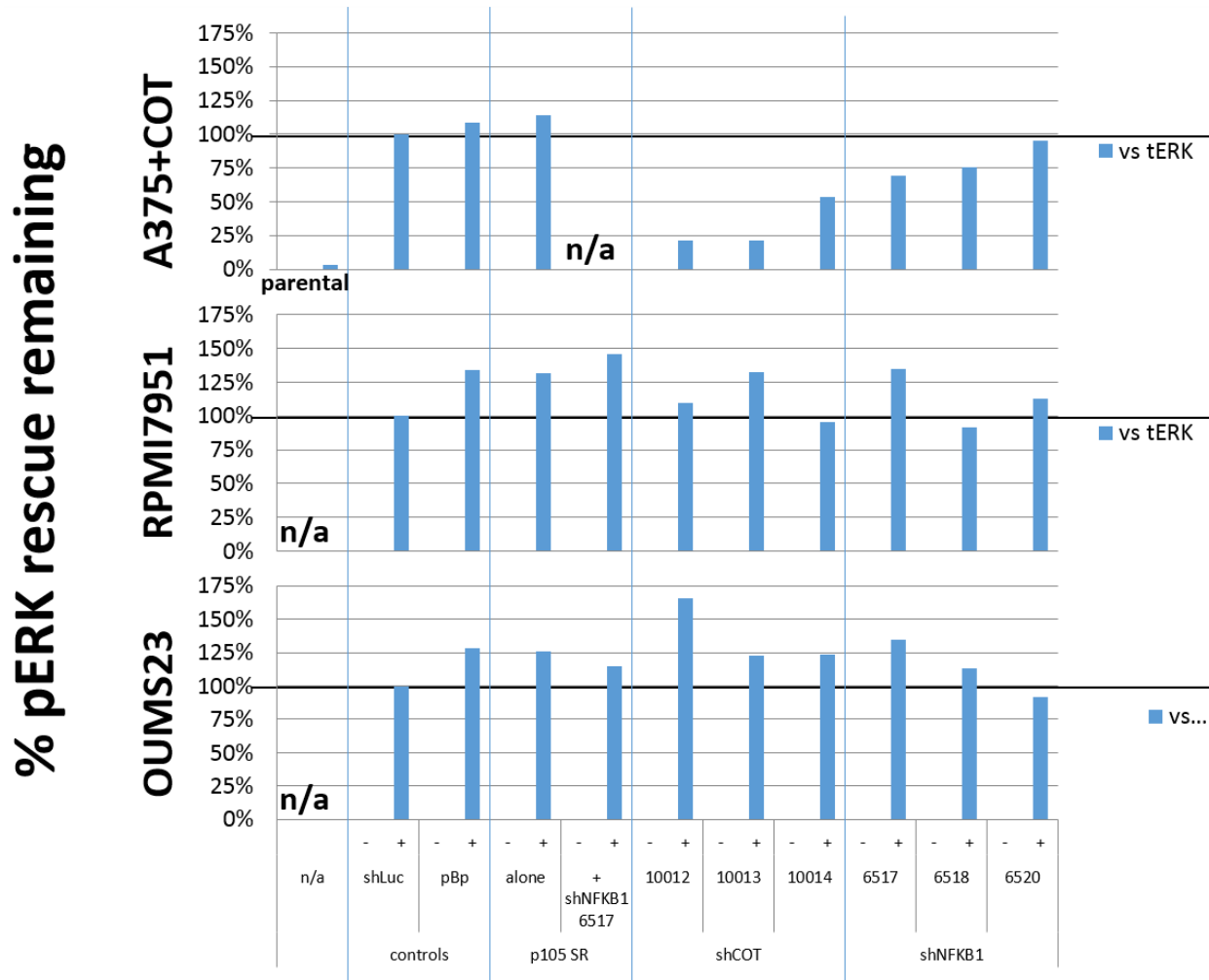
Figure 4.8: **Knockdown of p105 NFKB1 decreases residual pERK following PLX4720 treatment in the setting of exogenous, but not endogenous, COT expression.**
Residual pERK levels following PLX4720 treatment in A375 (exogenously expressing COT), RPMI7951, and OUMS23 (endogenously expressing COT), following NFKB1 knockdown (R) or other indicated perturbations. Percentage is relative to pERK maintained in negative control (shLuc) following PLX4720 treatment (black line). Quantification is from Figure 4.5A-C.

9. <u>Knockdown of NFKB1 partially resensitizes A375+COT cells to PLX4720.</u>

As a further test of the ability of COT and NFKB1 perturbations to affect COT-mediated

resistance, we performed pharmacological growth inhibition experiments on cells perturbed as

above. A375+COT and RPMI-7951 were used for these experiments; OUMS23 was omitted

due to technical difficulties. In A375+COT, as a positive control, COT shRNAs robustly re-

sensitized cells to PLX4720 (**Fig. 4.9A**). Consistent with the weaker effect of shNFKB1 in

decrementing COT and pERK rescue, shNFKB1 only marginally resensitized cells to PLX4720.

Indeed, measured PLX4720 GI50 was proportional to the amount of COT remaining across

various perturbations (**Fig. 4.9B**). Thus, it appears that the ~25% reduction in residual pERK

effected by shNFKB1 (**Fig. 4.8** was sufficient to effect only a marginal change in resistance to

PLX4720.
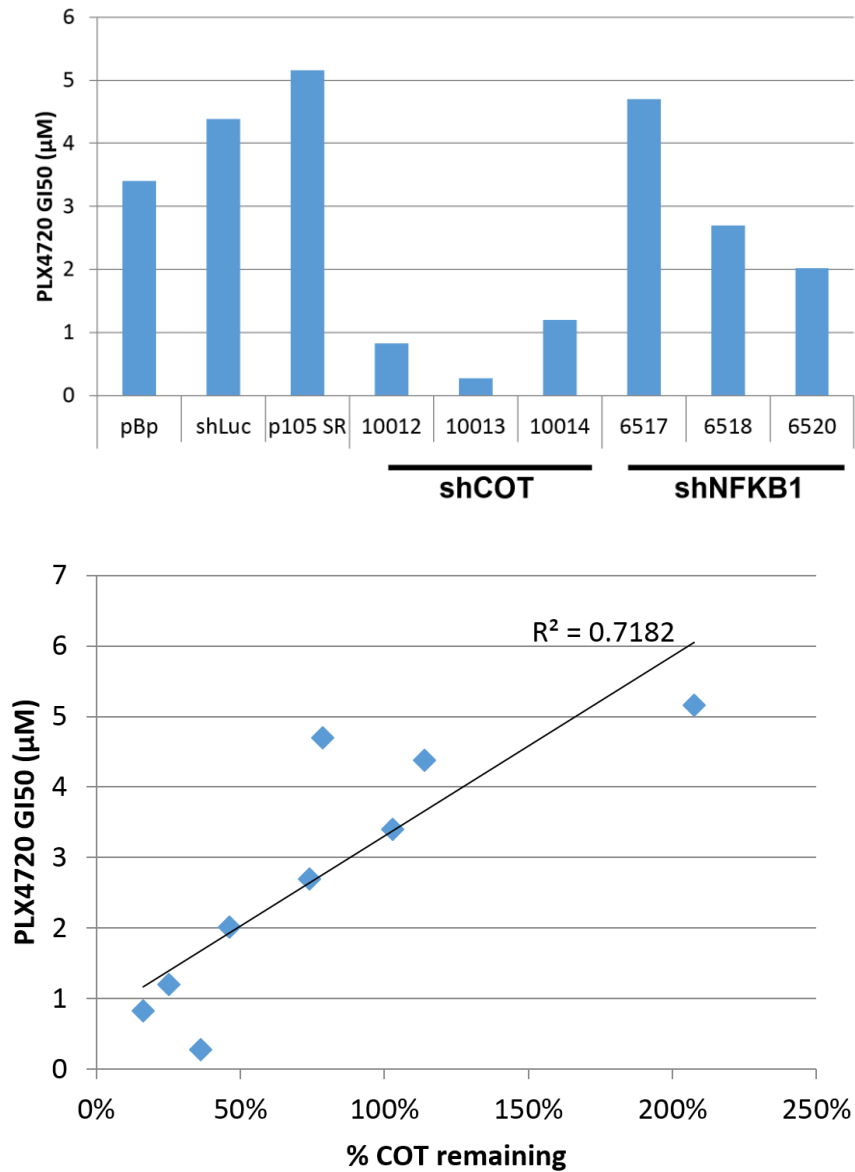
Figure 4.9: **Knockdown of COT partially resensitizes A375+COT cells to PLX4720.**
Top: shCOT substantially resensitizes A375+COT to PLX4720, whereas shNFKB1 effects
only a modest resensitization (2/3 hairpins)
Bottom: Correlation between % COT remaining and PLX4720 GI50 for various perturbations
of A375+COT.

10. Knockdown of neither COT nor NFKB1 sensitizes RPMI-7951 to PLX4720.

We queried whether a similar result obtained in RPMI-7951. Here, we found that neither shCOT

nor shNFKB1 reproducibly shifted the GI50 for PLX4720 (**Fig. 4.10**). This finding is consistent

with our prior observations that neither perturbation altered residual ERK following PLX4720

treatment. Thus, in the setting of endogenous COT expression in RPMI-7951, modulation of

COT either by shCOT or by shNFKB1 appears insufficient to alter the phenotype of intrinsic

resistance to PLX4720 and maintenance of MAPK pathway activity following PLX4720

treatment.
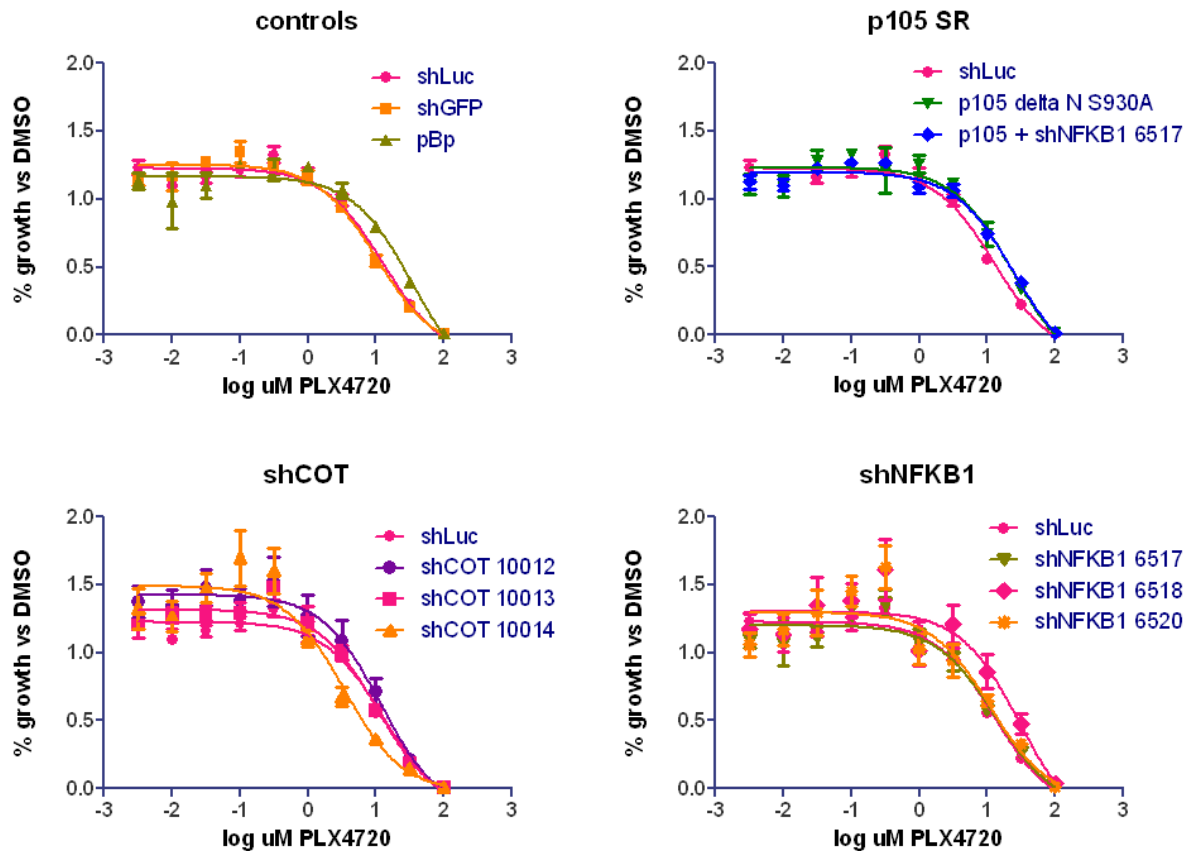
Figure 4.10: **Knockdown of neither COT nor NFKB1 sensitizes RPMI-7951 to PLX4720.**
Effects of control constructs, the p105 SR alone or in combination with knockdown of
endogenous p105, shCOT, and shNFKB1 on PLX4720 GI50.

Discussion and future directions

COT and p105 interaction in melanoma

These investigations have revealed several aspects of COT biology and interaction with p105 NFKB1. First, a reciprocal stabilization between COT and p105, similar to that reported in immune contexts [138-140], is evident in melanoma as well. Our work therefore demonstrates that this aspect of COT biology is conserved across cellular contexts. As a consequence, we found that perturbing p105 also modulates COT levels in melanoma. Indeed, in many cases, knockdown NFKB1 was more effective at reducing COT levels than was knockdown of COT itself. Thus, our core hypothesis of using p105 to perturb COT expression was validated.

Perturbing ectopic COT

The motivation for perturbing COT by perturbing p105 was to determine if p105 suppression might attenuate COT-mediated reactivation of pERK and therefore COT-dependent resistance following treatment with a RAF inhibitor. In the context of A375 cells exogenously expressing COT, it is known that COT is the primary mediator of PLX4720 resistance. Consistent with this fact, knockdown of COT in A375 exogenously expressing COT almost totally abrogated pERK rescue following PLX4720 treatment. Similarly, p105 knockdown also attenuated COT expression and pERK rescue (albeit in both cases less than the attenuation observed with shCOT). Thus, in an exogenous context, where COT is known to be a predominant resistance effector, knockdown of p105 is capable of affecting COT-mediated MAPK pathway reactivation. However, in this specific setting of A375, the fundamental limitation appears to be one of effect size: because shNFKB1 was less effective than shCOT at suppressing COT levels, shNFKB1 in turn led to only a ~25% reduction in pERK.

Perturbing endogenous COT

117

We obtained different results in the setting of endogenous COT expression (RPMI-7951 and OUMS23). Of note, RPMI-7951 is distinguished from other intrinsically resistant melanoma lines not only in its expression of COT, but also in retaining pERK following MAPK pathway inhibitor treatment (cf. **Fig. 2.3C**)—a phenomenon COT is sufficient to effect. In RPMI-7951 (and OUMS23), shNFKB1 was typically at least as effective as shCOT in reducing COT expression, thus eliminating a technical barrier in A375 to adequate abrogation of pERK rescue. However, shCOT and shNFKB1 neither altered residual pERK following PLX4720 treatment, nor, in RPMI-7951, re-sensitized cells to PLX4720. There are at least two, non-mutually exclusive possibilities to explain these results.

First, shCOT and/or shNFKB1 may have inadequately suppressed COT levels in RPMI-7951 and OUMS23. This appears to be the case in A375+COT, where the stronger COT suppression achieved by shCOT was sufficient to abrogate pERK rescue and phenotypic resistance, whereas the weaker COT suppression achieved by shNFKB1 was not. In RPMI-7951 and OUMS23, shCOT was less effective at suppressing COT than in A375+COT, suggesting that, in these cell lines, residual COT could have continued to phosphorylate ERK and maintain viability in the presence of PLX4720. This explanation appears less likely in the contest of shNFKB1, however, as knockdown of p105 frequently led to efficient suppression of endogenous COT. In either case, testing this hypothesis would require a more effective way to suppress COT expression or function. Unfortunately, we lack tools to do so: shCOT provided inadequate knockdown, and small molecule COT inhibitors have suboptimal potency and specificity.

Second, COT is not required for maintenance of pERK rescue and/or intrinsic resistance following PLX4720 to RPMI-7951 and OUMS23. Consistent with this hypothesis, shCOT did abrogate pERK rescue and phenotypic resistance in A375+COT, where COT is known to be the

118

only kinase rescuing pERK following PLX4720 treatment. Although shCOT achieved less COT knockdown in RPMI-7951 and OUMS23 than in A375+COT, shNFKB1 in RPMI-7951 and OUMS23 suppressed COT in those lines to a degree comparable to that of shCOT in A375+COT, yet showed no effect on pERK or drug resistance, suggesting that other mediators of pERK rescue and resistance might be active.

The possibility that COT is not required for maintenance of intrinsic resistance in cell lines such as RPMI-7951 and OUMS23 is noteworthy. Indeed, it is consistent with data from several other sources. First, RPMI-7951 is among the high-NF-κB, high-AXL melanoma cell lines studied in Chapters 2 and 3. Much as AXL, though individually sufficient to confer MAPK pathway inhibitor resistance, was found not to be required for maintenance of intrinsic resistance, these data suggest that the same is true of COT. Indeed, given that RPMI-7951 express not only COT but also AXL, another known resistance effector, it would have been surprising if perturbing only COT was sufficient to render the cells sensitive to MAPK pathway inhibition. Moreover, the simultaneous expression of multiple resistance effectors is consistent with findings from patient samples, where, for example, COT amplification has been found to co-exist with an activating MEK1^{C121S} mutation that also confers RAF inhibitor resistance. [144]

The possibility of multiple resistance effectors operating at once suggests several observations. First, targeting resistance (whether intrinsic or acquired) may require more than simply targeting a single resistance effector shown to be expressed in the resistant context. On the contrary, targeting multiple resistance effectors may be required. Second, what controls the balance between these resistance effectors? Do they antagonize each other or synergize with each other? Are they mutually controlled by a master regulator? Are they present in the same cells or are they contained within subpopulations of the relapsing tumor?

The characterization of an intrinsically resistant cellular state in Chapter 2 suggests potential answers to these questions. In initially sensitive cell lines continuously cultured in PLX4720, in at least some cases, resistant subclones gained COT expression, but in the context of a broader transition to the high-NF-κB state. Although this finding is an example of acquired, rather than intrinsic, resistance, it may suggest that COT as a resistance effector does not operate in isolation, but rather is one effector engaged by a broader cell state transition such as that characterized in Chapter 2. Indeed, as discussed in Chapter 2, it is not certain that cells in the intrinsically resistant state retain any fundamental dependency on the MAPK pathway. If not, then it appears unlikely that targeting any individual resistance effector would confer sensitivity.

Ultimately, a definitive demonstration of the role of COT in RPMI-7951 and OUMS23 would require more effective suppression of COT: continued rescue of pERK and continued PLX4720 resistance in the setting of definitively ablated COT signaling would demonstrate that COT was not the only operant resistance mechanism. In the absence of better loss-of-function reagents to carry out this experiment, however, the cumulative picture of intrinsic MAPK pathway inhibitor resistance appears to be one of a broad cell-state dichotomy differentiating sensitivity from resistance, rather than a background of baseline sensitivity on which expression of individual resistance effectors is superimposed.

Conclusion

In summary, we have elucidated several features of p105/COT biology in melanoma. We have shown that they interact in melanoma and that their levels are reciprocally regulated. Reciprocal regulation of BRAF/COT levels appears not to depend upon altered p105 levels or COT-p105 binding. shNFKB1, to a greater extent than IL-1β, suppresses p105 and hence COT levels. Indeed, following PLX4720 treatment, shNFKB1 modestly impairs the rescue of pERK and of

viability mediated by exogenous COT. In lines endogenously expressing COT, however, neither NFKB1 knockdown nor knockdown of COT itself is able to alter residual PLX4720 resistance or pERK following PLX4720 treatment. Although this finding may simply be due to inadequate COT suppression, it is consonant with the idea intrinsic resistance is due not simply to COT expression, but rather to a fundamentally distinct, intrinsically resistant cellular state (of which COT expression happens to be one feature). Thus, cumulatively, our core biological hypothesis of COT/p105 interaction has been confirmed. Moreover, this finding providing a proof of principle that resistance effectors can be perturbed by targeting binding partners. In this particular case, this result is unlikely to yield clinical utility both due to the modest magnitude of the effect and to the apparent non-requirement of COT for maintenance of intrinsic resistance. Nonetheless, this work illustrates a role for one component of the NF-κB pathway in regulating COT as a mechanism of acquired resistance. Moreover, the principle of targeting resistance effectors by perturbing binding partners may prove valuable as an additional approach to targeting other mediators of drug resistance in cancer.

Methods

Constructs

All shRNAs were in pLKO.1 vector.

target	name	TRC identifier	target sequence
Luciferase	shLuc	TRCN0000072243	CTTCGAAATGTCCGTTCGGTT
NFKB1	6517	TRCN0000006517	CGCCTGAATCATTCTCGATTT
NFKB1	6518	TRCN0000006518	CCAGAGTTTACATCTGATGAT

| NFKB1 | 6520 | TRCN0000006520 | CCTTTCCTCTACTATCCTGAA |

| MAP3K8 | 10012 | TRCN0000010012 | GGGCCATTCAACCAAAGCAGA |

| MAP3K8 | 10013 | TRCN0000010013 | CAAGAGCCGCAGACCTACTAA |

| MAP3K8 | 10014 | TRCN0000010014 | GCGTTCTAAGTCTCTGCTGCT |

shRNA glycerol stocks were obtained through OpenBioSystems. The p105 ΔN (494-971)

S930A construct, in pK1 vector, was a kind gift of Bruce Horwitz [143]. The IκBα super-

repressor construct has been previously published [61, 110] and was a kind gift from David

Barbie and Jesse Boehm. pBABE-Puro empty vector was a gift of Cory Johannessen. MEK1

and COT (in pLX980-Blast-V5 or pLX304-Blast-V5 vectors) were from The RNAi Consortium.

Cell culture

All cells were maintained in medium supplemented with 10% FBS and 1%

penicillin/streptomycin. Media used were as follows: A375: RPMI. RPMI-7951: MEM.

OUMS23: MEM. All cell lines were obtained from in-lab stocks.

Primary melanocytes

Primary melanocytes were grown in TICVA medium (Ham's F-10 (Cellgro), 7% FBS, 1%

penicillin/streptomycin, 2 mM glutamine (Cellgro), 100 μM IBMX, 50 ng ml−1 TPA (12-O-

tetradecanoyl-phorbol-13-acetate), 1 mM 3′,5′-cyclic AMP dibutyrate (dbcAMP; Sigma) and

1 μM sodium vanadate). Following lentiviral introduction of BRAF^{V600E}, cells were switched to

Ham's F10 + 10% FBS. Survival in Ham's was used to select for BRAF^{V600E} expressing cells as

BRAF^{V600E} permits survival in the absence of TICVA supplements.

Virus infection

For single lentivirus infections, A375 cells were seeded in 6w plates (at 1.25e5 cpw). The day after seeding, medium was changed to medium + 4 µg/mL polybrene. 125 µL of lentivirus was used per well. Plates were centrifuged during infection for 30 minutes at 2250 rpm (1178 x g) at 30 °C, followed by overnight incubation. The subsequent day, medium was changed for fresh medium, and puromycin was added to a final concentration of 1 µg/mL. Cells were selected for 3 days before harvest.

Infection with multiple viruses was carried out according to the following protocol:

Day 1: seed in 6 well plate. (RPMI-7951: 2.5e5; OUMS23: 2e5)

Day 2: add polybrene to 4 µg/mL final and infect 1 mL retrovirus (pBABE-Puro empty vector, pBABE-p-IκBα SR, pBABE-puro-p105 SR) plus 125 µL shRNA lentivirus. Plates were centrifuged 30 minutes at 2250 rpm (1178 x g) at 30 °C during infection.

Day 3: morning: change to fresh medium. Afternoon: add polybrene to 4 µg/mL final and infect 1 mL retrovirus (pBabePuro-empty, pBp-IκBα SR, pBp-p105 SR). For wells combining p105 SR and shNFKB1 6517, shRNA infection was also repeated. Plates were centrifuged 30 minutes at 2250 rpm (1178 x g) at 30 °C during infection.

Day 4: change infected cells to fresh medium plus puromycin 1 µg/mL final.

Day 7: add DMSO or PLX4720 at 1 µM.

Day 8: Harvest (for lysates) or reseed in 96w format (for GI50 determination). RPMI7951 was reseeded at 3500 cpw; A375+COT at 1750 cpw.

For A375, protocol was as above except 1e5 cells per well were seeded 1 day earlier and an initial overnight infection with 125 µL LacZ or COT was performed prior to shRNA/retrovirus

infection. In addition, cells were selected with both puromycin (1 mg/mL final) and blasticidin (10 mg/mL final).

<u>IL-1β stimulus</u>

A375 were seeded at 6.24e4/w in 12w plates. Beginning the following day, cells were stimulated for indicated length of time with recombinant IL-1β (CST 8900SF) to the indicated final concentration, and harvested at indicated timepoints.

<u>Lysate harvesting</u>

Cells were harvested by washing 1x in PBS, applying sufficient lysis buffer to cover the well (~ 40 uL for 12w plate, ~100 uL for 6w plate), and removing lysis buffer. Plates were not scraped and lysates were not pelleted. Cells were lysed in 1% NP40 buffer (150 mM NaCl, 50 mM Tris pH 7.5, 2 mM EDTA pH 8, 25 mM NaF and 1% NP-40), containing 2x EDTA-free protease inhibitor cocktail (Roche) and 1x phosphatase inhibitors I and II (EMD). Lysates were quantitated by BCA, normalized, and denatured by boiling in sample buffer plus 20 mM DTT.

Immunoprecipitations were performed overnight at 4 °C in 1% NP-40 lysis buffer, at 1 µg/µl total protein concentration, followed by binding to Protein A agarose (25 µl, 50% slurry; Pierce) for 2 h at 4 °C. Beads were pelleted and washed three times in lysis buffer before elution and denaturing (95 °C) in 2× reduced sample buffer (Invitrogen).

<u>Western Blotting</u>

Transfers were on iBlot nitrocellulose membrane using setting P0. Membranes were blocked 1 hour at room temperature in LiCor blocking buffer. Primary antibodies (1:1000 dilution unless otherwise indicated) were incubated overnight at 4°C in LiCor blocking buffer plus 0.1% Tween-

20. Secondary antibodies (1:10,000 dilution, LiCor) were incubated at room temperature for 90 minutes in LiCor blocking buffer plus 0.1% Tween-20 and 0.1% SDS. Imaging was on a LiCor Odyssey infrared imager.

Primary antibodies were as follows (CST = Cell Signaling Technology, SCBT = Santa Cruz Biotechnology): BRAF (13, BD Biosciences 612375), COT (N17, SCBT sc-1717, 1:200), V5 (Invitrogen R960-25), pMEK (41G9, CST 9154), tMEK (L38C12 CST 9122), p105 (CST 4717), p50 (CST 3035), IκBα (L35A5, CST 4814), MCM2 (D7G11, CST 3619), pRelA (S536, 93H1, CST 3033); tRelA (L8F6, CST 6956), pERK (T202/Y204, D13.14.4E, CST 4370); tERK (L34F12, CST 4696), GAPDH (D16H11, CST 5174),

CHAPTER 5. IDENTIFYING NOVEL MELANOMA DEPENDENCIES: QUERYING THE NF-κB PATHWAY AS A POTENTIAL MELANOMA ESSENTIALITY

Abstract

Although the RAF and MEK inhibition has shown outstanding clinical promise in the 60% of melanomas harboring a BRAF^{V600} mutation, they have yet to show equivalent results in melanomas not harboring this mutation. In an attempt to identify new melanoma dependencies not restricted by BRAF genotype, we used pooled shRNA screening data to nominate genes that appeared to be differentially essential across all melanoma cell lines relative to other cancers. Among the top hits in this analysis was MYD88, a signal transduction adapter of profound importance in innate immune signaling, including the NF-κB, and a recently elucidated dependency in several other cancer contexts. In light of our previous interest in NF-κB in melanoma, we sought to query more comprehensively whether the NF-κB pathway represented a potential melanoma dependency. To this end, we performed a comprehensive arrayed shRNA screen for essential members of the NF-κB pathway in melanoma. This screen nominated additional signaling effectors around MYD88 as well as the immune-related transcription factor IRF3. Subsequent validation studies revealed a link between growth inhibition and knockdown performance for IRF3 and a putative cross-talk between IRF3 and MYD88-dependent signal transduction not previously recognized. Cumulatively, these experiments nominate the NF-κB pathway as an effector of potential significance and suggest a possible functional role for IRF3 in melanoma.

Attributions

All experiments and analyses were performed by David Konieczkowski except as follows:

Screens described in **Fig. 5.1** were performed by Marika Linja and Laura Johnson. **Fig 5.1** is reproduced from Barbara Weir.

Analysis in **Fig. 5.2** was performed by Aviad Tsherniak.

Introduction

Previous chapters have considered the limitations of MAPK pathway inhibitors for BRAF^{V600}-mutant melanoma—namely, pre-existing intrinsic resistance and the development of acquired resistance. Even with a comprehensive understanding of the mechanisms and therapeutic vulnerabilities of these classes of resistance, however, MAPK pathway inhibitor therapy may still face a fundamental limitation: although MEK inhibition has shown some early promise in NRAS-mutant melanoma [145], it remains primarily BRAF^{V600}-mutant melanomas that have shown clinical response to MAPK pathway inhibitors. Therefore, in melanomas that harbor BRAF^{V600} mutations as well as those that do not, MAPK pathway inhibition alone is unlikely to be sufficient to achieve durable control. In principle, what is needed to overcome this limitation is a gene or signaling pathway, not linked to MAPK pathway genotype, and preferably druggable, that is essential at least in a large proportion of melanomas. Targeting such vulnerabilities could illuminate therapeutic inroads for melanomas lacking BRAF/NRAS mutations or co-targeting opportunities in BRAF/NRAS-mutant melanomas.

A long-standing interest in cancer biology has been the efficient identification of targets specifically required for tumor growth. In the past several years, high-throughput approaches

127

have been developed to facilitate the interrogation of such dependencies. One important

systematic approaches involves genome-scale pooled shRNA screening. In brief, pooled shRNA

screening relies on the fact that cells infected with an shRNA knocking down an essential gene

will proliferate at a reduced rate, and therefore will be outcompeted in a culture. Each cell line is

infected with a pooled library of lentiviruses (when this work was initiated, the library contained

~55,000 shRNAs), at a titer to ensure ≤1 integration event per cell. Infected cells are selected

with puromycin and cultured for 16 populations doublings to allow lethal shRNAs to deplete.

Genomic DNA is harvested and final shRNA abundance is deconvoluted by hybridization to a

custom microarray. After extensive data quality control and normalization, shRNAs

differentially lethal to cell lines of interest relative to other cell lines are identified by

comparative marker selection, and genes with more than one shRNA scoring are identified by a

variety of methods. [68],[146] (**Fig. 5.1**)

Pooled screening technology has found significant use in cancer. As discovery efforts, multiple

large-scale screening efforts have produced dependency profiles for multiple cancer cell types.

[147], [148], [149],[150] Broadly speaking, this approach has shown itself able to identify that

cell lines with driver mutations in known oncogenes are generally dependent on those oncogenes

(e.g., BRAF, KRAS, PIK3CA) [146], an important positive control for the sensitivity of this

method. Turned towards discovery of unknown dependencies, these screens have identified

novel lineage essentialities such as PAX8 in ovarian cancer.[150] This technology, however, has

not been comprehensively leveraged in melanoma to identify novel dependencies.

Results

1. <u>A pooled shRNA screening approach to identify novel melanoma dependencies</u>

In order to identify candidate dependencies within melanoma not linked to BRAF genotype, we

made use of two sources of genome-scale pooled shRNA screening data. First, within the lab, 16

genetically diverse melanoma short-term cultures (encompassing BRAF-mutant, NRAS-mutant,

and BRAF/NRAS-wild-type lines) had been subjected to pooled shRNA screening (M. Linja,

unpublished data). Although this dataset could in principle be analyzed on its own for genes

essential in melanoma, such analyses tend to be dominated by genes essential in all cell types

(e.g., ribosomal subunits) [147]. Therefore, we sought a second dataset of non-melanoma cell

lines for comparison. Separately, the Achilles 2 project and Broad RNAi Consortium had

screened (at the time this study was initiated) ~40 non-melanoma cancer cell lines using the

same shRNA library. [150] By comparing these two datasets, we could query for genes whose

essentiality was specific to the melanoma lineage (**Fig 5.1**). Critically, because our screened

melanoma collection included robust representation of all MAPK genotypes (BRAF-mutant,

NRAS-mutant, and wild-type), this analysis had the potential to detect true pan-lineage

essentialities that were independent of MAPK pathway mutational status.
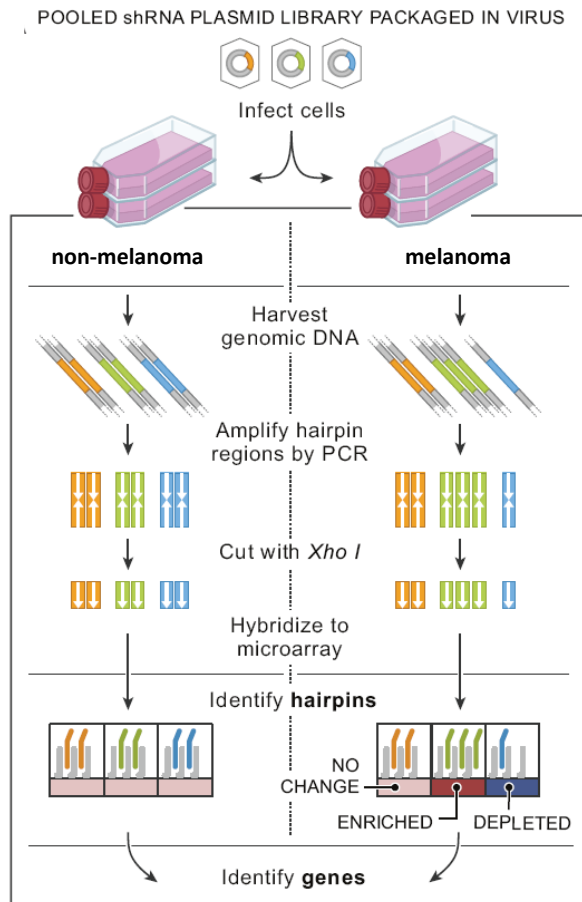
Figure 5.1: **A pooled shRNA screening approach to identify novel melanoma dependencies.**
Cells were infected with a pool of barcoded lentiviruses encoding an shRNA library and passaged for 16 population doublings to allow lethal hairpins to deplete. The relative abundance of each hairpin was determined by microarray. Gene essentialities were compared between melanoma and non-melanoma cell lines to identify novel putative melanoma lineage dependencies.

2. Pooled shRNA screening analysis nominates MYD88 as a novel melanoma dependency, suggesting a role for the NF-κB pathway

To identify such candidate melanoma dependencies, we compared the shRNA screening data from our melanoma cell lines with the non-melanoma cell lines from Achilles 2, identifying genes preferentially depleted in melanoma relative to other cancer cell lines. Following extensive quality control, normalization, and analysis, we identified MYD88 as among the genes most differentially essential in melanoma. (**Fig. 5.2**) MYD88 is a well-characterized adapter protein that links Toll-like receptors (TLRs) and the interleukin 1 receptor (IL1R) to downstream signal transduction, most notably NF-κB. In light of our prior investigation of the role of NF-κB pathway in MAPK pathway inhibitor resistance, the suggestion that NF-κB might also represent a melanoma lineage dependency was tantalizing.

Moreover, MYD88 has recently been implicated as a critical signal transduction node in several types of cancer. DLBCL and chronic lymphocytic leukemia harbor MYD88 activating mutations [151, 152]. MYD88 has also been found essential for colon cancer progression in Apc$^{Min/+}$ mice. [153],[154] Similar findings have been reported in other mouse models, particularly liver cancer. [155-157] While the screening identification of MYD88 as differentially essential in melanoma was not by itself definitive, when combined with (a) the known role of MYD88 in other cancers; and (b) our previous interest in NF-κB signaling in melanoma (cf. Ch. 2, 4), it was deemed worthy of additional study. Moreover, given the limited precision associated with pooled shRNA screening, we reasoned that a signal of MYD88 essentiality might in fact be a signpost for a larger NF-κB pathway dependency. For this reason, we set out to query whether the NF-κB pathway might represent a previously unrecognized melanoma lineage dependency.
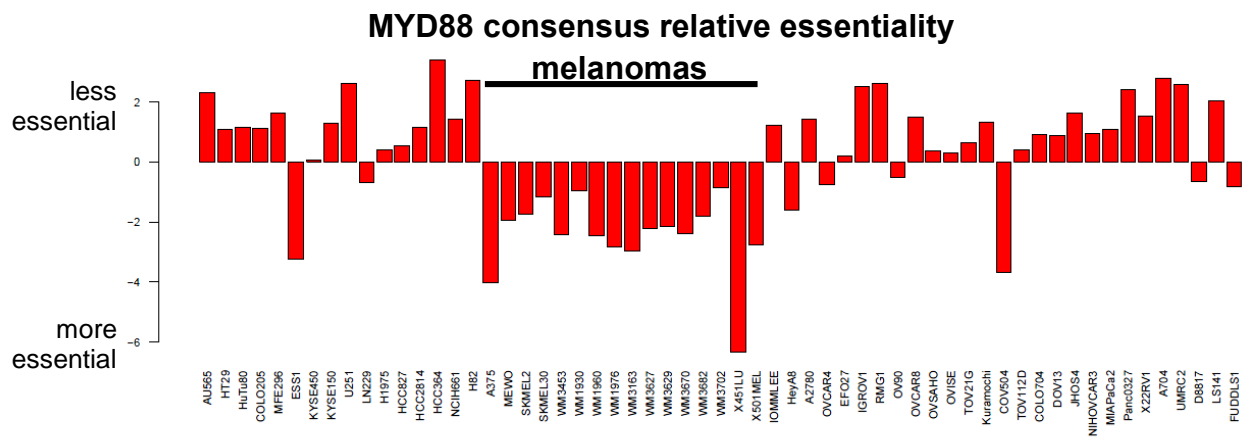
Figure 5.2: **Pooled shRNA screening analysis nominates MYD88 as candidate melanoma dependency, suggesting a role for the NF-κB pathway.**
Consensus essentiality profile (generated by ATARiS analysis) plotted for MYD88 across the collection of analyzed melanomas and non-melanomas. More negative numbers indicate greater essentiality.

3. Arrayed shRNA screen nominates NF-κB pathway members, including MYD88 and IRF3, as candidate melanoma dependencies.

Although our pooled screening analysis nominated MYD88 and by extension the NF-κB pathway as a candidate melanoma essentiality, large-scale pooled screening is by nature limited in its precision. As a complementary approach, we sought to map in detail a putative melanoma dependency on the NF-κB pathway using an arrayed shRNA screen. We screened ~5 shRNAs per gene for ~160 NF-κB pathway genes over a 7 day time course using three melanoma cell lines (1 BRAF-mutant, 1 NRAS-mutant, 1 BRAF/NRAS wild-type) so as to uncover dependencies shared across MAPK pathway genotypes. As a control, and in collaboration with the Barbie and Hahn labs, 8 lung adenocarcinoma lines were also screened. These lines provided a comparator group to identify shRNAs differentially toxic to melanoma but not globally toxic to all cancer cell lines.

Among the hits scoring as differentially essential in melanoma was LTBR, which has been previously characterized as a required upstream activator of the non-canonical NF-κB pathway in melanoma ([74], **Fig. 5.3**). Examining other top scoring hits (**Table 5.1**), we observed not only MYD88, but also numerous other members of the TLR/IL1R/MYD88 signaling module: CD14, a TLR4/TLR2 co-receptor; IRAK2, an immediate downstream adaptor of MYD88; Lyn, a Src-family Ser/Thr kinase which, among other functions, has been reported to phosphorylate TLRs following ligand binding; and ECSIT and TAB1, two parallel signaling components proximally downstream of the TLR/IL1R/MYD88 module (see **Fig. 5.3**). TRAF6—which bridges IRAK1/2 to TAK1 and ECSIT—did not emerge as a top hit in this arrayed screen. This might be due either to poor shRNA knockdown performance or to TRAF6 redundancy, as is observed for other TRAF family members. In addition, IRF3, a transcription factor induced downstream of

TLR signaling, but generally considered to by MYD88-independent, emerged as the single best hit, showing profound and highly selective depletion in the melanoma lines. In total, 7 out of the top 12 hits were related to the IL1R/TLR/MYD88/IRAK signaling module. (**Table 5.1**, **Fig. 5.3**).

In light of our query hypothesis that the NF-κB pathway might contain novel melanoma dependencies, it seemed noteworthy that the arrayed screen revealed multiple hits around one annotated functional module within the NF-κB pathway. These results suggested a preliminary validation of our hypothesis; moreover, they gave us a detailed gene-by-gene view of the components of this candidate essentiality. We therefore initiated further functional characterization of these genes.

Table 5.1: List of genes scoring as differentially essential in melanoma in NF-κB pathway arrayed shRNA screen.

Gene	P value rank	P value
IRF3	1	0.0012
CSNK2A1	2	0.0025
IRAK2	3	0.0034
LYN	4	0.0167
NOD1	5	0.0316
LTBR	6	0.0412
ECSIT	7	0.0497
CD14	8	0.0655
NFKBIE	9	0.0663
PRKCQ	10	0.0826
TAB1	11	0.0829
MYD88	12	0.0875
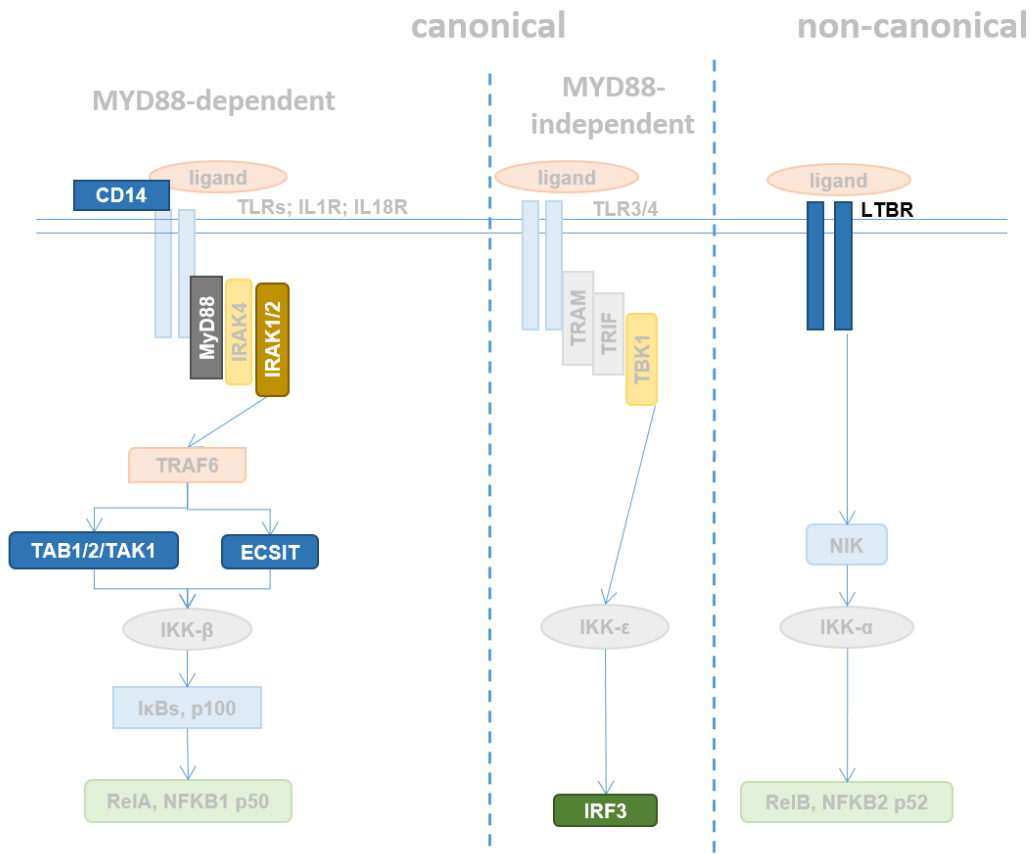
Figure 5.3: **Arrayed shRNA screen nominates NF-κB pathway members, including MYD88 and IRF3, as candidate melanoma dependencies.**
Top hits from arrayed shRNA validation screen (dark modules) are mapped onto various branches of the NF-κB pathway.

4. Assessment of MYD88 shRNA knockdown, pooled screening, and arrayed screening performance.

Because MYD88 was the index hit in our pooled screening analysis, and because the putative module of dependency identified in the arrayed screen involved MYD88, we first sought to query the behavior of MYD88 shRNAs. We reasoned that if MYD88 represented a legitimate biological dependency in melanoma, individual MYD88 shRNAs should behave consistently across contexts and in a manner correlated to their knockdown performance. To test this hypothesis, we compared the behavior of each MYD88 shRNA in the contexts where it had so far been tested. (**Fig. 5.4**) Surprisingly, we did not find a robust correlation between shRNAs that scored in the pooled analysis, the arrayed screen, and those that gave significant knockdown in low-throughput experiments. Imperfect correlation between screening results and independent knockdown studies has been observed elsewhere (unpublished Achilles screening data) and might relate to procedural differences between arrayed and pooled screens or "off-target" effects of individual shRNAs. Thus, the aggregate results of the arrayed screen and knockdown data generally supported the notion that an NF-κB signaling module might comprise a melanoma dependency, but the relative importance of MYD88 as a central node remained unclear.

		Wm3682				
		shMyD88				
	8024	8025	8026	8027	11223	shLuc
vinc						
MyD88						
Reproducible KD?	Y	Y	N	N	Y	
Scored in pooled?	±	Y	Y	N	n/a	
Scored in arrayed?	N	N	Y	Y	N	
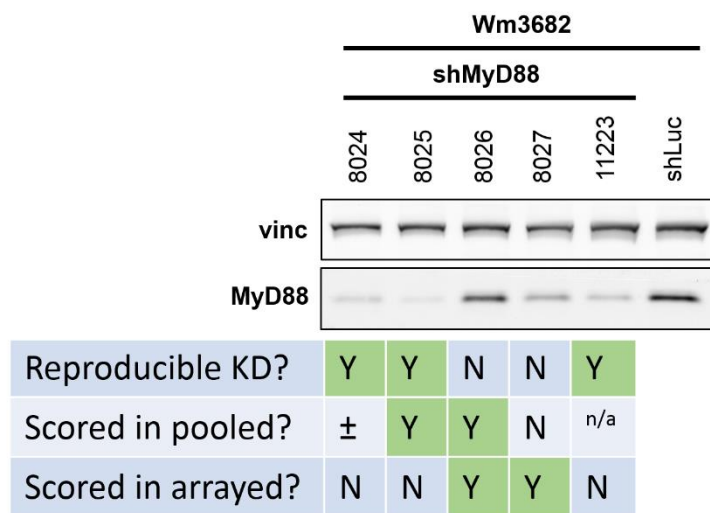
Figure 5.4: **Assessment of MYD88 shRNA knockdown, pooled screening, and arrayed screening performance.**
Representative knockdown performance of the MYD88 shRNAs, correlated with performance in the pooled and arrayed screens.

5. <u>Growth inhibitory effects of MYD88 shRNAs in melanoma and non-melanoma cell lines</u>

Because of the imperfect correlation between which shRNAs scored in the pooled screening analysis and which scored in the arrayed screen, it remained unclear which MYD88 shRNAs actually impaired the growth of melanoma cell lines. To clarify this question, we expressed all 5 available MYD88 shRNAs in the three melanoma cell lines used for the screen and performed 7-day growth inhibitory studies. (**Fig. 5.5A**) We found that the majority of the MYD88 shRNAs did confer a growth deficit, typically in the range of 50%. In particular, this was true of those shRNAs that scored in the pooled screening analysis as well as the arrayed screen. This finding confirmed that knockdown of MYD88 can confer a growth deficit on melanoma cell lines. Moreover a 50% growth deficit over a 7-day timecourse might result in a significant fitness disadvantage under pooled shRNA screening conditions (i.e., 16 population doublings)

We also sought to understand the extent to which these growth inhibitory effects were specific to melanoma. To address this question, we again expressed all 5 MYD88 shRNAs, but this time in a panel of 4 lung adenocarcinoma cell lines used in the control arm of the arrayed screen. (**Fig. 5.5B**) In many cases, we found that MYD88 shRNAs impaired the growth of non-melanoma cell lines to a comparable degree as they impaired melanoma cell lines. Moreover, no clear correlation was observed between growth inhibitory effects, in either melanoma or non-melanoma cell lines, and knockdown performance at the protein level (compare **Fig. 5.4**). This finding suggests that, while knockdown of MYD88 does impair the growth of melanoma cell lines, this phenotype may be due either to a dependency shared between melanoma and non-melanoma lines, or, at least in part, to non-specific growth inhibitor effects that are also shared with non-melanoma cell lines.
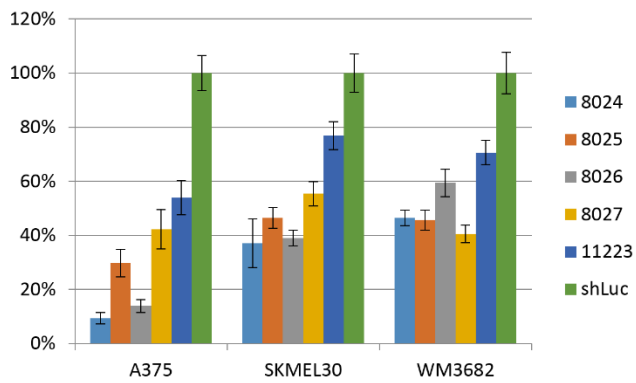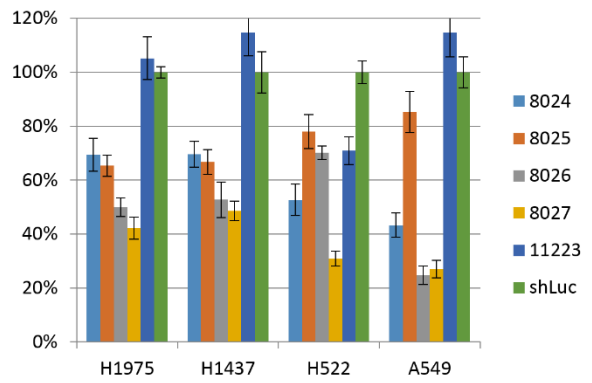
Figure 5.5: Growth inhibitory effects of MYD88 shRNAs in melanoma and non-melanoma cell lines.
Growth inhibitory effects of 5 MYD88 shRNAs on melanoma (a) and non-melanoma (b) cell lines from the arrayed screen.

6. <u>Correlation of arrayed screening and knockdown performance for selected targets.</u>

Although the correlation between knockdown and growth effects was imperfect for MYD88 shRNAs, our arrayed screen nominated a broader functional module of which MYD88 was just one member. We therefore sought to validate more comprehensively this module as a whole by querying a relationship between protein-level knockdown and screening phenotype (**Fig 5.6A**).

We reasoned that, if shRNAs scoring well in the arrayed screen (i.e., differentially lethal to melanoma vs. non-melanoma cells) also showed strong knockdown, the growth-inhibitory effects of such shRNAs were more likely due to "on-target" effects. In contrast, poor correlation between growth inhibition and knockdown would suggest that growth inhibition might be due to off-target toxicity. (**Fig 5.6B**) Because the arrayed screening analysis nominated hits differentially lethal in melanoma vs. non-melanoma cell lines, we used this (rather than absolute lethality in melanoma cell lines) as the metric for loss of viability. To test the hypothesis that differential shRNA lethality for our hits would correlate with protein-level knockdown, we infected A375 cells with shRNAs for the selected hits, harvested lysates, quantitated knockdown for each target of interest relative to actin loading control, and correlated that knockdown with the screening performance of each shRNA. Results are graphed in **Fig. 5.6C**.

As a negative control, we included TRAF6 (**Fig. 5.6C**, bottom right), a gene whose function has been linked to MYD88 but that did not did not score in either the pooled or arrayed screens. Consistent with this result, we found no correlation for TRAF6 between knockdown effectiveness and screening Z score.

We delineated several possible results. Strong knockdown with differential lethality (in melanoma vs. non-melanoma) (bottom left quadrant) is consistent with on-target killing;

conversely, weak knockdown with poor differential lethality (upper right quadrant) is consistent with an ineffective shRNA. On the other hand, strong knockdown with poor differential lethality (bottom right quadrant) is consistent either with off-target toxicity across cell lines, or with non-essentiality of the gene in melanoma; conversely, weak knockdown with strong differential lethality (upper left quadrant) is consistent with off-target toxicity specific to melanoma. We were therefore most interested in genes with multiple shRNAs scoring in the lower left quadrant.

Applying this framework to the hits, we noted that many of our hits had at least some shRNAs with excellent knockdown (e.g., IRAK2); however, these were not always among the most differentially lethal. Rather, some of the most differentially lethal shRNAs displayed relatively poor knockdown (e.g., IRAK2, TAB1, ECSIT). This result suggests that, for at least some of these shRNAs, observed differential lethality in melanoma might be due to off-target effects.

A notable exception to this trend, however, was seen in shRNAs targeting IRF3, the top single hit in the arrayed screen. Here, the shRNAs most differentially lethal were also among those achieving best knockdown. Although two shRNAs also gave >50% knockdown without differential lethality, this could be due to off-target toxicity of these shRNAs common across cell lines. For this reason, and because IRF3 was the strongest hit from the arrayed shRNA screen, we sought to functionally query the IRF3 signaling in melanoma.

Figure 5.6: Correlation of arrayed screening and knockdown performance for selected targets.
(**a**) Example of 96w knockdown validation Western blot.
(**b**) Schematic of graph plotting percent expression remaining relative to screening Z score. Lower left quadrant is consistent with on-target killing. Upper left quadrant is consistent with off-target toxicity specific to melanoma. Upper right quadrant is consistent with ineffective shRNAs. Lower right quadrant is consistent with either off-target toxicity across all cell lines, or non-essentiality of the targeted gene in melanoma.
(**c**) Plots of percent expression remaining and screening Z score for every screened hairpin for the indicated 8 genes.
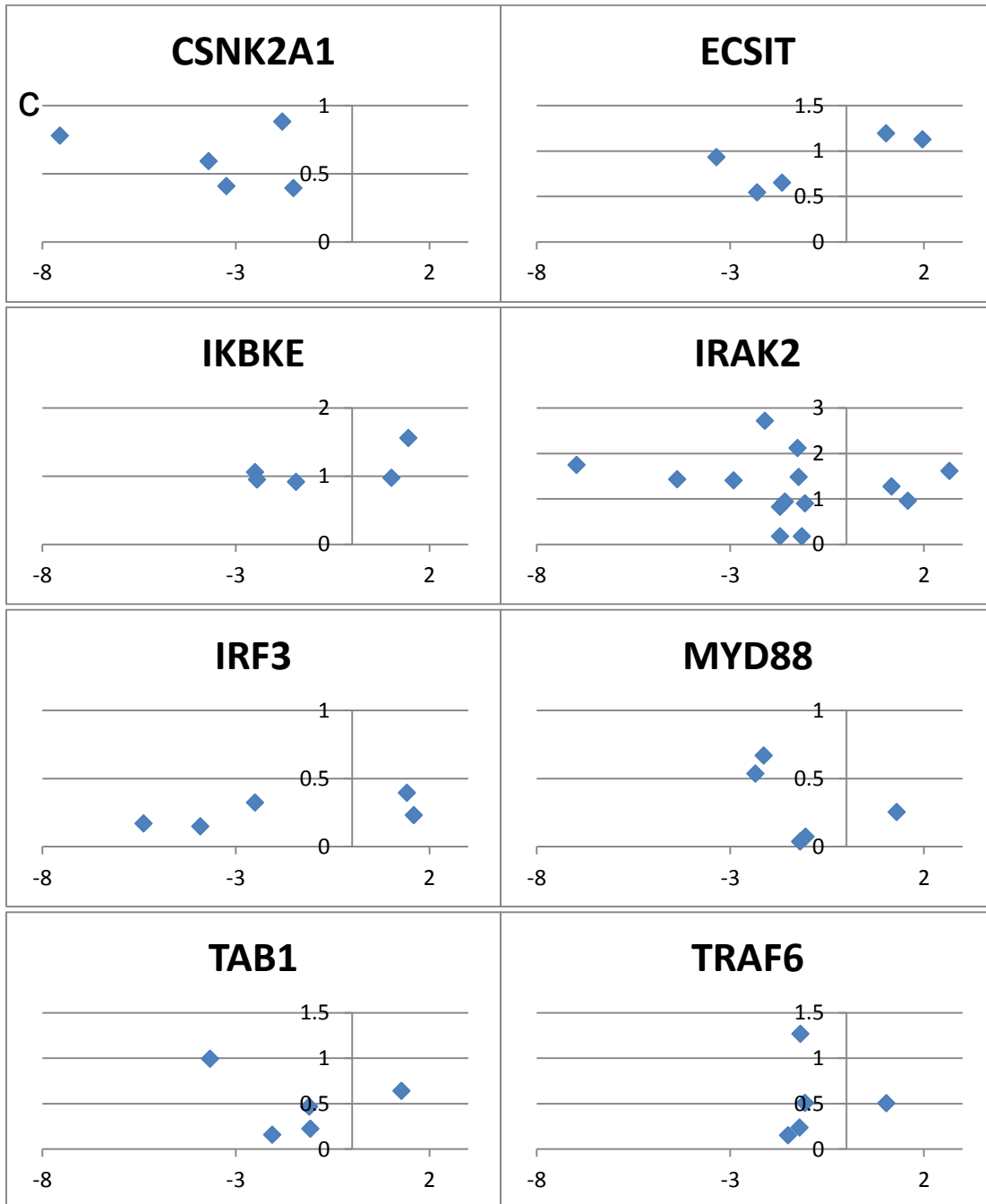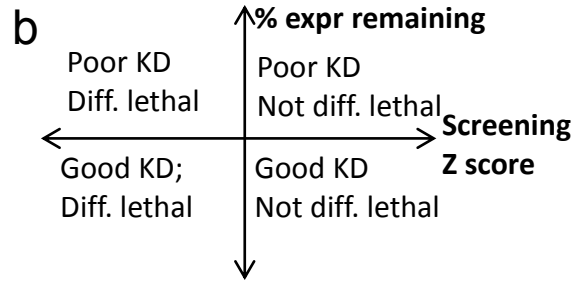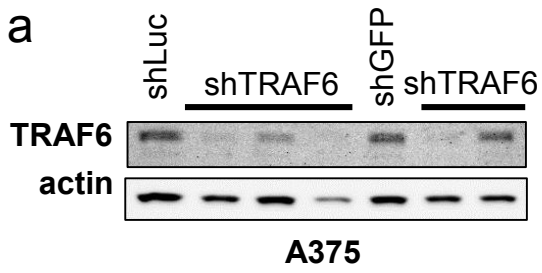
Figure 5.6 (continued)

7. <u>Functional relationships among MYD88, IRF3, and NF-κB pathway.</u>

Our cumulative results identified a putative module of dependency within the NF-κB pathway around MYD88 and a particular validated dependency on IRF3. Historically, these components have been classified in separate arms of the NF-κB pathway (**Fig. 5.3**), with hits around MYD88 involved in transducing phosphoactivation of the RelA transcription factor in response to ligands such as LPS and IL-1β, whereas IRF3 is itself a downstream transcription factor, activated in a MYD88-independent fashion by viral antigens (e.g., dsRNA). Given the potential functional relevance of these modules in melanoma but the lack of a known functional relationship between them, we sought to query whether signaling cross-talk might exist in this context. A functional relationship between these two genes could explain why both of them were identified as putative melanoma dependencies.

To test this, we queried signaling following knockdown of MYD88 and IRF3, using 3 independent shRNAs for each gene. Because pIRF3 is the readout for IRF3 activation, however, we needed to perturb an additional component in the IRF3 signaling pathway to ascertain signaling effects on IRF3. Therefore, we also knocked down TBK1, a kinase essential for TLR signaling to IRF3. After these perturbations, we then left cells untreated (**Fig. 5.7**, left panel) or perturbed them with IL-1β (**Fig. 5.7**, middle panel), which should activate signaling through MYD88 but not IRF3, or with poly(I:C), an artificial TLR3 ligand (**Fig. 5.7**, right panel), which should lead to IRF3 activation in a MYD88-independent manner. As an additional control, we included an uninfected control in the unstimulated panel (right-most lane, left panel). We observed no signaling differences at baseline between the uninfected control and the shLuc negative control shRNA, suggesting that neither lentiviral infection or shRNA expression itself was perturbing these innate immune signaling pathways.
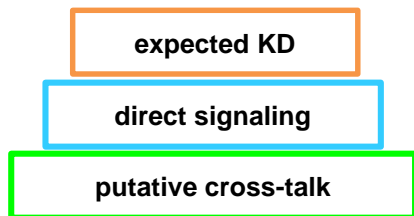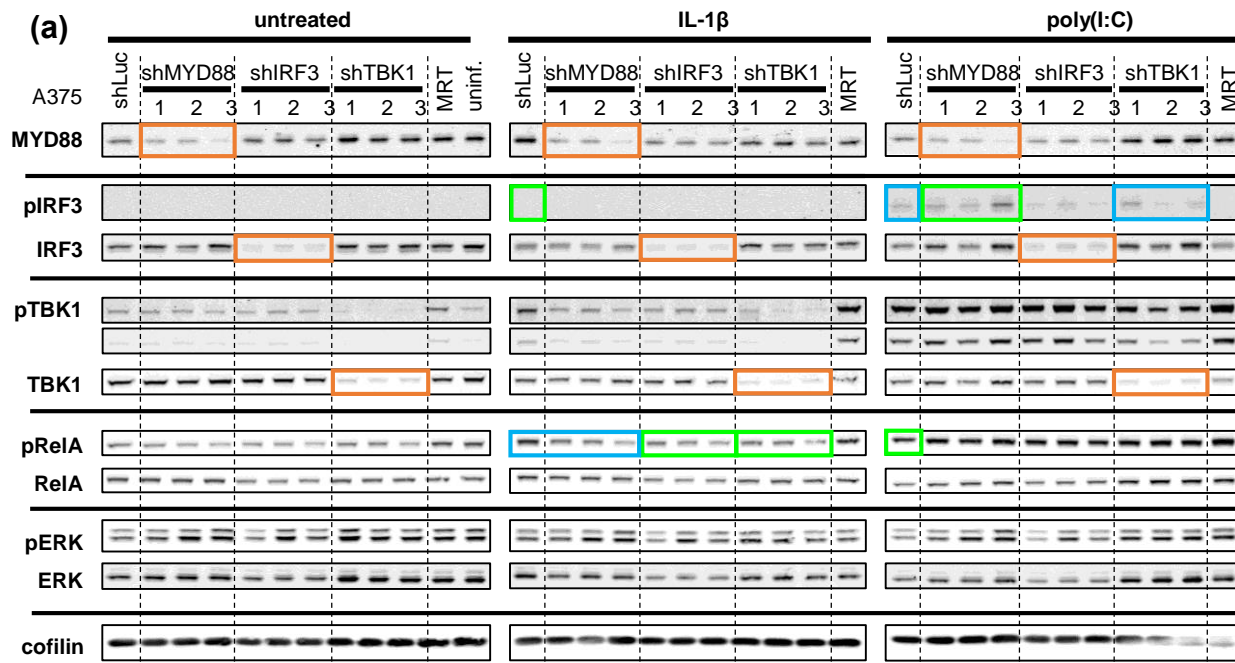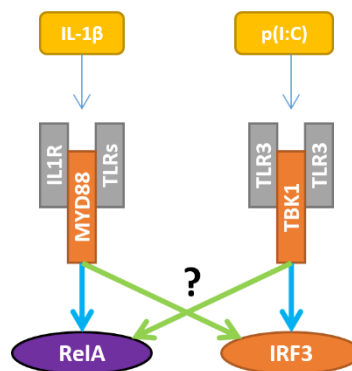
Figure 5.7: Functional relationships among MYD88, IRF3, and NF-κB pathway.
(a) A375 cells were infected with shRNAs as indicated, selected 3 days with puromycin, then left untreated or stimulated with IL-1β (25 ng/mL) or poly(I:C) (1000 ng). In addition to TBK1 shRNAs, TBK1 inhibitor MRT67307 (5 μM) was used as a second TBK1 loss-of-function reagent. Activation of downstream pathways was assessed by Western blot. Orange boxes indicate knockdown of shRNA targets; blue boxes indicate impairment of signaling directly downstream of either IL-1β or poly(I:C) stimulus; green boxes indicate putative cross-talk between these pathways.
(b) Schematic of pathway crosstalk queried in this experiment.

First, we confirmed adequate knockdown of targets (orange boxes). Next, we queried the effect

of knockdown of these targets in the unstimulated state. At baseline, knockdown of MYD88 or

IRF3 had no obvious effects on phosphorylation of RelA, a commonly used marker of NF-κB

pathway activity, or on phosphorylation of ERK. One mark of IRF3 activation is its

phosphorylation at S396[158]; however, we observed no pIRF3 at baseline. This finding may

imply that basal IRF3 activity in melanoma is simply below our detection limit, or that baseline

IRF3 activity may operate through a mechanism of activation other than phosphorylation of the

site queried by our antibody.

Next, we assessed whether "canonical" signaling downstream of shRNA targets was impaired by

knockdown (**Fig. 5.7**, blue boxes). Indeed, shMYD88 abrogated IL-1β-induced increase in

pRelA (center panel), and shTBK1 decreased poly(I:C)-mediated pIRF3 (right panel). These

findings demonstrate that both of the signaling modules nominated by our screen are competent

to transduce signals in melanoma—an important demonstration of their potential functional role

in this lineage. Together, these experiments confirmed that we achieved (a) adequate stimulation

of signaling through the relevant modules and (b) adequate knockdown of our targets at both a

protein level and functional level. This experiment was therefore powered to detect cross-talk

between these pathways or its abrogation.

We next queried whether any cross-talk might be detected between the canonical NF-κB

(including MYD88) and IRF3 signaling modules (**Fig. 5.7**, green boxes). Despite robust

increase in pRelA, IL-1B did not lead to discernible IRF3 phosphorylation (center panel),

implying that signaling through MYD88 may not be sufficient to activate pIRF3. Further,

shMYD88 did not impair poly(I:C)-mediated pIRF3 (right panel), arguing that MYD88 is not

necessary for activation of pIRF3 at least by poly(I:C) and at the levels of suppression achieved

in these experiments. We thus concluded that signaling through MYD88 may not contribute to IRF3 activity.

Conversely, we also assessed cross-talk from the IRF3 module to the MYD88 module. First, we queried whether poly(I:C) was sufficient to activate mediators typically considered downstream of MYD88. Indeed, we found that poly(I:C), in addition to activation of pIRF3, conferred robust RelA phosphorylation (**Fig. 5.7**, right panel). This suggests that an upstream stimulus through TLR3 can signal not only to IRF3 but also to the NF-κB effector module. Interestingly, this increase in pRelA was not abrogated by TBK1 knockdown, raising the possibility that cross-talk may proceed through other proximal signaling intermediates. Although MYD88 might conceivably represent one such intermediate, its involvement appears unlikely because shMYD88 also did not reduce poly(I:C)-induced RelA phosphorylation. Thus, we conclude that while poly(I:C) is sufficient to signal into the canonical NF-κB module, MYD88 may not be required for this cross-talk.

Having established that signals through the TBK1/IRF3 module were sufficient to activate pRelA, we next asked whether the TBK1/IRF3 signaling module was necessary for IL-1β-induced RelA phosphorylation. Surprisingly, we found that shIRF3 and shTBK1 reduced IL-1β-induced pRelA to an extent comparable to that achieved by shMYD88 (**Fig. 5.7**, center panel). It is possible that, in the case of TBK1, this phenomenon might occur due to cross-talk between TBK1-containing and MYD88-containing complexes. (Note, for example, the upregulation of MYD88 upon TBK1 knockdown, left panel.) It is less clear however, how IRF3—as a putatively downstream transcription factor—might be required for MYD88-dependent signal transduction. Nonetheless, these perturbational experiments suggest that the TBK1/IRF3 module may be necessary for canonical NF-κB signaling in melanoma.

Discussion and future directions

Nomination of NF-κB modules as candidate melanoma dependencies

Cumulatively, this study leveraged a particular analysis of existing pooled shRNA screening datasets to design and execute an arrayed follow-up screen. Furthermore, validation of hits was achieved by knockdown confirmation and by functionally querying the nominated signaling pathways.

Pooled shRNA screening analysis initially nominated MYD88 as one component of a potential melanoma lineage dependency. A subsequent arrayed shRNA screen identified IRF3, as well as MYD88 and other genes in close functional relationship to it, as candidate melanoma dependencies. The putative module of dependency around MYD88 appeared to involve the canonical NF-κB pathway. Although subsequent validation revealed an imperfect correlation shRNA knockdown and screening performance for some hits, including MYD88, such disparity is not entirely unexpected given the different formats used (pooled, arrayed, and low-throughput), the potential for off-target shRNA effects, and the different effects of shRNAs within specific cellular contexts.

Moreover, our arrayed screen nominated IRF3, a transcription factor critical for antiviral response but historically placed in a separate, MYD88-independent NF-κB pathway, as another candidate melanoma dependency. Not only was IRF3 the top hit in our arrayed screen for differential lethality in melanoma, it also showed the best knockdown/lethality correlation. This result is novel for melanoma, as these modules have not previously been suggested as melanoma dependencies. In particular, IRF3, given the strength of its phenotype and knockdown correlation, appears worthy of further investigation to characterize the mechanism of its dependency in melanoma.

Subsequent work has assessed the functional importance of these putative essentialities. Although demonstrating their activity at baseline proved challenging, we have shown that the signaling modules around MYD88 and IRF3 can be active in melanoma following stimulus, a finding that reaffirms these candidate dependencies can be functional signaling modules in melanoma. Second, we queried cross-talk between the two modules. We did not uncover any evidence of that the MYD88 module is necessary or sufficient for signaling to IRF3. We did, however, find that poly(I:C) mediated stimulus of IRF3 was also sufficient to activate the canonical NF-κB pathway. More striking, both IRF3 and its upstream kinase TBK1 appeared to be essential for optimum IL-1β signaling through MYD88. This result is novel and unexpected, not only in melanoma biology, but even in the innate immune context, where MYD88 and IRF3 have historically been considered a part of separate pathways.

Future directions for shRNA screening in melanoma

To the extent that MYD88 and/or IRF3 represent authentic melanoma dependencies, cross-talk between them implies the possibility of new signaling effects that could be determinants of this dependency. The nature of such signals, as well as their relevance to melanoma survival, remains obscure. Thus, future efforts—in addition to extending the initially promising validation of IRF3 as a melanoma dependency—will need to take into account the challenge of characterizing the downstream signal mediated by IRF3, and how that signal intersects with both the MYD88 module and with melanoma survival. This as-yet uncharacterized signaling pathway, being novel both in its mechanistic details and in its status as a melanoma dependency, is a promising target for future investigation.

In addition to pursuit of specific questions around IRF3 and MYD88, another avenue for further investigation is extending the analysis of shRNA screening in melanoma. Of note, our current

analysis did not attempt to segregate melanomas by expression class (MITF or NF-κB), as no intrinsically resistant, high-NF-κB lines were present in the initial pooled screening dataset. In light of the now understood importance of the high NF-κB class, and its profoundly different biology, an important avenue for further investigation will be querying this class for unique essentialities potentially not shared by other high-MITF melanoma. This could take place either at the genome-scale level, using pooled screening, or in a more targeted fashion using the NF-κB arrayed screening shRNA set that we have curated.

Although we have carried out an initial analysis for differential dependency in melanoma, there are many other resources that can be leveraged to ask additional questions. For example, using both shRNA screening and copy number data could allow one to look for genes both amplified and essential in melanoma; a similar analysis with expression data could identify genes both overexpressed and essential in melanoma. The potential to integrate other data sources offers many additional lenses through when to view shRNA screening data which more sharply focus the hypothesis being queried in the shRNA analysis. In addition, use of two orthogonal, independent data sources (e.g., pooled screening and copy number data) is a powerful way to filter out the false positives of either approach. Therefore, a systematic approach should be undertaken to (a) catalog what data sources are currently available for the melanoma lineage, (b) comprehensively delineate what biological questions can be asked by the appropriate intersection of these data sources, and (c) perform the identified analyses in order to search for any particularly noteworthy hits worthy of further investigation.

Conclusion

Taken together, the data in this aim nominate two novel candidate dependencies in melanoma: a module around MYD88, and IRF3. This screen thus provides evidence for the essentiality of at

least some signaling nodes in the NF-κB pathway in melanoma. However, our data also suggest that, in melanoma, the signaling circuitry within and/or between these canonically MYD88-dependent and MYD88-independent modules may not be as compartmentalized as thought. Rather, the IRF3/ "MYD88-independent" module appears to be both necessary and sufficient to effect signaling through the module around MYD88. This finding sets the stage for further functional investigation as well as suggests broad strategies for the future analysis of pooled screening data in melanoma.

Methods

Pooled screening data analysis

Raw microarray .CEL files were normalized, background corrected, probeset-averaged, and log-transformed in dChip. Outlier replicates within a cell line were filtered on the basis of MvA plots. Remaining replicates were collapsed to a single value and normalized to the concentration of each shRNA in the initial plasmid pool using a metric that penalizes shRNAs with large variation in the initial plasmid pool (modified log fold change). The resulting score distributions was normalized using the PMAD metric. Modules for all normalization steps following dChip are available on GenePattern. Finally, following normalization, genes were analyzed in one of two ways. First, essentiality scores for each gene in each cell line were calculated using the ATARiS tool [146]; differential essentiality was then calculated on the basis of fold change between melanoma and non-melanoma. Second, using the RIGER method, individual shRNAs were compared between the melanoma and non-melanoma classes on the basis of log fold change. Subsequently, this ranked list of shRNAs was collapsed to a ranked list of genes by

weighting the best shRNA 25% (to account for the possibility of it being off-target) and the second-best shRNA 75%.

Cell culture

All cells were maintained in medium supplemented with 10% FBS and 1% penicillin/streptomycin. The following cell lines were maintained in RPMI-1640: A375, Skmel30, Wm3682. A375, Skmel30, and Wm3682 were obtained from in-lab stocks; H1975, H1437, H522, and A549 were obtained from David Barbie.

Arrayed screening

shRNA-bearing lentiviruses for the screening set were produced by The RNAi Consortium (Broad Institute) and re-arrayed into 384w format. A375 cells were seeded at 400 cpw, SKMEL30 at 900 cpw, and WM3682 at 600 cpw. Each plate included empty well, empty vector, and irrelevant shRNA controls for subsequent data quality control. 24 hours after cell plating, media was changed to include 4 μg/μL polybrene, and cells were infected with 1-1.5 μL virus followed by a 30 min spin at 2250 rpm (1178 x g) at 30 °C. 24 hours after infection, selection was begun with 1 μg/μL puromycin. Cells were grown 5 days, and viability was determined by CellTiter-Glo assay. Cell lines were screened in quadruplicate; 3 replicates were selected with puromycin, and 1 replicate was not selected with puromycin in order to calculate infection efficiency. shRNAs were filtered by infection efficiency, and data were normalized between plates by converting raw luminescence values to robust Z scores. In order to go from ranked shRNAs to a ranked gene list, we used a weighted average of the ranks of the two best shRNAs for a given gene, with 25% weight on the best-scoring shRNA (to account for the possibility of that shRNA having an off-target effect) and 75% weight on the second-best

shRNA. The inclusion of 2 shRNAs reflects the finding that, for this library, out of 5 shRNAs against a gene, typically 2-3 give good knockdown.

Medium-throughput knockdown validation

For validation of knockdown/screening correlation, shRNAs targeting genes of interest were re-arrayed into a single 96-well plate. A375 cells were seeded into 96-well plates. The following day, cells were changed to medium containing 4 µg/mL puromycin, infected with 1.5 µL shRNA lentivirus per well, and spin infected for 60 minutes at 2250 rpm (1178 x g) at 30 °C. Medium was immediately changed following infection. The next day, puromycin was added to a concentration to 1 µg/mL final. After 3 days of selection, lysates were harvested using a multi-channel pipette. To increase lysate concentration, lysates were pooled from 3 replicate plates.

shRNA growth inhibition

For shRNA growth experiments, cell lines were infected in 6 well format followed by 3 days selection with puromycin (1 µg/mL final). Cells were then reseeded into 96 well format at 1000-3000 cpw. 7 days after seeding, viability was read out using CellTiter-Glo and compared to shLuc.

IRF3/MYD88 cross-talk

For shRNA knockdown followed by stimulus, A375 cells were seeded at 7.4e4 cpw in a 12-well plate. The next day, following addition of polybrene to 4 µg/mL final, cells were spin infected at 2250 rpm (1178 x g) at 30 °C for 30 minutes with 40-60 µL virus per well. Beginning the next day, cells were selected for 2 days with 1 µg/mL puromycin. After 2 days of selection, medium was removed, cells were washed once in PBS to remove dead cells (due to shMYD88 and

shIRF3 lethality), and cells were returned to medium plus puromycin, with or without 5 µM

MRT 67307. The next day, cells were treated for 90 minutes with IL-1β (100 ng/mL, Cell

Signaling Technologies) or transfected (FuGene 6, Roche) with poly(I:C) (1000 ng, Invivogen).

<u>Lysate harvesting</u>

Cells were harvested by washing 1x in PBS, applying sufficient lysis buffer to cover the well (~

40 uL for 12w plate, ~100 uL for 6w plate, ~250 µL for 10 cm plate), and removing lysis buffer.

Plates were not scraped and lysates were not pelleted. Cells were lysed in 1% NP40 buffer

(150 mM NaCl, 50 mM Tris pH 7.5, 2 mM EDTA pH 8, 25 mM NaF and 1% NP-40), containing

2x EDTA-free protease inhibitor cocktail (Roche) and 1x phosphatase inhibitors I and II (EMD).

Lysates were quantitated by BCA, normalized, and denatured by boiling in sample buffer plus 20

mM DTT.

<u>Western blotting</u>

All gels to be probed for MYD88 were transferred to Immobilon-FL PVDF membranes.

Membranes were blocked 1 hour at room temperature in LiCor blocking buffer. Primary

antibodies (1:1000 dilution unless otherwise indicated) were incubated overnight at 4°C in LiCor

blocking buffer plus 0.1% Tween-20. Secondary antibodies (1:10,000 dilution, LiCor) were

incubated at room temperature for 90 minutes in LiCor blocking buffer plus 0.1% Tween-20 and

0.1% SDS. Imaging was on a LiCor Odyssey infrared imager.

The following primary antibodies were used. CST = Cell Signaling Technology, SCBT = Santa

Cruz Biotechnology. MYD88 (D80F5. CST 4283), pIRF3 (4D4G, CST 4947), IRF3 (D83B9,

CST 4302), TBK1 (D1B4, CST 3504), pTBK1 (D52C2, CST 5483), CSNK2A1 (CST 2656),

ECSIT (Abcam ab-21288), IKBKE (72B587, SCBT sc-52931), TAB1 (C25E9, CST 3226),

IRAK2 (CST 4367), TRAF6 (CST 4743).

shRNAs

All shRNAs were in pLKO.1 vector.

target	name	TRC identifier	target sequence
Luciferase	shLuc	TRCN0000072243	CTTCGAAATGTCCGTTCGGTT
MYD88	1 / 8024	TRCN0000008024	CCACCAACTTTGTACCTTGAT
MYD88	8025	TRCN0000008025	GCAGAGCAAGGAATGTGACTT
MYD88	8026	TRCN0000008026	ACAGACAAACTATCGACTGAA
MYD88	2 / 8027	TRCN0000008027	CATCAAGTACAAGGCAATGAA
MYD88	3 / 11223	TRCN0000011223	CCTGTCTCTGTTCTTGAACGT
IRF3	1	TRCN0000005921	GCCAACCTGGAAGAGGAATTT
IRF3	2	TRCN0000005922	CGCAAAGAAGGGTTGCGTTTA
IRF3	3	TRCN0000005923	GATCTGATTACCTTCACGGAA

shTBK1 D1, D2, and D3 were a gift from David Barbie.

Approach to the problem

A guiding theme of this dissertation has been the limits of currently available MAPK pathway

therapeutics in melanoma. Although BRAF^{V600} mutations have emerged as a powerful predictor

of response to MAPK pathway inhibition, there remain three limitations to this therapeutic

approach. First, not all BRAF^{V600}-mutant melanomas respond to MAPK pathway inhibition

(intrinsic resistance). Second, of those that do respond, most eventually relapse (acquired

resistance). Third, for both those melanomas harboring BRAF^{V600} mutations as well as those

lacking them, durable control is likely to require the identification of therapeutically tractable

vulnerabilities beyond the MAPK pathway. We have endeavored to probe these challenges by

identifying molecular determinants of intrinsic resistance, investigating ways to perturb

mediators of acquired resistance, and screening for melanoma dependencies not linked to MAPK

pathway mutational status.

In addressing the problem of intrinsic resistance, we discovered that many BRAF^{V600}-mutant

melanomas intrinsically resistant to MAPK pathway inhibition exhibit a transcriptional state

distinct from those sensitive to MAPK pathway inhibition. Intriguingly, this cellular state is

characterized by low expression of the melanocyte lineage transcription factor MITF (and its

target genes), but activation of the NF-κB pathway and expression of marker genes including the

receptor tyrosine kinase AXL. This high-NF-κB state can arise in melanocytes secondary to

aberrant MAPK activation by BRAF^{V600E}, but its induction can be at least partially antagonized

by dysregulated MITF. In established melanoma cells, these states remain plastic and mutually

antagonistic.

The gene encoding the AXL receptor tyrosine kinase, which was strongly associated with the intrinsically resistant state, was previously identified as an effector of acquired MAPK pathway inhibitor resistance. We validated this observation, but also demonstrated that several intrinsically resistant lines do not depend upon AXL for maintenance of intrinsic resistance. Thus, AXL expression is sufficient but not necessary for resistance to RAF/MEK inhibitors. This finding is consistent (a) with the extensive expression differences we observed between intrinsic sensitivity and resistance, which encompass many genes in addition to AXL, and (b) the fact that AXL was induced by NF-κB activation, implying that, while it may be one downstream effector of intrinsic resistance, it is not the master regulator of this phenotype.

Our studies of acquired resistance focused on the role of NFKB1 p105 in modulating the stability of COT, a known resistance effector. This approach, which was hypothesis-driven rather than unbiased, was motivated by two considerations: (1) the notion that a mediator of acquired resistance could be regulated by NF-κB, and (2) the current paucity of potent and selective small molecule COT inhibitors. We observed that suppression of p105 (by shRNA knockdown) was indeed an effective means to reduce COT protein levels in melanoma cells. Following exogenous COT expression, where COT was known to be the only active resistance effector, p105 perturbation was sufficient to impair (albeit to a modest degree) COT-mediated rescue of pERK and viability following PLX4720 treatment. However, in intrinsically resistant cell lines expressing COT, even robust suppression of COT did not affect pERK or viability following PLX4720 treatment. This result is consonant with our observations from the preceding chapters that the phenotype of intrinsic resistance is broader than a single resistance effector, and therefore, that perturbing individual effectors appears not to sensitize melanoma cells to MAPK pathway inhibitors.

157

Finally, to address the need to discover additional melanoma dependencies, we analyzed large-scale pooled shRNA screening data generated across a collection of melanoma and non-melanoma cell lines. An informative observation from the primary pooled shRNA screen was that MYD88, an adaptor protein required for signal transduction into the NF-κB pathway, emerged as putatively essential in melanoma. This finding, noteworthy in light of our prior interest in NF-κB, led us to perform a follow-up arrayed shRNA screen to characterize NF-κB pathway dependencies in melanoma. This screen nominated two signaling modules: one, centered around MYD88, that implicated signal transduction to the canonical NF-κB transcription factor RelA; and a second, historically considered MYD88-independent, consisting of the IRF3 transcription factor. Subsequent mechanistic studies suggested a role for IRF3 in signal transduction through a MYD88-dependent signaling module in melanoma cells. While the nature of the contributions by IRF3 to melanoma signaling and dependency remains to be more fully elucidated, this work has nominated both IRF3 and the module around MYD88 as promising targets within the NF-κB pathway for future investigation.

Emergence of NF-κB as a common theme in melanoma

A unifying finding from these investigations was the emergence of the NF-κB pathway as a common theme in melanoma. Although prior studies have examined the NF-κB pathway in melanoma (see Introduction), this pathway has not been a major focus of the melanoma field to date.

This work has highlighted several reasons for renewed interest in NF-κB signaling in melanoma. We have shown that COT, an effector of acquired MAPK pathway inhibitor resistance, is regulated in melanoma by binding to p105 NFKB1. Through shRNA screening, we nominated two modules within the NF-κB pathway as putative melanoma dependencies. Last, we have

158

shown that intrinsic resistance to MAPK pathway inhibitor in BRAF^{V600} mutant melanoma is associated with a high-NF-κB/low-MITF transcriptional state, and that reciprocity between MITF and NF-κB may underlie the phenomenon of intrinsic resistance.

Questions for future investigation

Perhaps the broadest question is whether the multiple observations involving the NF-κB pathway are merely coincidental, or whether they reflect a unifying biological process contributing to melanoma initiation and/or progression. Several lines of evidence suggest an underlying connectivity amongst these observations. For example, although the we have shown protein stability of the resistance effector COT to be modulated by NFKB1 p105, the fact that the only COT-expressing BRAF^{V600E} melanoma cell line belonged to the high NF-κB subclass suggests that COT transcription also may be linked to the high-NF-κB state. Another line of evidence linking these observations emerged when sensitive cell lines were cultured to resistance in PLX4720; here, one of the resistant clones that emerged had not only transitioned to the high-NF-κB state, but also gained COT overexpression. Thus, in addition to p105-mediated regulation of COT protein stability, the high-NF-κB state may be linked to COT expression.

Another line of evidence for a possible linkage between the high-NF-κB state and COT dysregulation comes from studies of non-transformed human melanocytes. At baseline, these melanocytes express COT, but upon introduction of BRAF^{V600E} and subsequent induction of NF-κB, they lose COT expression (**Fig. 4.1**). In this case, the context of COT expression is opposite from that observed in melanoma cell lines: in melanocytes, COT is expressed in the high-MITF state before BRAF^{V600E} introduction, whereas in melanoma cell lines it is expressed in the low-MITF state associated with intrinsic resistance. Thus, although the directionality of COT regulation appears to differ between these two contexts, it appears that in both cases, gain or loss

159

of COT expression is not a single-gene perturbation, but rather one component of a broader shift in cellular state linked to NF-κB activation.

More generally, the MITF-low/NF-κB-high cellular state in melanoma may comprise an important area of future investigation. As discussed in Chapter 2, there is much mechanistic detail still to uncover about the origin of this state. How does BRAF^{V600E} induce NF-κB activation, AXL expression, and MITF suppression? How do most melanomas maintain MITF expression in the setting of BRAF^{V600E} mutation? Moreover, we have characterized that originally drug-sensitive, high-MITF cells can transition to the high-NF-κB state during acquisition of resistance, regardless of which individual resistance effectors (e.g., COT, AXL, p61 BRAF) they express. Thus, is this high-NF-κB state, in addition to being a feature of intrinsic resistance, also a unifying feature of acquired resistance? If so, and if we can characterize the mediators of the transition into this state during MAPK pathway inhibitor therapy, it is possible that this transition could be blocked or delayed therapeutically. Such an intervention would potentially extend the durability of response to MAPK pathway inhibitors in BRAF^{V600}-mutant melanoma by forestalling acquisition of resistance.

Another question pertains to how the high NF-κB state is induced by BRAF^{V600E} in melanocytes, yet marks resistance to MAPK pathway inhibition in melanoma. Why, fundamentally, are the high NF-κB melanomas resistant to MAPK pathway inhibition? Given the low levels in these melanomas of expression and activity of MITF, the canonical master regulator of the melanocyte lineage, can the high-NF-κB state be conceptualized as an alternative cellular fate decision? If so, does it correspond to a previous developmental state in the natural history of melanocytes or the neural crest?

The fact that melanomas intrinsically resistant to MAPK pathway inhibition exhibit a distinct transcriptional state carries with it obvious potential therapeutic implications. Indeed, we have shown initial clinical data that pre-treatment AXL expression (representing high-NF-κB cellular state) predicts a shorter response to MAPK pathway inhibition. While this finding suggests the prognostic importance of these transcriptional states, it comes with two caveats. First, this finding does not suggest excluding patients with AXL-positive melanoma from MAPK pathway inhibitor therapy, as some such patients experienced progression-free survival of up to 12 months on dabrafenib + trametinib treatment. Second, the fact that some AXL-positive patients experienced relatively durable responses to MAPK pathway inhibition suggests the need for a more refined signature of intrinsic resistance capable of more reliably guiding clinical prognosis.

Beyond MAPK pathway inhibitors, the other class of targeted therapeutics currently approved or in late-phase trials for melanoma consists of drugs such as ipilimumab or anti-PD1 antibodies that block immune checkpoint mechanisms. Interestingly, a recent report describes that TNFα-mediated downregulation of melanoma antigens leads to resistance to resistance to adoptive cytotoxic T cell transfer therapy. [159] Although the connection was not discussed in this report, these melanoma antigens are primarily MITF target genes (e.g., gp100/PMEL/SILV; cf. Ch. 2; [160]). Conceivably, a similar mechanism of resistance may operate for ipilimumab and associated therapies as well, which likely rely on immune recognition of melanoma antigens. Thus, melanomas that are intrinsically resistant to MAPK pathway inhibition and express low levels of MITF and its melanoma antigen target genes may prove resistant to immunomodulatory therapies as well.

Given the paucity of current therapeutic options for melanomas that are intrinsically resistant to RAF/MEK inhibition, a critical direction for future investigation will be the elucidation of

tractable therapeutic vulnerabilities in this set of melanomas. Here, two options present themselves: attempting to confer sensitivity to MAPK pathway inhibitors, and finding novel vulnerabilities outside of the MAPK pathway. As detailed in Chapters 3 and 4, attempts to sensitize intrinsically resistant cells to MAPK pathway inhibitors by impairing the function of individual resistance effectors (COT and AXL) proved disappointing, at least in vitro. However, it is possible that other perturbations exist which would render these cells sensitive to MAPK pathway inhibition; these targets could be discovered either through computational approaches or through shRNA screens for sensitization to MAPK pathway inhibitors, as detailed in Chapter 5.

In addition to such efforts to sensitize intrinsically resistant melanomas to MAPK pathway inhibition, shRNA screening efforts such as those detailed in Chapter 5 may offer a path to identify novel candidate dependencies outside of the MAPK pathway. Such dependencies, in principle, might be either (a) shared across all melanomas, regardless of MITF expression status or (b) unique to this high-NF-κB melanoma subclass. Indeed, the nomination of a candidate NF-κB dependency across melanomas (involving MYD88 and/or IRF3) may suggest that, while the high-NF-κB subclass exhibits a prominent NF-κB-driven phenotype, this pathway may be operant in other genetic or molecular subtypes of melanoma. A question for further investigation, then, will be the extent to which NF-κB signaling, as associated with intrinsic resistance, shares any functional overlap with the putative NF-κB modules of dependency identified in our shRNA screening. Regardless of the answer to this question, a comparison of genetic essentialities (whether through genome-wide, pooled shRNA screening or by probing the NF-κB pathway using a curated arrayed shRNA screening set) between high-NF-κB melanomas, high-MITF melanomas, and non-melanoma cancer cell lines should prove useful for identifying novel dependencies that could be targeted by future therapeutic regimens and combinations.

If the high-NF-κB cellular state presents a challenge to targeted therapy, it possible that, conversely, the high-MITF state presents an unexpected opportunity. Our index finding in Chapter 2 was that high MITF expression marks sensitivity to MAPK pathway inhibition. Although we have not explored the question here, it is possible that this finding obtains not only in BRAF^{V600}-mutant melanoma, but also in other melanoma genotypes. Several clinical trials have been reported for MEK inhibition in NRAS-mutant melanoma; results, however, have generally been less impressive than those achieved in BRAF^{V600}-mutant melanoma. If the findings obtained here extend across melanoma genotypes, one might hypothesize that MITF expression could be used to identify NRAS-mutant melanomas more likely to respond to MEK inhibition. If this finding bears out, it has the potential to expand significantly the therapeutic utility of MAPK pathway inhibition in melanoma.

Conclusion

Considered as a whole, this work has employed a series of systematic and hypothesis-driven approaches to investigate factors that limit the efficacy and durability of MAPK pathway inhibition in melanoma. A unifying theme from these studies is that the NF-κB pathway may have key roles in melanoma not previously appreciated. In particular, NF-κB signaling appears to be modulate and be modulated by both MAPK pathway signaling and MITF regulation, thus connecting considerations of targeted therapeutic sensitivity and resistance to those of melanocytic lineage identity. While the present work may heighten interest the NF-κB pathway in melanoma, much mechanistic detail also remains to be elucidated. Significant future work will therefore be required to synthesize a comprehensive understanding of the role of NF-κB in melanoma dependency, drug resistance, and cellular state.

REFERENCES

1.   Siegel, R., D. Naishadham, and A. Jemal, *Cancer statistics, 2013.* CA Cancer J Clin, 2013. **63**(1): p. 11-30.

2.   Eide, M.J. and M.A. Weinstock, *Association of UV index, latitude, and melanoma incidence in nonwhite populations--US Surveillance, Epidemiology, and End Results (SEER) Program, 1992 to 2001.* Arch Dermatol, 2005. **141**(4): p. 477-81.

3.   Rivers, J.K., *Melanoma.* Lancet, 1996. **347**(9004): p. 803-6.

4.   Kamb, A., et al., *Analysis of the p16 gene (CDKN2) as a candidate for the chromosome 9p melanoma susceptibility locus.* Nat Genet, 1994. **8**(1): p. 23-6.

5.   Hussussian, C.J., et al., *Germline p16 mutations in familial melanoma.* Nat Genet, 1994. **8**(1): p. 15-21.

6.   Zuo, L., et al., *Germline mutations in the p16INK4a binding domain of CDK4 in familial melanoma.* Nat Genet, 1996. **12**(1): p. 97-9.

7.   Draper, G.J., B.M. Sanders, and J.E. Kingston, *Second primary neoplasms in patients with retinoblastoma.* Br J Cancer, 1986. **53**(5): p. 661-71.

8.   Fletcher, O., et al., *Lifetime risks of common cancers among retinoblastoma survivors.* J Natl Cancer Inst, 2004. **96**(5): p. 357-63.

9.   Gandini, S., et al., *Meta-analysis of risk factors for cutaneous melanoma: III. Family history, actinic damage and phenotypic factors.* Eur J Cancer, 2005. **41**(14): p. 2040-59.

10.   Mitra, D., et al., *An ultraviolet-radiation-independent pathway to melanoma carcinogenesis in the red hair/fair skin background.* Nature, 2012. **491**(7424): p. 449-53.

11.   Yokoyama, S., et al., *A novel recurrent mutation in MITF predisposes to familial and sporadic melanoma.* Nature, 2011. **480**(7375): p. 99-103.

12.   Horn, S., et al., *TERT promoter mutations in familial and sporadic melanoma.* Science, 2013. **339**(6122): p. 959-61.

13.   Breslow, A., *Thickness, cross-sectional areas and depth of invasion in the prognosis of cutaneous melanoma.* Ann Surg, 1970. **172**(5): p. 902-8.

14.   Jelfs, P.L., et al., *Cutaneous malignant melanoma in Australia, 1989.* Med J Aust, 1994. **161**(3): p. 182-7.

15.   King, R., et al., *Microphthalmia transcription factor expression in cutaneous benign, malignant melanocytic, and nonmelanocytic tumors.* Am J Surg Pathol, 2001. **25**(1): p. 51-7.

16.   Busam, K.J., et al., *Analysis of microphthalmia transcription factor expression in normal tissues and tumors, and comparison of its expression with S-100 protein, gp100, and tyrosinase in desmoplastic malignant melanoma.* Am J Surg Pathol, 2001. **25**(2): p. 197-204.

17.   Granter, S.R., et al., *Microphthalmia transcription factor: not a sensitive or specific marker for the diagnosis of desmoplastic melanoma and spindle cell (non-desmoplastic) melanoma.* Am J Dermatopathol, 2001. **23**(3): p. 185-9.

18.   Veronesi, U., et al., *Thin stage I primary cutaneous malignant melanoma. Comparison of excision with margins of 1 or 3 cm.* N Engl J Med, 1988. **318**(18): p. 1159-62.

19.   Crosby, T., et al., *Systemic treatments for metastatic cutaneous melanoma.* Cochrane Database Syst Rev, 2000(2): p. CD001215.

20.   Middleton, M.R., et al., *Randomized phase III study of temozolomide versus dacarbazine in the treatment of patients with advanced metastatic malignant melanoma.* J Clin Oncol, 2000. **18**(1): p. 158-66.

21.   Davies, H., et al., *Mutations of the BRAF gene in human cancer.* Nature, 2002. **417**(6892): p. 949-54.

22.   Hingorani, S.R., et al., *Suppression of BRAF(V599E) in human melanoma abrogates transformation.* Cancer Res, 2003. **63**(17): p. 5198-202.

23.   Wellbrock, C., et al., *V599EB-RAF is an oncogene in melanocytes.* Cancer Res, 2004. **64**(7): p. 2338-42.

24.   Karasarides, M., et al., *B-RAF is a therapeutic target in melanoma.* Oncogene, 2004. **23**(37): p. 6292-8.

25.   Ball, N.J., et al., *Ras mutations in human melanoma: a marker of malignant progression.* J Invest Dermatol, 1994. **102**(3): p. 285-90.

26.   Carr, J. and R.M. Mackie, *Point mutations in the N-ras oncogene in malignant melanoma and congenital naevi.* Br J Dermatol, 1994. **131**(1): p. 72-7.

27.   Nikolaev, S.I., et al., *Exome sequencing identifies recurrent somatic MAP2K1 and MAP2K2 mutations in melanoma.* Nat Genet, 2012. **44**(2): p. 133-9.

28.   Wei, X., et al., *Exome sequencing identifies GRIN2A as frequently mutated in melanoma.* Nat Genet, 2011. **43**(5): p. 442-6.

29.   Berger, M.F., et al., *Melanoma genome sequencing reveals frequent PREX2 mutations.* Nature, 2012. **485**(7399): p. 502-6.

30.   Krauthammer, M., et al., *Exome sequencing identifies recurrent somatic RAC1 mutations in melanoma.* Nat Genet, 2012. **44**(9): p. 1006-14.

31.   Huang, F.W., et al., *Highly recurrent TERT promoter mutations in human melanoma.* Science, 2013. **339**(6122): p. 957-9.

32.   Berger, M.F., et al., *Integrative analysis of the melanoma transcriptome.* Genome Res, 2010. **20**(4): p. 413-27.

33.   Pleasance, E.D., et al., *A comprehensive catalogue of somatic mutations from a human cancer genome.* Nature, 2010. **463**(7278): p. 191-6.

34.   Hodis, E., et al., *A landscape of driver mutations in melanoma.* Cell, 2012. **150**(2): p. 251-63.

35.   Curtin, J.A., et al., *Distinct sets of genetic alterations in melanoma.* N Engl J Med, 2005. **353**(20): p. 2135-47.

36.   Garraway, L.A., et al., *Integrative genomic analyses identify MITF as a lineage survival oncogene amplified in malignant melanoma.* Nature, 2005. **436**(7047): p. 117-22.

37.   Levy, C., M. Khaled, and D.E. Fisher, *MITF: master regulator of melanocyte development and melanoma oncogene.* Trends Mol Med, 2006. **12**(9): p. 406-14.

38.   Liu, J.J. and D.E. Fisher, *Lighting a path to pigmentation: mechanisms of MITF induction by UV.* Pigment Cell Melanoma Res, 2010. **23**(6): p. 741-5.

39.   Du, J., et al., *Critical role of CDK2 for melanoma growth linked to its melanocyte-specific transcriptional regulation by MITF.* Cancer Cell, 2004. **6**(6): p. 565-76.

40.   Vance, K.W., et al., *Tbx2 is overexpressed and plays an important role in maintaining proliferation and suppression of senescence in melanomas.* Cancer Res, 2005. **65**(6): p. 2260-8.

41.   McGill, G.G., et al., *Bcl2 regulation by the melanocyte master regulator Mitf modulates lineage survival and melanoma cell viability.* Cell, 2002. **109**(6): p. 707-18.

42.   Dynek, J.N., et al., *Microphthalmia-associated transcription factor is a critical transcriptional regulator of melanoma inhibitor of apoptosis in melanomas.* Cancer Res, 2008. **68**(9): p. 3124-32.

43.   Ghosh, S. and D. Baltimore, *Activation in vitro of NF-kappa B by phosphorylation of its inhibitor I kappa B.* Nature, 1990. **344**(6267): p. 678-82.

44.   Woronicz, J.D., et al., *IkappaB kinase-beta: NF-kappaB activation and complex formation with IkappaB kinase-alpha and NIK.* Science, 1997. **278**(5339): p. 866-9.

45.   Henkel, T., et al., *Rapid proteolysis of I kappa B-alpha is necessary for activation of transcription factor NF-kappa B.* Nature, 1993. **365**(6442): p. 182-5.

46. Senftleben, U., et al., *Activation by IKKalpha of a second, evolutionary conserved, NF-kappa B signaling pathway.* Science, 2001. **293**(5534): p. 1495-9.

47. Yin, L., et al., *Defective lymphotoxin-beta receptor-induced NF-kappaB transcriptional activity in NIK-deficient mice.* Science, 2001. **291**(5511): p. 2162-5.

48. Theilen, G.H., R.F. Zeigel, and M.J. Twiehaus, *Biological studies with RE virus (strain T) that induces reticuloendotheliosis in turkeys, chickens, and Japanese quail.* J Natl Cancer Inst, 1966. **37**(6): p. 731-43.

49. Chen, I.S., K.C. Wilhelmsen, and H.M. Temin, *Structure and expression of c-rel, the cellular homolog to the oncogene of reticuloendotheliosis virus strain T.* J Virol, 1983. **45**(1): p. 104-13.

50. Carrasco, D., et al., *The v-rel oncogene promotes malignant T-cell leukemia/lymphoma in transgenic mice.* EMBO J, 1996. **15**(14): p. 3640-50.

51. Gilmore, T.D., *Multiple mutations contribute to the oncogenicity of the retroviral oncoprotein v-Rel.* Oncogene, 1999. **18**(49): p. 6925-37.

52. Lu, D., et al., *Alterations at the rel locus in human lymphoma.* Oncogene, 1991. **6**(7): p. 1235-41.

53. Joos, S., et al., *Primary mediastinal (thymic) B-cell lymphoma is characterized by gains of chromosomal material including 9p and amplification of the REL gene.* Blood, 1996. **87**(4): p. 1571-8.

54. Houldsworth, J., et al., *REL proto-oncogene is frequently amplified in extranodal diffuse large cell lymphoma.* Blood, 1996. **87**(1): p. 25-9.

55. Ngo, V.N., et al., *A loss-of-function RNA interference screen for molecular targets in cancer.* Nature, 2006. **441**(7089): p. 106-10.

56. Lenz, G., et al., *Oncogenic CARD11 mutations in human diffuse large B cell lymphoma.* Science, 2008. **319**(5870): p. 1676-9.

57. Davis, R.E., et al., *Chronic active B-cell-receptor signalling in diffuse large B-cell lymphoma.* Nature, 2010. **463**(7277): p. 88-92.

58. Kato, M., et al., *Frequent inactivation of A20 in B-cell lymphomas.* Nature, 2009. **459**(7247): p. 712-6.

59. Compagno, M., et al., *Mutations of multiple genes cause deregulation of NF-kappaB in diffuse large B-cell lymphoma.* Nature, 2009. **459**(7247): p. 717-21.

60. Shembade, N., A. Ma, and E.W. Harhaj, *Inhibition of NF-kappaB signaling by A20 through disruption of ubiquitin enzyme complexes.* Science, 2010. **327**(5969): p. 1135-9.

61.   Boehm, J.S., et al., *Integrative genomic approaches identify IKBKE as a breast cancer oncogene.* Cell, 2007. **129**(6): p. 1065-79.

62.   Finco, T.S. and A.S. Baldwin, Jr., *Kappa B site-dependent induction of gene expression by diverse inducers of nuclear factor kappa B requires Raf-1.* J Biol Chem, 1993. **268**(24): p. 17676-9.

63.   Finco, T.S., et al., *Oncogenic Ha-Ras-induced signaling activates NF-kappaB transcriptional activity, which is required for cellular transformation.* J Biol Chem, 1997. **272**(39): p. 24113-6.

64.   Norris, J.L. and A.S. Baldwin, Jr., *Oncogenic Ras enhances NF-kappaB transcriptional activity through Raf-dependent and Raf-independent mitogen-activated protein kinase signaling pathways.* J Biol Chem, 1999. **274**(20): p. 13841-6.

65.   Chien, Y. and M.A. White, *Characterization of RalB-Sec5-TBK1 function in human oncogenesis.* Methods Enzymol, 2008. **438**: p. 321-9.

66.   Mayo, M.W., et al., *Requirement of NF-kappaB activation to suppress p53-independent apoptosis induced by oncogenic Ras.* Science, 1997. **278**(5344): p. 1812-5.

67.   Meylan, E., et al., *Requirement for NF-kappaB signalling in a mouse model of lung adenocarcinoma.* Nature, 2009. **462**(7269): p. 104-7.

68.   Barbie, D.A., et al., *Systematic RNA interference reveals that oncogenic KRAS-driven cancers require TBK1.* Nature, 2009. **462**(7269): p. 108-12.

69.   Yang, J. and A. Richmond, *Constitutive IkappaB kinase activity correlates with nuclear factor-kappaB activation in human melanoma cells.* Cancer Res, 2001. **61**(12): p. 4901-9.

70.   McNulty, S.E., N.B. Tohidian, and F.L. Meyskens, Jr., *RelA, p50 and inhibitor of kappa B alpha are elevated in human metastatic melanoma cells and respond aberrantly to ultraviolet light B.* Pigment Cell Res, 2001. **14**(6): p. 456-65.

71.   McNulty, S.E., et al., *Comparative expression of NFkappaB proteins in melanocytes of normal skin vs. benign intradermal naevus and human metastatic melanoma biopsies.* Pigment Cell Res, 2004. **17**(2): p. 173-80.

72.   Gao, K., et al., *Prognostic significance of nuclear factor-kappaB p105/p50 in human melanoma and its role in cell migration.* Cancer Res, 2006. **66**(17): p. 8382-8.

73.   Dhawan, P. and A. Richmond, *A novel NF-kappa B-inducing kinase-MAPK signaling pathway up-regulates NF-kappa B activity in melanoma cells.* J Biol Chem, 2002. **277**(10): p. 7920-8.

74.   Dhawan, P., et al., *The lymphotoxin-beta receptor is an upstream activator of NF-kappaB-mediated transcription in melanoma cells.* J Biol Chem, 2008. **283**(22): p. 15399-408.

75.   Yang, J., et al., *BMS-345541 targets inhibitor of kappaB kinase and induces apoptosis in melanoma: involvement of nuclear factor kappaB and mitochondria pathways.* Clin Cancer Res, 2006. **12**(3 Pt 1): p. 950-60.

76.   Yang, J., et al., *Systemic targeting inhibitor of kappaB kinase inhibits melanoma tumor growth.* Cancer Res, 2007. **67**(7): p. 3127-34.

77.   Yang, J., et al., *Conditional ablation of Ikkb inhibits melanoma tumor development in mice.* J Clin Invest, 2010. **120**(7): p. 2563-74.

78.   Ferradini, L., et al., *Analysis of T cell receptor variability in tumor-infiltrating lymphocytes from a human regressive melanoma. Evidence for in situ T cell clonal expansion.* J Clin Invest, 1993. **91**(3): p. 1183-90.

79.   Hodi, F.S., et al., *Improved survival with ipilimumab in patients with metastatic melanoma.* N Engl J Med, 2010. **363**(8): p. 711-23.

80.   Robert, C., et al., *Ipilimumab plus dacarbazine for previously untreated metastatic melanoma.* N Engl J Med, 2011. **364**(26): p. 2517-26.

81.   Iwai, Y., et al., *Involvement of PD-L1 on tumor cells in the escape from host immune system and tumor immunotherapy by PD-L1 blockade.* Proc Natl Acad Sci U S A, 2002. **99**(19): p. 12293-7.

82.   Brahmer, J.R., et al., *Safety and activity of anti-PD-L1 antibody in patients with advanced cancer.* N Engl J Med, 2012. **366**(26): p. 2455-65.

83.   Topalian, S.L., et al., *Safety, activity, and immune correlates of anti-PD-1 antibody in cancer.* N Engl J Med, 2012. **366**(26): p. 2443-54.

84.   Flaherty, K.T., F.S. Hodi, and D.E. Fisher, *From genes to drugs: targeted strategies for melanoma.* Nat Rev Cancer, 2012. **12**(5): p. 349-61.

85.   Solit, D.B., et al., *BRAF mutation predicts sensitivity to MEK inhibition.* Nature, 2006. **439**(7074): p. 358-62.

86.   Tsai, J., et al., *Discovery of a selective inhibitor of oncogenic B-Raf kinase with potent antimelanoma activity.* Proc Natl Acad Sci U S A, 2008. **105**(8): p. 3041-6.

87.   Chapman, P.B., et al., *Improved survival with vemurafenib in melanoma with BRAF V600E mutation.* N Engl J Med, 2011. **364**(26): p. 2507-16.

88.   Sosman, J.A., et al., *Survival in BRAF V600-mutant advanced melanoma treated with vemurafenib.* N Engl J Med, 2012. **366**(8): p. 707-14.

89.   Flaherty, K.T., et al., *Combined BRAF and MEK inhibition in melanoma with BRAF V600 mutations.* N Engl J Med, 2012. **367**(18): p. 1694-703.

90.   Poulikakos, P.I., et al., *RAF inhibitor resistance is mediated by dimerization of aberrantly spliced BRAF(V600E).* Nature, 2011. **480**(7377): p. 387-90.

91.   Montagut, C., et al., *Elevated CRAF as a potential mechanism of acquired resistance to BRAF inhibition in melanoma.* Cancer Res, 2008. **68**(12): p. 4853-61.

92.   Johannessen, C.M., et al., *COT drives resistance to RAF inhibition through MAP kinase pathway reactivation.* Nature, 2010. **468**(7326): p. 968-72.

93.   Nazarian, R., et al., *Melanomas acquire resistance to B-RAF(V600E) inhibition by RTK or N-RAS upregulation.* Nature, 2010. **468**(7326): p. 973-7.

94.   Whittaker, S.R., et al., *A genome-scale RNA interference screen implicates NF1 loss in resistance to RAF inhibition.* Cancer Discov, 2013. **3**(3): p. 350-62.

95.   Lito, P., et al., *Relief of profound feedback inhibition of mitogenic signaling by RAF inhibitors attenuates their activity in BRAFV600E melanomas.* Cancer Cell, 2012. **22**(5): p. 668-82.

96.   Straussman, R., et al., *Tumour micro-environment elicits innate resistance to RAF inhibitors through HGF secretion.* Nature, 2012. **487**(7408): p. 500-4.

97.   Emery, C.M., et al., *MEK1 mutations confer resistance to MEK and B-RAF inhibition.* Proc Natl Acad Sci U S A, 2009. **106**(48): p. 20411-6.

98.   Haq, R., et al., *BCL2A1 is a lineage-specific antiapoptotic melanoma oncogene that confers resistance to BRAF inhibition.* Proc Natl Acad Sci U S A, 2013. **110**(11): p. 4321-6.

99.   Flaherty, K.T., et al., *Inhibition of mutated, activated BRAF in metastatic melanoma.* N Engl J Med, 2010. **363**(9): p. 809-19.

100.   Barretina, J., et al., *The Cancer Cell Line Encyclopedia enables predictive modelling of anticancer drug sensitivity.* Nature, 2012. **483**(7391): p. 603-7.

101.   Bittner, M., et al., *Molecular classification of cutaneous malignant melanoma by gene expression profiling.* Nature, 2000. **406**(6795): p. 536-40.

102.   Sensi, M., et al., *Human cutaneous melanomas lacking MITF and melanocyte differentiation antigens express a functional Axl receptor kinase.* J Invest Dermatol, 2011. **131**(12): p. 2448-57.

103.   Bertolotto, C., et al., *Microphthalmia gene product as a signal transducer in cAMP-induced differentiation of melanocytes.* J Cell Biol, 1998. **142**(3): p. 827-35.

104.   Price, E.R., et al., *alpha-Melanocyte-stimulating hormone signaling regulates expression of microphthalmia, a gene deficient in Waardenburg syndrome.* J Biol Chem, 1998. **273**(49): p. 33042-7.

105. Gray-Schopfer, V.C., et al., *Tumor necrosis factor-alpha blocks apoptosis in melanoma cells when BRAF signaling is inhibited.* Cancer Res, 2007. **67**(1): p. 122-9.

106. Sequist, L.V., et al., *Genotypic and histological evolution of lung cancers acquiring resistance to EGFR inhibitors.* Sci Transl Med, 2011. **3**(75): p. 75ra26.

107. Hemesath, T.J., et al., *MAP kinase links the transcription factor Microphthalmia to c-Kit signalling in melanocytes.* Nature, 1998. **391**(6664): p. 298-301.

108. Wu, M., et al., *c-Kit triggers dual phosphorylations, which couple activation and degradation of the essential melanocyte factor Mi.* Genes Dev, 2000. **14**(3): p. 301-12.

109. Pratilas, C.A., et al., *(V600E)BRAF is associated with disabled feedback inhibition of RAF-MEK signaling and elevated transcriptional output of the pathway.* Proc Natl Acad Sci U S A, 2009. **106**(11): p. 4519-24.

110. Brown, K., et al., *Control of I kappa B-alpha proteolysis by site-specific, signal-induced phosphorylation.* Science, 1995. **267**(5203): p. 1485-8.

111. Garnett, M.J., et al., *Systematic identification of genomic markers of drug sensitivity in cancer cells.* Nature, 2012. **483**(7391): p. 570-5.

112. Lin, W.M., et al., *Modeling genomic diversity and tumor dependency in malignant melanoma.* Cancer Res, 2008. **68**(3): p. 664-73.

113. Wood, K.C., et al., *MicroSCALE screening reveals genetic modifiers of therapeutic response in melanoma.* Sci Signal, 2012. **5**(224): p. rs4.

114. Subramanian, A., et al., *Gene set enrichment analysis: a knowledge-based approach for interpreting genome-wide expression profiles.* Proc Natl Acad Sci U S A, 2005. **102**(43): p. 15545-50.

115. Jagani, Z., et al., *Loss of the tumor suppressor Snf5 leads to aberrant activation of the Hedgehog-Gli pathway.* Nat Med, 2010. **16**(12): p. 1429-33.

116. Tamayo, P., et al., *Predicting relapse in patients with medulloblastoma by integrating evidence from clinical and genomic features.* J Clin Oncol, 2011. **29**(11): p. 1415-23.

117. Xing, F., et al., *Concurrent loss of the PTEN and RB1 tumor suppressors attenuates RAF dependence in melanomas harboring (V600E)BRAF.* Oncogene, 2012. **31**(4): p. 446-57.

118. Nagata, K., et al., *Identification of the product of growth arrest-specific gene 6 as a common ligand for Axl, Sky, and Mer receptor tyrosine kinases.* J Biol Chem, 1996. **271**(47): p. 30022-7.

119. Tai, K.Y., et al., *Axl promotes cell invasion by inducing MMP-9 activity through activation of NF-kappaB and Brg-1.* Oncogene, 2008. **27**(29): p. 4044-55.

120.   Demarchi, F., et al., *Gas6 anti-apoptotic signaling requires NF-kappa B activation.* J Biol Chem, 2001. **276**(34): p. 31738-44.

121.   Liu, E., B. Hjelle, and J.M. Bishop, *Transforming genes in chronic myelogenous leukemia.* Proc Natl Acad Sci U S A, 1988. **85**(6): p. 1952-6.

122.   Quong, R.Y., et al., *Protein kinases in normal and transformed melanocytes.* Melanoma Res, 1994. **4**(5): p. 313-9.

123.   van Ginkel, P.R., et al., *Expression of the receptor tyrosine kinase Axl promotes ocular melanoma cell survival.* Cancer Res, 2004. **64**(1): p. 128-34.

124.   Zhang, Z., et al., *Activation of the AXL kinase causes resistance to EGFR-targeted therapy in lung cancer.* Nat Genet, 2012. **44**(8): p. 852-60.

125.   Liu, L., et al., *Novel mechanism of lapatinib resistance in HER2-positive breast tumor cells: activation of AXL.* Cancer Res, 2009. **69**(17): p. 6871-8.

126.   Mahadevan, D., et al., *A novel tyrosine kinase switch is a mechanism of imatinib resistance in gastrointestinal stromal tumors.* Oncogene, 2007. **26**(27): p. 3909-19.

127.   Miyoshi, J., et al., *Structure and transforming potential of the human cot oncogene encoding a putative protein kinase.* Mol Cell Biol, 1991. **11**(8): p. 4088-96.

128.   Patriotis, C., et al., *Tpl-2 acts in concert with Ras and Raf-1 to activate mitogen-activated protein kinase.* Proc Natl Acad Sci U S A, 1994. **91**(21): p. 9755-9.

129.   Dumitru, C.D., et al., *TNF-alpha induction by LPS is regulated posttranscriptionally via a Tpl2/ERK-dependent pathway.* Cell, 2000. **103**(7): p. 1071-83.

130.   Banerjee, A., et al., *Diverse Toll-like receptors utilize Tpl2 to activate extracellular signal-regulated kinase (ERK) in hemopoietic cells.* Proc Natl Acad Sci U S A, 2006. **103**(9): p. 3274-9.

131.   Gewurz, B.E., et al., *Genome-wide siRNA screen for mediators of NF-kappaB activation.* Proc Natl Acad Sci U S A, 2012. **109**(7): p. 2467-72.

132.   Kaila, N., et al., *Identification of a novel class of selective Tpl2 kinase inhibitors: 4-Alkylamino-[1,7]naphthyridine-3-carbonitriles.* Bioorg Med Chem, 2007. **15**(19): p. 6425-42.

133.   Green, N., et al., *Inhibitors of tumor progression loci-2 (Tpl2) kinase and tumor necrosis factor alpha (TNF-alpha) production: selectivity and in vivo antiinflammatory activity of novel 8-substituted-4-anilino-6-aminoquinoline-3-carbonitriles.* J Med Chem, 2007. **50**(19): p. 4728-45.

134. Wu, J., et al., *Selective inhibitors of tumor progression loci-2 (Tpl2) kinase with potent inhibition of TNF-alpha production in human whole blood.* Bioorg Med Chem Lett, 2009. **19**(13): p. 3485-8.

135. Cusack, K., et al., *Identification of a selective thieno[2,3-c]pyridine inhibitor of COT kinase and TNF-alpha production.* Bioorg Med Chem Lett, 2009. **19**(6): p. 1722-5.

136. Hu, Y., et al., *Discovery of indazoles as inhibitors of Tpl2 kinase.* Bioorg Med Chem Lett, 2011. **21**(16): p. 4758-61.

137. Cohen, P., *Targeting protein kinases for the development of anti-inflammatory drugs.* Curr Opin Cell Biol, 2009. **21**(2): p. 317-24.

138. Belich, M.P., et al., *TPL-2 kinase regulates the proteolysis of the NF-kappaB-inhibitory protein NF-kappaB1 p105.* Nature, 1999. **397**(6717): p. 363-8.

139. Waterfield, M.R., et al., *NF-kappaB1/p105 regulates lipopolysaccharide-stimulated MAP kinase signaling by governing the stability and function of the Tpl2 kinase.* Mol Cell, 2003. **11**(3): p. 685-94.

140. Beinke, S., et al., *NF-kappaB1 p105 negatively regulates TPL-2 MEK kinase activity.* Mol Cell Biol, 2003. **23**(14): p. 4739-52.

141. Beinke, S., et al., *Lipopolysaccharide activation of the TPL-2/MEK/extracellular signal-regulated kinase mitogen-activated protein kinase cascade is regulated by IkappaB kinase-induced proteolysis of NF-kappaB1 p105.* Mol Cell Biol, 2004. **24**(21): p. 9658-67.

142. Yang, H.T., et al., *NF-kappaB1 inhibits TLR-induced IFN-beta production in macrophages through TPL-2-dependent ERK activation.* J Immunol, 2011. **186**(4): p. 1989-96.

143. Zhao, X., et al., *Nfkb1 inhibits LPS-induced IFN-beta and IL-12 p40 production in macrophages by distinct mechanisms.* PLoS One, 2012. **7**(3): p. e32811.

144. Wagle, N., et al., *Dissecting therapeutic resistance to RAF inhibition in melanoma by tumor genomic profiling.* J Clin Oncol, 2011. **29**(22): p. 3085-96.

145. Ascierto, P.A., et al., *MEK162 for patients with advanced melanoma harbouring NRAS or Val600 BRAF mutations: a non-randomised, open-label phase 2 study.* Lancet Oncol, 2013. **14**(3): p. 249-56.

146. Shao, D.D., et al., *ATARiS: computational quantification of gene suppression phenotypes from multisample RNAi screens.* Genome Res, 2013. **23**(4): p. 665-78.

147. Luo, B., et al., *Highly parallel identification of essential genes in cancer cells.* Proc Natl Acad Sci U S A, 2008. **105**(51): p. 20380-5.

148. Brough, R., et al., *Functional viability profiles of breast cancer.* Cancer Discov, 2011. **1**(3): p. 260-73.

149. Marcotte, R., et al., *Essential gene profiles in breast, pancreatic, and ovarian cancer cells.* Cancer Discov, 2012. **2**(2): p. 172-89.

150. Cheung, H.W., et al., *Systematic investigation of genetic vulnerabilities across cancer cell lines reveals lineage-specific dependencies in ovarian cancer.* Proc Natl Acad Sci U S A, 2011. **108**(30): p. 12372-7.

151. Puente, X.S., et al., *Whole-genome sequencing identifies recurrent mutations in chronic lymphocytic leukaemia.* Nature, 2011. **475**(7354): p. 101-5.

152. Ngo, V.N., et al., *Oncogenically active MYD88 mutations in human lymphoma.* Nature, 2011. **470**(7332): p. 115-9.

153. Lee, S.H., et al., *ERK activation drives intestinal tumorigenesis in Apc(min/+) mice.* Nat Med, 2010. **16**(6): p. 665-70.

154. Rakoff-Nahoum, S. and R. Medzhitov, *Regulation of spontaneous intestinal tumorigenesis through the adaptor protein MyD88.* Science, 2007. **317**(5834): p. 124-7.

155. Pikarsky, E., et al., *NF-kappaB functions as a tumour promoter in inflammation-associated cancer.* Nature, 2004. **431**(7007): p. 461-6.

156. Maeda, S., et al., *IKKbeta couples hepatocyte death to cytokine-driven compensatory proliferation that promotes chemical hepatocarcinogenesis.* Cell, 2005. **121**(7): p. 977-90.

157. Naugler, W.E., et al., *Gender disparity in liver cancer due to sex differences in MyD88-dependent IL-6 production.* Science, 2007. **317**(5834): p. 121-4.

158. Lin, R., et al., *Virus-dependent phosphorylation of the IRF-3 transcription factor regulates nuclear translocation, transactivation potential, and proteasome-mediated degradation.* Mol Cell Biol, 1998. **18**(5): p. 2986-96.

159. Landsberg, J., et al., *Melanomas resist T-cell therapy through inflammation-induced reversible dedifferentiation.* Nature, 2012. **490**(7420): p. 412-6.

160. Du, J., et al., *MLANA/MART1 and SILV/PMEL17/GP100 are transcriptionally regulated by MITF in melanocytes and melanoma.* Am J Pathol, 2003. **163**(1): p. 333-43.